Role of MinD and related proteins in chromosome partitioning in *Bacillus subtilis* during sporulation

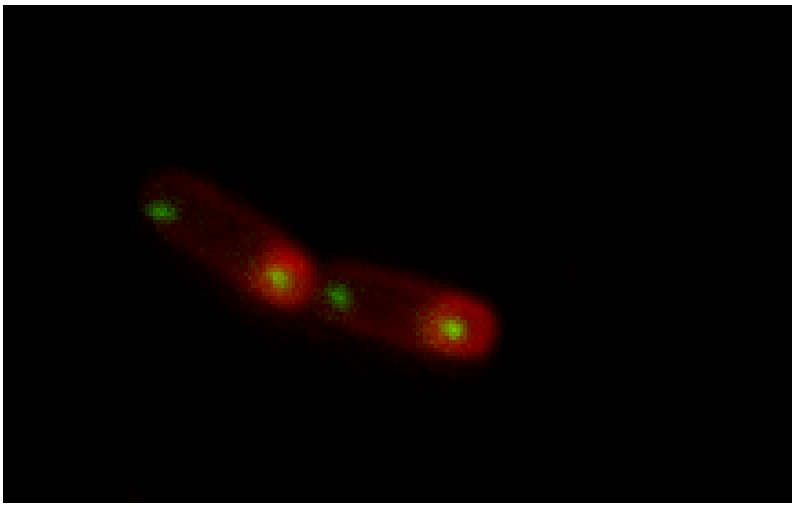

ROK LENARCIC

A THESIS SUBMITTED FOR THE DEGREE OF DOCTOR OF PHILOSOPHY
NEWCASTLE UNIVERSITY

JULY, 2011

Abstract

When conditions for growth are unfavourable, cells of *Bacillus subtilis* are able to enter sporulation cycle which leads to formation of highly resistant spores; dormant form of the organism that is able to survive harsh conditions and can germinate when environmental conditions are favourable for growth again.

Asymmetric division in the early stages of sporulation divides the sporulating cell into 2 unequal compartments; the bigger mother cell and the smaller prespore. Asymmetric septation also results in asymmetric chromosome distribution, with the prespore containing only about 30% of one chromosome at completion of septation, and the mother cell containing the rest of this chromosome plus one intact one. Although the programs of gene expression in the two compartments are different, each compartment contains one intact chromosome. This is crucial for the development of the spore and the viability of its progeny. Therefore dedicated systems are employed to ensure that one intact copy of the chromosome ends in the prespore, including conformational change of the chromosomes and attachment of the chromosomes to the cell poles,

In this work the cell division protein MinD (part of the 'Min' system) is shown to play an important role during the trapping of initial part of the chromosome into the prespore. Absence of MinD causes a trapping defect such that the chromosomal region surround the origin of replication (*oriC*) is excluded from the prespore, but the flanking regions to the left and right of *oriC* are segregated into the prespore.

Further analysis showed that this defect of the MinD mutants is not due to the loss of the Min function *per se*, or to possible over-replication of the chromosomes during sporulation in the absence of MinD. We also show that absence of DNA binding protein Soj can suppress this trapping defect of MinD, although the exact mechanism of the suppression is still unclear. We propose that during spore development Soj imposes some topological control over the *oriC* region of the chromosome to prevent its release from the quarter positions or/and its migration to the cell poles, and that this activity is counteracted by MinD.

Acknowledgements

I would like to thank everyone who contributed and helped me to finish my thesis. First, thanks to Jeff Errington for accepting me in his Institute and allowing me to work in this great environment. Thanks a lot to my great supervisors, Dr. Ling Juan Wu and Dr. Leendert Hamoen, for making my life in laboratory much easier and for all the great help, support, and discussing my results during my PhD and also for the great help while I was writing up the thesis. Thanks to Ian Selmes for regularly preparing and ordering all the media and reagents that I needed. I would like to thank all the past and present members of the lab, especially my friends Pamela, Katka, Elisa and Erkam for sharing the good and bad times in the lab, Patri for being 'the lab sunshine' and making me smile anytime I needed and also for useful suggestions and Jan-Willem, Heath and Robyn, Sven and Nadja for some strains and discussing my results.

Thanks a lot to my friends Michael and Clampits, David and Stan for a great time in Newcastle outside the lab during my spare time.

Many thanks to my friends at home for supporting me throughout my PhD and sharing a great time when I was back home and visiting me regularly in Newcastle, especially Nastja, Jure, Mitja and Rok. Hvala vam!!

And finally, thanks a lot to my little brother and my fantastic parents for all the support, help and visiting me in Newcastle. Most importantly, thank you for the financial support during the last year and a half to make it possible to finish my PhD. Hvala vam!!

Table of contents

List of figures

List of tables

Abbreviations

Table 1: List of abbreviations

ADP	adenosine diphosphate
amp	ampicilin
ATP	adenosine triphosphate
B. subtilis	*Bacillus subtilis*
CAA	casamino acids
chl	choramphenicol
CBB-G	Comassie Brilliant Blue stain
CFP	cyano fluorescent protein
DAPI	4,6-diamidino-2-phenylindole
dH_2O	deionised water
DMSO	dimethyl sulfoxide
DNA	deoxyribonucleic acid
DTT	Dithiothreitol
E. coli	*Escherichia coli*
EDTA	ethylenediaminetetraacetic acid
Erm	Erythromycin
et al.	*et alii* (and others)
GFP	green fluorescent protein

GDP	guanosine diphosphate
GTP	guanosine triphosphate
h	hour/hours
IPTG	isopropyl β-D-1-thiogalactopyranoside
kan	kanamycin
LiAc	lithium acetate
LB	Luria-Bertani broth
MBP	maltose binding protein
min	minute/minutes
MM	minimal medium
MOPS	3-(N-morpholino)-2-hydroxypropanesulphonic acid
NA	nutrient agar
neo	Neomycin
OD	optical density
ONPG	*ortho*-Nitrophenyl-β-galactoside
ori	origin of replication of the chromosome
PAB	Penassay broth
PAGE	polyacrylamide gel electrophoresis
PBS	phosphate buffered saline solutions

PCR	polymerase chain reaction
phl	Phleomycin
PMSF	phenylmethanesulfonylfluoride
PVDF	polyvinylidene fluoride
Q-PCR	quantitative polymerase chain reaction
RNA	ribonucleic acid
rpm	rounds per minute
SDS	sodium lauryl sulfate
SMM	Spizizen minimal medium
spec	Spectinomycin
S.pombe	*Schizosaccharomyces pombe*
SSC	sodium chloride – sodium citrate solution
ter	terminus of replication region of the chromosome
tet	tetracyclin
X-gal	5-bromo-4-chloro-3-indolyl-beta-D-galactopyranoside
YFP	yellow fluorescent protein

All chemicals are represented by standard symbols

Chapter 1: Introduction

1.1. *Model organism* Bacillus subtilis *and overview of its life cycle*

Bacillus subtilis is a rod shaped, Gram-positive bacterium of which the primary habitat is the upper layer of soil. In this ecosystem, *B. subtilis* experiences a wide variety of environmental changes and nutrient limitations. To survive in such an environment, *B. subtilis* has in its life cycle not only vegetative growth, but also sporulation; formation of highly resistant spores (Budde et al., 2006; Waites et al., 1970). In contrast to vegetative bacterial cells, spores can survive treatments that very efficiently kill vegetative bacterial forms; high temperatures (even 100°C), ionizing radiation, detergents, chemical solvents and hydrolytic enzymes (Nicholson et al., 2000). Spores can remain dormant for immense periods of time, according to some estimations even millions of years (Cano and Borucki, 1995; Vreeland et al., 2000).

Because sporulation is time and energy consuming and is an irreversible process, it is important to regulate this process precisely. The key switch in the transition from vegetative growth to sporulation is the transcription factor Spo0A. Activation of this master regulator is modulated by a wide variety of physiological signals such as cell density, DNA replication, DNA damage or nutrient availability (Errington, 2003; Levin and Grossman, 1998; Sonenshein, 2000; Stephenson and Hoch, 2002). Here the landmark event is asymmetric cell septation, which gives rise to two different cell compartments. The small compartment is called the prespore and the bigger compartment is called the mother cell. Expression of genes needs to be highly regulated in both compartments in order to complete the sporulation process successfully and release a mature spore that contains a full copy of genetic information (Hilbert and Piggot, 2004).

Under favourable environmental conditions, when the spore senses sugars or aminoacids, it can break its dormancy and resume growth. This process is called germination. At the end of the process, an actively growing cell that can continue vegetative growth is formed (Keijser et al., 2007). While vegetative cell grows, it duplicates its genetic material and forms division septum at midcell.

1.2. Vegetative growth and cell division

In an environment that offers enough nutrients, *B. subtilis* cells undergo vegetative growth; replication of a living cell. At the end of the division process, two identical daughter cells are produced, each inherits one full copy of the genetic material of the ancestor cell. The cell cycle of the vegetative growth can then repeat, as long as there are sufficient nutrients available for growth (Wang and Levin, 2009). During each cell cycle, the chromosome needs to undergo a single complete round of replication. Following replication, the sister chromosomes need to move apart to the quarter positions so that division can occur (Lee and Grossman, 2006; Pavlendova et al., 2007; Sharpe et al., 1998; Wu, 2004). In bacteria, these processes are coupled and need to be well coordinated. During chromosome segregation, the cell prepares for one important event; cell division (Figure 1.1), by assembling several proteins to form a multicomponent divisome (Errington et al., 2003; Sharpe et al., 1998). The central protein of divisome assembly is a tubulin-like protein FtsZ, which forms the so called Z-ring at the division site and serves as the scaffold for the assembly of most of the other essential components of the cell-division machinery (Errington et al., 2003).

It still remains unclear what the signal is for the cell to start a new replication cycle. Much work has been done with *E. coli* and many studies suggested that DNA

replication is coupled with increased cell mass (Boye and Nordstrom, 2003; Churchward et al., 1981; Wold et al., 1994). However, more recent data suggest that cell mass might not be the key signal for the cell to start the replication cycle (Bates and Kleckner, 2005).

Very recently, in *B. subtilis* a metabolic sensor controlling cell division has been discovered. This sensor couples nutrition availability with cell division. The main effector is glucosyltransferase UgtP that is part of the glucolipid biosynthesis pathway. UgtP localises to the division site in a nutrient-dependent manner; this means that the information about nutrition availability is transferred directly to the division machinery. UgtP inhibits assembly of FtsZ and it serves to maintain a constant ratio between FtsZ rings and cell length regardless of growth rate (Weart et al., 2007). Furthermore, some protein-protein interactions have been discovered that point to potential signalling pathways that could act to coordinate DNA replication with the global cell physiology (Noirot-Gros et al., 2002).

1.2.1. Cell Elongation

In rod shaped bacteria, it is important to maintain cell shape and to synthesise the correct amount of cell wall during growth, so that the whole area of the cell is protected by the cell wall. In order to achieve this, growth of cell wall must be coordinated properly together with the cell elongation and cell division, when at the new cell poles newly synthesised cell wall is needed. Tight coordination of these processes is needed to prevent cell lysis. This is because cell wall needs to be dynamic during the cell cycle, in the way that allows continuous synthesis, remodelling and

turnover (Claessen et al., 2008). Early research of cell wall synthesis demonstrated two models: one that is responsible for the sidewall cell wall synthesis during the cell elongation (Lederberg, 1957) and another one that is responsible for the synthesis of the cell wall during the cell division (Schwarz et al., 1969). Both processes also have employed specific penicillin binding proteins (Wei et al., 2003; Yanouri et al., 1993).

However, the main transglycosylase/transpeptidase that controls synthesis of new cell wall is PBP1, which is during the cell division relocated to the division site. To achieve this move, GpsB relocates PBP1 from MreC complex to the division site complex via a direct interaction with EzrA; a membrane bound protein at the division site (Claessen et al., 2008).

However, although cell wall protects cell from damage and osmotic lysis and was therefore thought to be essential, it is possible to construct bacterial strains without cell wall. Such viable bacterial cell is called L-form. Not much is understood yet about how L-forms divide, although there seems no need for FtsZ polymerisation in these strains (Leaver et al., 2009).

Cell shape is maintained by actin homologues - MreB and Mbl that form dynamic helical structures underneath the membrane (Jones et al., 2001; Vats and Rothfield, 2007). These helices are anchored to the membrane via interaction with membrane localised MreC and MreD (Divakaruni et al., 2007).

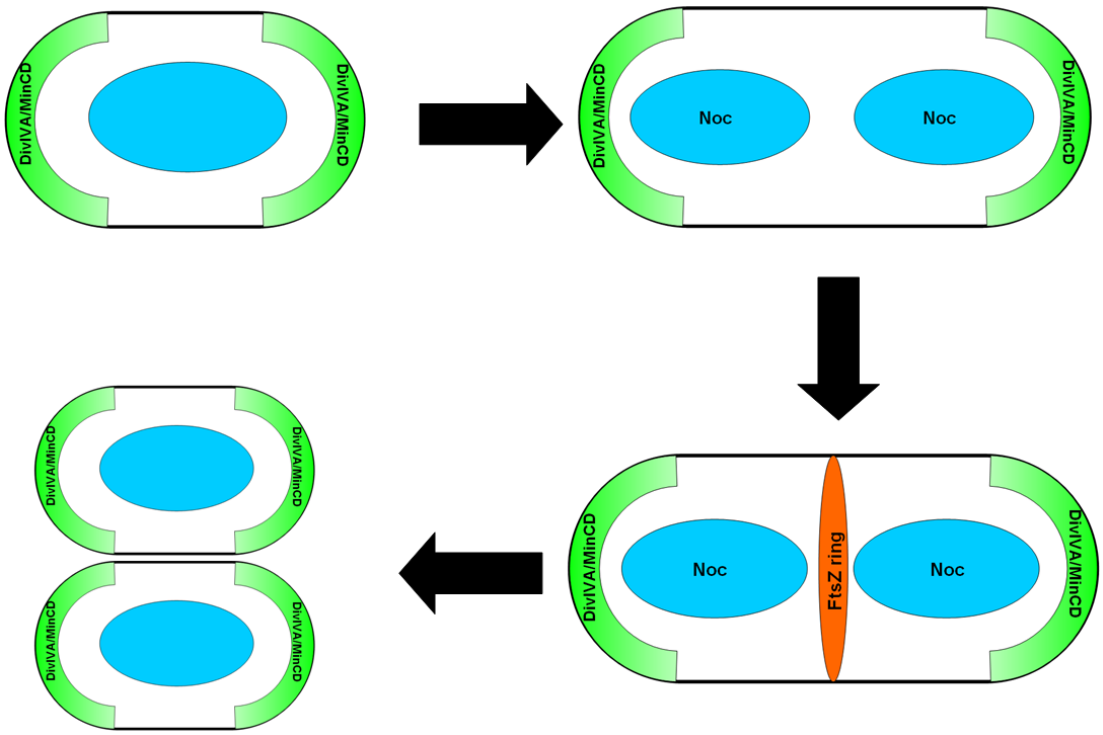

Figure 1.1: Vegetative growth of *B. subtilis*.
After the replication of the chromosomes, the division septum is formed at the midcell. Formation of the division septum is crucial and therefore spatially regulated by two mechanisms: Noc and Min. Noc prevents formation of the division septum at the vicinity of the chromosome and Min prevents septum formation at the cell poles. The combined effects of Noc and Min determine the mid-cell position as the site for the cell division. After a successful cell division, each of the two sister cells inherit a full copy of the genetic material.

1.2.2. Chromosome replication

Before cell division, the DNA of the cell has to be replicated to ensure one full copy of the genetic material is available for each daughter cell (Figure 1.1). DNA replication cycle is divided into three stages: initiation of replication, DNA elongation and termination of replication (Sherratt, 2003). Chromosome replication initiates from *oriC* (origin of replication) and proceeds bidirectionally (Berkmen and Grossman, 2006; Fuller et al., 1984; Matsui et al., 1985; Sharpe et al., 1998). It is carried out by a large multiprotein complex called replisome (Baker and Bell, 1998; Kelman and O'Donnell, 1995; Noirot-Gros et al., 2002). After elongation of the replicating chromosome when the two replication forks meet in the so called terminus region (*terC),* termination occurs. The *terC* is just opposite of the *oriC*. Termination of the chromosome replication is carried out by specific termination proteins (Bussiere and Bastia, 1999; Lewis et al., 1989; Lewis and Wake, 1991; Wake, 1997). The separation of newly replicated chromosomes begins well before DNA replication is completed (Sherratt, 2003).

The main initiator protein of DNA replication is DnaA (Messer et al., 2001; Moriya et al., 1990). It is a DNA binding protein that binds to DnaA boxes; sequence specific binding sites (Mott and Berger, 2007). DnaA boxes have been reported to be 9-pb repeat elements; DnaA binds with high affinity to sequence 5'-TTATNCACA-3' (Ishikawa et al., 2007; Schaper and Messer, 1995) but there are slight variations found in different DnaA boxes at the *oriC*. DnaA binding sites are well conserved among different bacterial species, but the arrangement and number of them might differ (Messer, 2002). *B. subtilis* has eight intergenic regions on which DnaA forms stable complexes (Ishikawa et al., 2007).

DnaA recognises specific sequence of a DnaA box by its domain IV at the C terminal end of the protein (Messer et al., 1999). Domain IV possesses DNA signature sequence that mediates recognition of the DnaA binding site on the chromosome and 'basic loop', which contains a conserved arginine that is crucial for DNA binding (Blaesing et al., 2000). Binding to the DNA sequence is stimulated by ATP (Fukuoka et al., 1990)

The DnaA-*oriC* complex opens double stranded DNA at the AT rich 13-bp long sequence left of the *oriC* (Krause et al., 1997). The DnaA protein not only binds to DNA at the *oriC* but also directs the assembly of other components of the replisome (assembly of proteins involved in the replication machinery complex). In *B. subtilis* these are DnaB (primosome subunit), DnaC (helicase), DnaD (primosome subunit), DnaE (DNA polymerase), DnaG (helicase) DnaI (primosome subunit), DnaN (DNA sliding clamp), DnaX (replisome subunit), HolA and HolB (both replisome subunits), PcrA (DNA helicase), PolC (DNA polymerase III) and PriA (primosome subunit) (Bruand and Ehrlich, 1995; Bruand et al., 1995; Noirot-Gros et al., 2002; Ogasawara et al., 1986; Sakamoto et al., 1995). Replication machinery, once assembled, is localised preferentially at midcell and the DNA template moves through this rather stationary polymerase complex (Lemon and Grossman, 1998).

Consistent with this model it has been shown that the *oriC* regions move towards the cell poles soon after initiation of DNA replication (Sharpe and Errington, 1999). When about 60 % of the chromosome is replicated, the division septum starts to form. At that time, the terminus region of the chromosome is still being replicated (Wu et al., 1995). After cell division, both copies of *oriC* are located at the midcell of the

newborn daughter cells and stay at this position most of the cell cycle till the next round of replication is initiated. The *terC* regions are located close to the newborn cell poles after cell division and then migrate to the midcell (Wu, 2004).

1.2.3. Positioning of the division septum

The placement of the division septum is crucial for successful cell division. Division septum has to be placed such that it does not damage the genetic material of the cell and also each of the sister cells needs to inherit one full copy of the chromosomes. To assure the accurate and correct placement of the division machinery, there are two distinct important mechanisms: the Min system and the nucleoid occlusion system (Barak and Wilkinson, 2007; Marston et al., 1998; Wu et al., 2009). Both of them are described in more detail below. The Min system inhibits formation of Z-ring at the cell poles (Adler et al., 1967; Marston and Errington, 1999b) and prevents formation of small anucleate minicells, while the nucleoid occlusion system acts to prevent formation of the FtsZ-ring in the vicinity of the nucleoid (Barak and Wilkinson, 2007; Wu and Errington, 2004). The protein in the nucleoid occlusion system is Noc, that associates with the chromosome. Deletion of both the *minCD* and *noc* genes in *B. subtilis* causes arrest of cell division and cells grow into long filaments. Fluorescence microscopy showed that double mutants fail to concentrate FtsZ at potential division site. Instead, FtsZ is more widely spread along the cell and it has difficulties polymerising into a productive Z-ring (Wu and Errington, 2004). Another protein required in placing division site is EzrA. It is important for correctly regulating the timing and positioning of FtsZ ring at the division site (Chung et al., 2007; Levin et al., 1999) and it has been shown to co-localise with FtsZ (Haeusser et al., 2004).

Noc also acts to co-ordinate cell division with DNA replication. FtsZ assembly can occur after a significant portion of the chromosome (~60 %) has been replicated (Wu et al., 1995). FtsZ starts to assemble at midcell once the bulk of the newly replicated chromosomes have been removed from the midcell position before completion of replication (Harry et al., 1999; Regamey et al., 2000).

1.2.3.1. The Min system

As mentioned above, the Min system is employed to prevent septation near the poles during vegetative growth (Barak and Wilkinson, 2007; de Boer et al., 1991). The Min system was discovered when the so called minicell mutants were observed in *E. coli* (Adler et al., 1967). These mutants often form septa near the cell pole instead of at midcell, leading to the formation of small spherical cells that lack DNA (Figure 1.2). The residual cell is longer than a normal cell and it contains two nucleoids (Rothfield et al., 2005). Further work led to the identification of the *minCDE* genetic locus, whose products, MinC, MinD and MinE, work together to prevent formation of division septum near the poles of the cell (de Boer et al., 1989). A division inhibitor of FtsZ ring formation is MinC that interacts with FtsZ and inhibits the assembly of the Z-ring with its C-terminal domain (Dajkovic et al., 2008; Hu et al., 1999; Shiomi and Margolin, 2007).

It has been shown that MinD is capable of binding and hydrolysing ATP. When ATP binds to MinD, it activates MinC (Hayashi et al., 2001). By Yeast two-hybrid experiments, it was shown that MinD interacts directly with MinC (and also with MinE) (Huang et al., 1996). MinD is also responsible for recruiting MinC to the membrane and for activating MinC by concentrating it at the cell poles. But the

positioning of MinC in *E. coli* is not static, as it oscillates between the poles of the cell with a period of about 50 seconds. Oscillation is driven by MinE protein, which is a topological specificity factor. Also MinE is recruited to the membrane by MinD. Next, MinE induces MinD and thereby MinC to oscilate between cell poles (Szeto et al., 2004; Zhou et al., 2005). In the presence of MinE, MinC and MinD are redistributed into a membrane associated polar zone, extending from the cell pole towards midcell (Hu and Lutkenhaus, 2001; Kruse et al., 2007; Raskin and de Boer, 1999a; Rowland et al., 2000). MinE polymerizes into the E-ring which acts to prevent the MinCDE polar zone from extending beyond midcell, thus preventing MinC from blocking division at the midcell position. The consequence of MinE mutation is blocked division throughout the cell and cells become filamentous (Shih et al., 2002). The biochemical basis for the oscillation of Min proteins in *E. coli* is the reversible binding of MinD to the membrane, a process that is regulated by MinE. MinD binds to the membrane through the C-terminus. This step requires ATP and oligomerization of MinD. The release from the membrane is then induced by MinE (Hu and Lutkenhaus, 2001; Lackner et al., 2003; Suefuji et al., 2002).

There are homologous proteins of MinD and MinC in many other bacteria (Nguyen et al., 2008; Ramirez-Arcos et al., 2001; Szeto et al., 2001). Both proteins are present in many Gram-negative and Gram-positive bacterial species and MinD shows a high degree of sequence conservation (Rothfield et al., 2005). *E. coli* and *B. subtilis* MinD share 44% identical residues. It is a member of a family of ATPases with diverse functions. This group of proteins also includes ParA and Soj, which are involved in plasmid and chromosome partitioning (Hiraga, 2000). Fluorescence microscopy indicates that most of the MinD protein in *B. subtilis* is located close to the cell

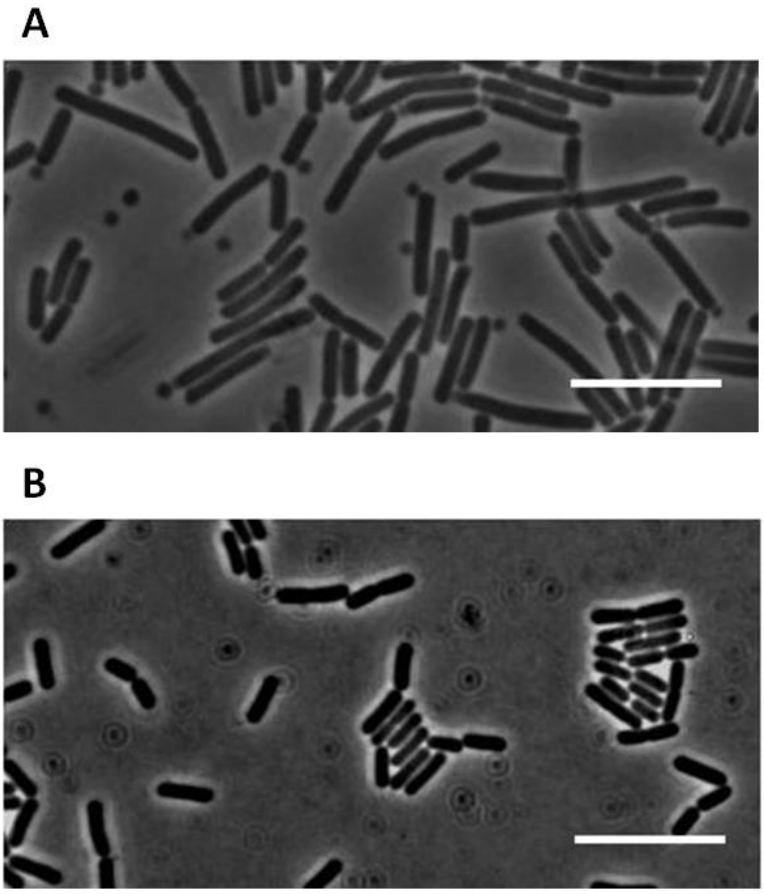

Figure 1.2: *minD* null mutant compared to wild type.
minD null mutant cells often form anucleate minicells at the cell poles and are considerably longer (A) than the wild type cells (B). Scale bar is 10 μm.

envelope which may suggest that it associates with the membrane (Marston et al., 1998).

The role of MinCD in *B. subtilis* cell division is similar to that in *E. coli*. It prevents polymerization of FtsZ near the poles of the cell (Gregory et al., 2008; Levin et al., 1998). One important difference between the *E. coli* and *B. subtilis* Min systems is that *B. subtilis* does not have a homologue of MinE. Instead, it has a functional homologue DivIVA. Like MinE in *E. coli*, DivIVA is a topological marker that determines the spatial activity zone of MinCD inhibitor in *B. subtilis*. It is widely distributed among Gram-positive species (Thomaides et al., 2001). In contrast to *E. coli* MinE that oscillates through the cell, DivIVA has no significant movement in *B. subtilis* cells (Edwards and Errington, 1997; Thomaides et al., 2001). DivIVA is concentrated at the cell poles during vegetative growth and also at the newly formed cell poles after cell division (Edwards and Errington, 1997; Marston et al., 1998) and has been shown to form a complex with FtsZ and MinD during the vegetative growth (Perry and Edwards, 2006). It has an important role in targeting the MinCD inhibitor complex of *B. subtilis* to the cell poles and to retain it at the cell poles (Marston et al., 1998). Barak et al. showed existence of lipid spirals in the cell membrane, consisting of anionic phospholipids. These lipid spirals are recognised by MinD. This indicates a higher organisation of regulation of FtsZ ring formation (Barak et al., 2008) and probably represent the mechanism by which MinD can control FtsZ ring formation.

Very recently, there was a new protein identified that is the link between MinD and DivIVA; MinJ (Patrick and Kearns, 2008). It interacts with both MinD and DivIVA

and is responsible for recruiting MinCD complex to the cell pole (Bramkamp et al., 2008).

After replication and segregation of chromosomes, the midcell region is free of MinCD and therefore FtsZ can assemble at this position. After completing Z-ring formation, and when the septum is almost complete, DivIVA is recruited to the midcell site, which in turn recruits MinCD to the newly formed septum, and therefore initiation of division close to the new septum is inhibited (Harry and Lewis, 2003; Marston and Errington, 1999b).

1.2.3.2. The Noc system

As it is important to prevent assembly of division machinery at the cell poles and producing minicells it is also important to prevent cell division over the nucleoid and to cause breakage of the chromosome. Therefore *B. subtilis* possess another very important system that negatively regulates assembly of FtsZ ring; the 'Noc' system or nucleoid occlusion system. The main player of this system is the Noc protein (YyaA), closely related to the Spo0J/ParB family of proteins. It binds to DNA and blocks cell division in the vicinity of the DNA (Sievers et al., 2002; Woldringh et al., 1990; Wu and Errington, 2004). Although first experiments suggested that Noc binds DNA non-specifically, very recent data revealed clear Noc-binding sequence; NBS. It is a 14-bp long inverted repeat with the sequence 5'-ATTTCCCGGGAAAT-3'. There are 74 NBS asymmetrically distributed on the chromosome of *B. subtilis*. Interestingly, there is no NBS around the replication terminus region which is probably important for temporal regulation of cell division (Wu et al., 2009). The exact mechanism of how

Noc works is still unclear, but it seems that its activity requires binding of Noc to DNA. It also remains unclear whether Noc inhibits assembly of division machinery by a direct interaction with FtsZ, as does its functional homologue in *E. coli*: SlmA (Bernhardt and de Boer, 2005). SlmA and Noc do not share any primary sequence homology, but they exhibit similar properties (Bernhardt and de Boer, 2005; Wu and Errington, 2004).

1.2.4. Forming the division septum

As already mentioned, the central protein of division septum is a cytosolic protein FtsZ; it assembles by polymerisation into a so called Z-ring in the cytosol at the division site and serves as a scaffold for assembly of all other proteins that are part of the division machinery. FtsZ is a homologue of tubulin and can be found in virtually all eubacteria, archaea and also in many eukaryotic organelles (Barak and Wilkinson, 2007; Lowe and Amos, 1998; Nogales et al., 1998; Rothfield et al., 2005; van den Ent et al., 2001). The protein is widely conserved among all those species (Osawa and Erickson, 2006). The similarity with tubulin is not only structural but they also share similar mechanism of polymerisation. This involves hydrolysis of GTP that is activated by a cation-coordinating loop. Experimental data showed that the GTP cap at the end of FtsZ polymer can stabilise it, but when the GTP is hydrolysed to GDP, the FtsZ polymer tends to disassemble rapidly (Rothfield et al., 2005; Scheffers et al., 2000). It has been shown for *E.coli* FtsZ that it can assemble into a Z-ring *in vivo* within 3 min and disassemble more rapidly, in 1 min (Sun and Margolin, 1998).

Peters at al. reported formation of FtsZ- helical patern along the entire cell which is then restricted to the centre of the cell prior to Z-ring formation. The dynamics and subunit exchange (dependent on GTP hydrolysis) probably play an important role before the helices restructure into a stable Z-ring (Peters et al., 2007). Once formed, the Z-ring is stable and persists for a considerable part of the cell cycle before it undergoes constriction (Weart and Levin, 2003).

Being on the top of hierarchy of assembly of the division machinery, FtsZ is required by all other proteins for their localisation to the division site. FtsA has been shown to localise with FtsZ prior to formation of the Z-ring, when they localise in a helical pattern (Peters et al., 2007). FtsA interacts directly with FtsZ and its role is probably to tether FtsZ to the membrane (Din et al., 1998; Yan et al., 2000). ZapA has been shown to be involved in recruitment of other cell division proteins to the division site (Gueiros-Filho and Losick, 2002). Gamba and colleagues showed that assembly of the divisome in *B. subtilis* takes place in two steps. In first step, the above mentioned proteins assemble (FtsZ, FtsA, ZapA and EzrA) and with the time delay of about 20 % of the cell cycle others are recruited to the division site. These include GpsB, FtsL, DivIB, DivIC, FtsW, Pbp2b and DivIVA (Gamba et al., 2009).

Very recently, discovery of a new cell division protein has been reported; SepF. It localises to the cell division septum and is employed in the later stage of septation. It has been shown to interact directly with FtsZ and is proposed to be involved in promoting Z-ring formation (Hamoen et al., 2006; Ishikawa et al., 2006; Singh et al., 2008).

Not much is known about the function of the other components of the divisome. FtsL, DivIB, DivIC and PBP-2B all have a single transmembrane span and a substantial extracellular domain (Errington et al., 2003). They might be involved in directing peptidoglycan synthesis machinery to the division site. FtsL is an essential part of division machinery that might be involved in regulation of cell division (Bramkamp et al., 2006; Sievers and Errington, 2000a). It has been shown to interact with FtsL-like protein DivIC (Sievers and Errington, 2000b), probably to stabilise it (Daniel et al., 1998; Sievers and Errington, 2000b). DivIC is required for proper septation (Katis et al., 1997; Levin and Losick, 1994; Sievers and Errington, 2000b). The role of DivIB could be to protect FtsL from degradation at higher temperatures (Daniel and Errington, 2000). Taken together, these 3 proteins might form some complex of which the main function is peptidoglycan-synthesis machinery (Errington et al., 2003). PBP 2B has a similar localisation pattern as the other 3 membrane proteins. It is a high-molecular-weight penicillin-binding protein that catalyses the late stages of peptidoglycan sythesis by introducing cross-links into septal peptidoglycan (Daniel et al., 2000).

1.3. The sporulation process of Bacillus subtilis

Living in soil, *B. subtilis* often faces harsh conditions and is lack of nutrients. To survive in such an environment it developed several different strategies; motility, chemotaxis, DNA uptake or transformation, production of antibiotics and sporulation. Sporulation (Figure 1.3) is an ultimate escape in order to survive as it requires huge amounts of energy and it takes a long time. Also, it requires a high density of cells rather than a low density of cells when cell growth is favoured. The decision to

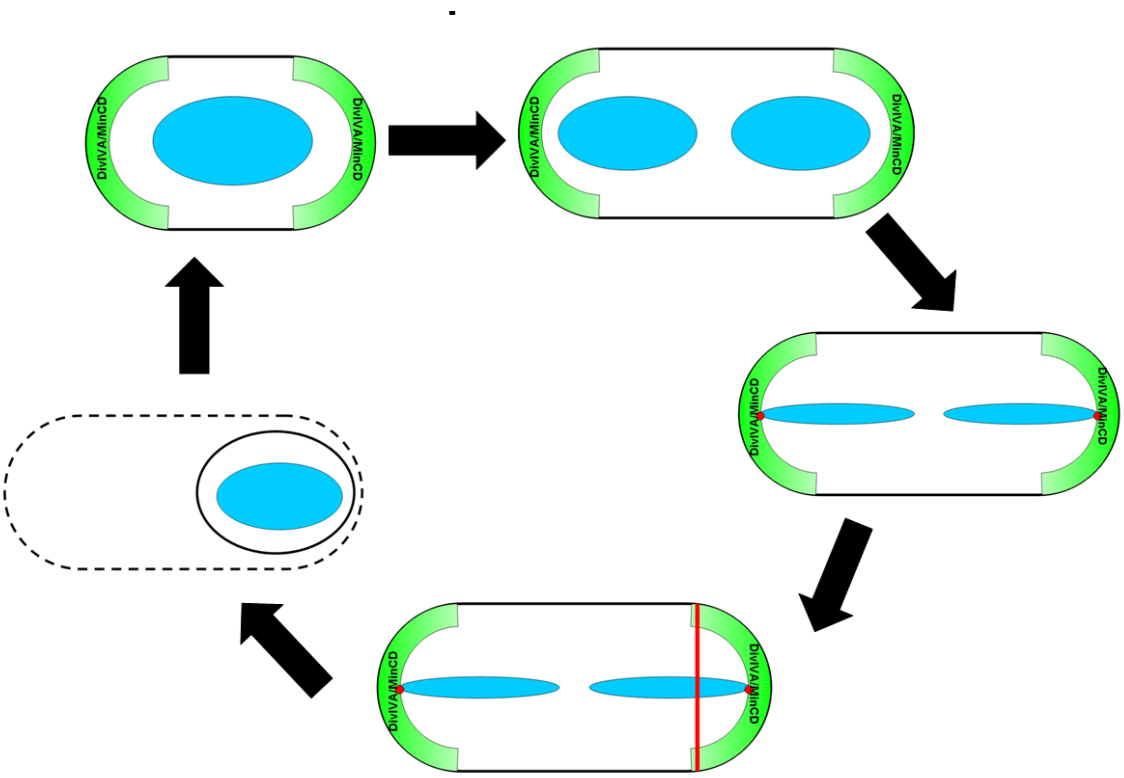

Figure 1.3: Sporulation process of *B. subtilis.*
Each cell that is going to sporulate has to complete replication of its chromosome. After replication, chromosomes adopt a new conformation; axial filament. Both chromosomes are attached to the cell pole with their *oriC* regions. This is followed by the formation of the asymmetric septum such that it traps 30 % of the chromosome in the prespore. The remaining part is then exported from the mother cell into the prespore. After the engulfment of the membrane, the spore coat is constructed and the spore is released by the lysis of the mother cell.

sporulate can only be made at certain stage of cell cycle, this is in stationary phase (Grossman and Losick, 1988).

1.3.1. Initiation of sporulation

Once initiated, the time and energy consuming sporulation process is irreversible. It is also lethal for all cells that are unable to complete the process once it has been initiated and therefore it is very important for sporulation to be tightly regulated. Although probably the most common signal for sporulation initiation is nutrient starvation, there is no single nutritional effect acting as a stimulus. Instead, *B. subtilis* possesses a complex decision-making apparatus that can sense a huge range of external and also internal signals. All those signals act on the phosphorylation of the master transcriptional regulator for entrance into sporulation, Spo0A (Burbulys et al., 1991). The pathway that phosphorylates Spo0A is called 'phosphorelay' and involves two intermediates (Spo0F, Spo0B) which are phosphorylated prior to Spo0A. They are phosphorylated by kinases (KinA, KinB, KinC, KinD, KinE), each of them responding to different environmental, cell cycle or metabolic signals. The phosphorylated form of Spo0A is an essential positive regulator of sporulation which activates directly or indirectly several hundred sporulation genes (Fawcett et al., 2000). Most important of these involves the formation of polar septum (Levin and Losick, 1996) and sporulation-specific genes such as *spoIIA*, *spoIIE* and *spoIIG* (Stragier and Losick, 1996).

1.3.2. Chromosome replication

Initiation of sporulation is coupled with DNA replication, because each sporulating cell needs two full copies of their genetic material. The key protein coupling the replication of the DNA and sporulation initiation is Sda (suppressor of DnaA) (Burkholder et al., 2001; Veening et al., 2009). It is a checkpoint that is activated directly by DnaA, the key protein in chromosome replication initiation (Burkholder et al., 2001). DnaA binds to the *sda* promoter to activate it (Ishikawa et al., 2007). Sda serves as a genetic timer allowing Spo0A~P to reach the required level to initiate sporulation. It can indirectly inhibit the primary kinases of the phosphorelay.

Recently, Murray and Errington showed that Soj is involved in controlling DnaA, the DNA replication initiator. The two proteins can interact directly. Soj acts as a spatially regulated molecular switch that can activate or inhibit initiation of DNA replication via DnaA. By interacting with DnaA, Soj causes over-replication of the chromosomes and consequently inhibits sporulation by activating the DNA replication initiation checkpoint protein Sda (Murray and Errington, 2008).

Chromosome replication is a crucial event prior to successful sporulation. Both full copies of the chromosome need to be without any damage. One copy is destined to move into the prespore and the other remains in the mother cell. This is important because sporulation specific proteins that are involved in maturation of the endospore are expressed from both copies of the chromosome; some are active in the mother cell, others are active in the prespore (Ireton and Grossman, 1994).

Chromosome replication starts at the *oriC* of the chromosome (origin of replication). DnaA protein binds to the region of the chromosome around *oriC* and by assembling

into a homo-oligomer it mediates open complex formation. This then allows assembly of the initiation complex followed by recruitment of all the other components of the replisome; the protein complex that leads replication of the chromosome (see chapter 1.2.2.). It has been shown that mutations in many of the Dna proteins required for initiation of DNA replication (DnaA, DnaB, DnaD) inhibit sporulation (Lemon et al., 2000). This is done through a replication initiation checkpoint that works via Sda. Sda can inhibit the histidine protein kinase KinA, that activates phosphorelay patway by phosphatising Spo0F (Burkholder et al., 2001).

1.3.3. Remodelling of the chromosome at the onset of sporulation

Soon after chromosomes are replicated and the sporulation initiated, the nucleoids undergo a conformational change from its normal compact shape to an elongated form called axial filament (Ben-Yehuda et al., 2003; Ryter et al., 1966; Wu, 2004). As a result, the chromosomes extend from one pole to the other. Formation of the axial filament is accompanied by movement of the *oriC* region towards the cell poles (Figure 1.3). This is important, because it is followed by formation of an asymmetric septum so that 30 % of the chromosome is trapped in the prespore (Graumann and Losick, 2001).

Work of Thomaides et al. has shown the importance of the DivIVA protein in the process of anchoring the axial filament to the cell pole. During the vegetative growth, DivIVA is in a complex with FtsZ and MinD, but the topological change allows DivIVA to form a complex with Spo0J during the sporulation. This interaction with the chromosome segregation machinery helps to position the *oriC* at the outer edge of

the chromosome to the cell pole (Perry and Edwards, 2006), which is one of the possible mechanisms allowing extraction of the chromosome from the quarter positions. DivIVA is a cell pole determinant localised at the cell poles during vegetative growth and also during sporulation (Perry and Edwards, 2004). It maintaines its polar localization during sporulation and does not localise to the asymmetric septum (Thomaides et al., 2001).

The chromosome segregation machinery that anchors axial filament to the cell poles consist of DNA-binding proteins (Figure 1.4); these proteins are Spo0J (homologue of partitioning ParB protein), Soj (homologue of partitioning ParA protein) and RacA (functions as a kinetochore) and they act together with DivIVA to deliver the *oriC* region of the chromosome to the cell pole (Lee and Grossman, 2006; Pavlendova et al., 2007; Perry and Edwards, 2006; Wu and Errington, 2003).

Soj (ParA) and Spo0J (ParB) are in the *par* operon; a well studied partitioning system that can be found in many bacteria. It is often encoded by low-copy number plasmids to ensure accurate plasmid partitioning (Williams and Thomas, 1992). The well conserved *par* system consists of ParA – a Walker type ATPase that binds DNA, ParB – a DNA binding protein that interacts with ParA, and ParS – the site bound by ParB (Gerdes et al., 2000).

Spo0J (ParB) of *B. subtilis* has eight binding sites on the chromosome in about 1 Mbp region around the *oriC* region (Lin and Grossman, 1998) and two more distant sites (Breier and Grossman, 2007). Spo0J molecules form condensed discrete foci in the presence of Soj, by condensing the region of the chromosome around the *oriC* (Autret

and Errington, 2003; Lee et al., 2003). To achieve this, it seems that dynamic behaviour of Soj is important (Marston and Errington, 1999a). Condensed Spo0J foci then migrate to the extreme poles of the cell to ensure that *oriC* is captured in the prespore when the asymmetric septum is formed. Spo0J also plays a role in orientation of the chromosome during vegetative growth and sporulation (Glaser et al., 1997; Ireton et al., 1994).

However, Soj and Spo0J are not sufficient for this process. There is another protein that is employed in anchoring the chromosomes to the cell pole: RacA (for Remodelling and Anchoring of the Chromosome) (Figure 1.4). RacA is expressed specifically only in the early stage of sporulation. It preferentially binds to 25 GC rich binding sites around the origin region (612 kb) (Ben-Yehuda et al., 2005). When bound to DNA, RacA forms a highly stable DNA-protein complex, which is targeted to the cell pole in a DivIVA-dependent manner (Ben-Yehuda et al., 2005). Mutations in RacA cause twofold decrease in DNA trapping into the prespore compartment. Cells often form prespores without or with very little DNA, but if they contain DNA, they continue to sporulate normally (Ben-Yehuda et al., 2003; Wu and Errington, 2003). In addition, many of RacA mutant sporangia with empty prespores undergo a second round of polar division, because when there is no DNA in prespore, there cannot be gene expression in the prespore compartment which is required for the continuation of the sporulation process. It has been suggested that, when RacA binds to DivIVA, it displaces MinCD from DivIVA (Ben-Yehuda et al., 2003). RacA seems to be important also for formation of the axial filament (Figure 1.3).

1.3.4. Asymmetric septum formation

The movement of the *oriC* region of the chromosome close to the cell pole is followed by the formation of an asymmetric septum (Errington, 2003; Graumann and Losick, 2001), which divides the sporulating cell into the small prespore and the large mother cell compartment (Figure 1.3). Since the axial filament extends from one pole to the other, formation of the asymmetric septum traps about 30% of one of the chromosomes into the prespore. This part of the chromosome includes the *oriC* region (Wu and Errington, 1994). The rest of the chromosome is translocated from the mother cell into the prespore by the SpoIIIE protein (Wu and Errington, 1994) (Figure 1.4). This protein forms a pore in the septum and its C-terminal part is capable of tracking along DNA in an ATP-dependent manner. The mislocated segment of chromosome is then transported in the prespore (Bath et al., 2000; Bogush et al., 2007). This process is described in more detail in section 1.3.5..

Most of the division proteins involved in asymmetric septation during sporulation are similar to those in vegetative growth of *B. subtilis* (Errington et al., 2003). One important difference is that the formation of an asymmetric septum during sporulation takes place before chromosome segregation is completed. In contrast to septum formation during the vegetative growth where the 'Noc' system prevents formation of the septum over the nucleoid, asymmetric septum is formed over the nucleoid (Figure 1.4). Correct positioning of the sporulation septum is dependent on Spo0A and σ^H (Ben-Yehuda and Losick, 2002) Spo0A is required for the switch of the division site from midcell to the cell pole. It controls migration of the Z-ring from the midcell, where it is assembled, to the polar site (Ben-Yehuda and Losick, 2002). After assembly at the midcell, the Z ring disassembles and form spirals towards the cell

poles. Formation of the spirals is an intermediate prior to asymmetric septum formation. Higher amounts of FtsZ and active SpoIIE are required in this process. The switch is not well understood yet, as well as how the activities of Min and Noc systems are overcome (Errington, 2003).

The important role of MinCD complex has been shown also during the asymmetric septum formation. It inhibits asymmetric septation at the midcell position, because cells lacking MinCD show formation of the thin septa during the sporulation not only at the cell pole, but also at the midcell (Barak et al., 1998). However, the asymmetric septum formed during sporulation is much thinner than the cell division septum during vegetative growth, possessing less cell-wall material. Moreover, most of the peptidoglycan separating the two lipid bilayers in the asymmetric septum is removed soon after septation is completed. This is probably important because communication (signal transduction) between the two compartments is needed during sporulation (Sharp and Pogliano, 1999).

1.3.5. Chromosome transfer into the prespore and the SpoIIIE protein

As mentioned, the asymmetric septum is formed so that it traps about 30 % of the chromosome in the prespore. The remaining 70 % is exported from the mother cell by DNA exporter SpoIIIE (Wu and Errington, 1994). SpoIIIE is a homologue of the *E.coli* FtsK protein. They both belong to a group of conserved DNA transporters (Barre, 2007). The protein is anchored to the membrane by very hydrophobic N-terminus (Wang and Lutkenhaus, 1998). The hydrophilic C-terminus lies in the

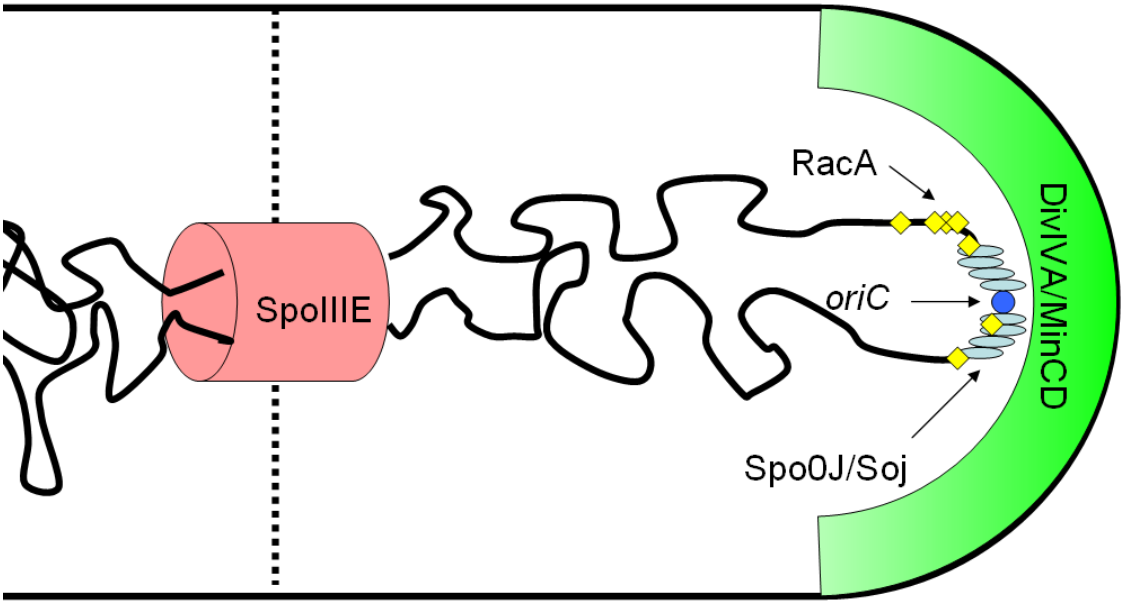

Figure 1.4: Proteins involved in chromosome segregation during sporulation. Spo0J and Soj act together to condense regions of the chromosome around *oriC* to form a compact structure which is then anchored to the cell pole through RacA, another DNA binding protein. RacA attaches chromosome to the cell pole in a DivIVA dependant manner. After asymmetric septum formation, one third of the chromosome is already trapped in the prespore, the remaining part is then exported from the mother cell into the prespore by SpoIIIE DNA translocase, assembled in the asymmetric septum.

cytoplasm and is responsible for translocation along the DNA molecule in an ATP dependent manner (Bath et al., 2000).

SpoIIIE protein assembles in the middle of the asymmetric septum to form functional exporter in the mother cell, from where it exports DNA into the prespore (Becker and Pogliano, 2007; Wu and Errington, 1997). The mechanism that dictates in which compartment SpoIIIE exporter assembles is chromosome polarity (Becker and Pogliano, 2007) and the position of the *oriC* region of the chromosome. Sharp and Pogliano also showed that in the absence of MinCD, SpoIIIE can be assembled in the prespore rather than in the mothercell side of the asymmetric septum, causing DNA to be exported from the prespore into the mother cell (Sharp and Pogliano, 2002). To ensure that DNA is exported only from the mother cell into the prespore, both mechanisms are needed: the presence of MinCD inhibitor to repress SpoIIIE assembly in the prespore, and polarity of DNA molecule (Ptacin et al., 2008). During the sporulation, each of the chromosome arms is transported through the independent SpoIIIE channels simultaneously (Burton et al., 2007).

During translocation of the chromosome into the prespore, all the DNA bound proteins are stripped off the chromosome. This includes RNA polymerases, transcription factors, proteins employed in remodelling of the chromosome. This is done by the ATPase domain of the SpoIIIE translocase. The fact that the chromosome enters the prespore naked probably helps to reprogram the prespore specific gene expression (Marquis et al., 2008).

Because SpoIIIE forms a pore in the septum, it needs to allow only movement of the DNA but not movement of the other molecules such as sigma factors. Wu and Errington reported 2 classes of mutants in *spoIIIE*; class I mutants that affect only DNA transfer through the pore and class II mutants, that cannot export DNA and also cannot prevent σ^F to appear and be active in the mother cell (Wu and Errington, 1994).

SpoIIIE is also involved in the latest stage of chromosome segregation, separation of the chromosome termini (Bogush et al., 2007). During sporulation, only a single chromosome terminus region can be detected in the cell, although the engulfment of the spore has already begun. When the engulfment process is nearly completed, the second chromosome terminus region can be detected in the prespore. Although the chromosome replication is presumably finished, the two chromosome terminus regions remain together until segregated by SpoIIIE (Bogush et al., 2007).

SpoIIIE has been reported to play also an important role that is distinguished from DNA transfer. It is involved in fusion of the membranes at the cell apex to finish the engulfment process of spore maturation (Sharp and Pogliano, 1999).

1.3.6. Prespore specific gene expression

Formation of the asymmetric septum divides cell into the prespore and the mother cell compartments. Compartmentalisation of the sporulating cell allows activity of different sigma factors in each compartment and expression of different genes (Errington, 1993). Prior to asymmetric septation there are two sigma factors

synthesised in the cell, σ^E and σ^F (Gholamhoseinian and Piggot, 1989; Partridge and Errington, 1993). Both are held in an inactive form until the septum is formed. Once the asymmetric septum is formed, the σ^F in the prespore becomes active first (Figure 1.5). Its activation depends on anti-sigma factor SpoIIAB and anti-anti-sigma factor SpoIIAA (Schmidt et al., 1990). SpoIIAB is a protein kinase that interacts with and phosphorylates SpoIIAA. SpoIIAA displaces σ^F from the SpoIIAB- σ^F complex prior to accepting phosphate from the SpoIIAB (Duncan and Losick, 1993; Min et al., 1993; Wu et al., 1998). To dephosphorylate phosphorylated SpoIIAA, SpoIIE is needed with its phosphatase activity. SpoIIE is a membrane bound serine protease, localised to the asymmetric septum. It is probably responsible for the timing and localization of σ^F activation in the prespore (Arigoni et al., 1996; Barak et al., 1996; Duncan et al., 1995; Feucht et al., 2002). Once in an active form, σ^F activates some important *spo* loci among which are *spoIIR* (required for activation of σ^E in the mother cell) (Karow et al., 1995) and *spoIIIG* (late prespore specific sigma factor σ^G) (Sun et al., 1991).

Following the activation of σ^F in the preposre, σ^E is activated in the mother cell (Figure 1.5) by a complex mechanism which is not yet fully understood. Inactive σ^E is activated by proteolytic processing by SpoIIGA; a serine protease. SpoIIGA requires activity of SpoIIR that is controlled by σ^F and secreted from the prespore. This inter-compartmental signalling is crucial for the activation of σ^E. Active σ^E then establishes different programme of gene expression than σ^F in the prespore. It activates genes required for engulfment of the prespore by the mother cell and also genes that are blocking another, second asymmetric division in the mother cell (Eichenberger et al., 2001; Feucht et al., 2003). This is important because cells with disporic phenotype are

unable to finish the sporulation process and therefore they lyse (Illing and Errington, 1991a).

1.3.7. Engulfment of the prespore

Engulfment of the prespore is the process that results in prespore being entirely surrounded by the mother cell. It begins with degradation of cell wall material in the asymmetric septum. At the end of the process, the two edges of the septal membranes migrate around the prespore to meet at the apex of the cell (Illing and Errington, 1991a). This process requires SpoIID, SpoIIM and SpoIIP, the expression of all of them is σ^E dependent (Frandsen and Stragier, 1995; Rong et al., 1986; Smith and Youngman, 1993). They migrate around the prespore at the leading edge of migrating membranes. All three proteins have transmembrane and extracytoplasmic domains (Errington, 2003). Although the englufment process is initiated in the mother cell, not all the proteins required for the engulfment are expressed form the mother cell. One important protein expressed in the prespore by σ^F is SpoIIQ, which is required for membrane fusion (Londono-Vallejo et al., 1997). Together with above mentioned proteins, the SpoIIIE also migrates from the septum to the apex of the cell where it has been shown to play a role in membrane fusion (Sharp and Pogliano, 1999). When membranes fuse, the engulfment process is completed and detached prespore is released in the mother cell.

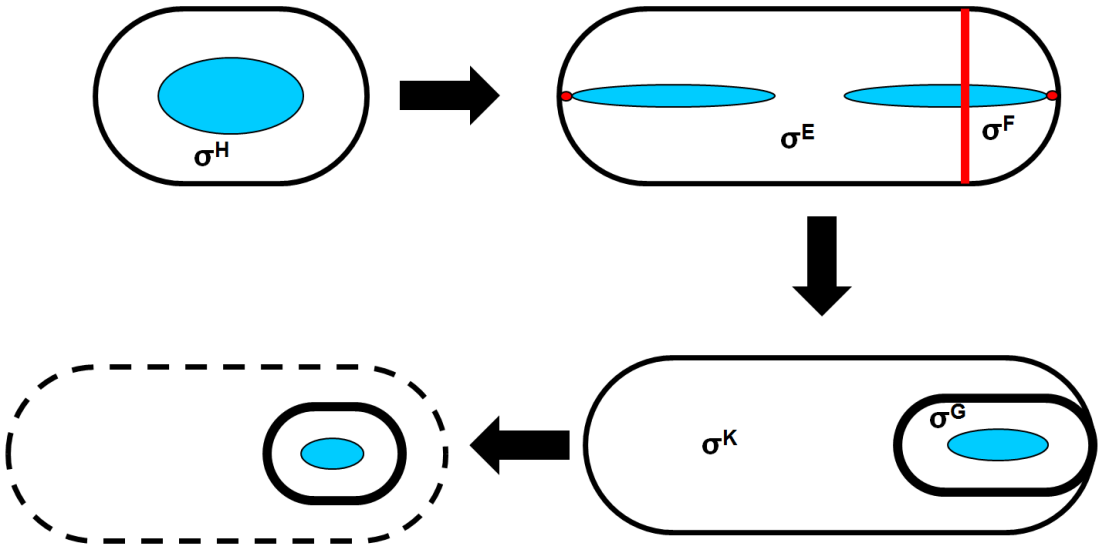

Figure 1.5: Sigma factors controlling the sporulation process.
After initiation of sporulation (σ^H), chromosomes are anchored to the cell poles, followed by formation of the asymmetric septum, which divides the sporulating cell in two compartments: the smaller prespore and the bigger mother cell. In the prespore, σ^F become active while in the mother cell σ^E. When the prespore is engulfed, the σ^G become active in the prespore and σ^K in the mother cell, to encapsulate the prespore. When the process is finished, the mother cell lyses and the mature spore is released.

1.3.8. Prespore maturation and release of the spore

After the prespore is engulfed by the mothercell, the next sporulation specific sigma factor becomes active in the endospore: σ^G (Sun et al., 1989) followed by σ^K in the mothercell (Figure 1.5). Both, σ^G and σ^K are responsible for expression of the genes that are required for endospore maturation to the final stage when it is released from the mothercell. The synthesis of the late transcription factor σ^G in the prespore is directed by σ^F and synthesis of the late transcription factor σ^K in the mothercell is directed by σ^E (Sun et al., 1991). Soon after the engulfment process is completed, the *spoIIIG* gene is transcribed encoding σ^G. The activation of σ^G is complex and not yet fully understood, but it seems to be coupled to the engulfment process (Sun et al., 2000). The timing of activation is very important, because it can direct transcription of its own gene (Sun et al., 1991). σ^G undergoes posttranslational regulation by SpoIIIJ, SpoIIAB and products of *spoIIIAA* operon (Coppolecchia et al., 1991; Errington et al., 1992; Illing and Errington, 1991b).

Soon after the activation of σ^G in the prespore, σ^K gets active in the mother cell. It is synthesised as an inactive precursor, pro- σ^K. In its activation, intercompartmental signalling is important and it seems that activation takes place next to the membrane. In the prespore, SpoIVB is expressed by σ^G (Cutting et al., 1991a). It is inserted into the inner membrane of the prespore where it undergoes autoproteolysis and releases signalling fragment that difuses across the membrane into the mother cell to interact with σ^K activation complex. This complex is inserted in the outer prespore membrane (Rudner and Losick, 2002; Wakeley et al., 2000). The σ^K activation complex consists of SpoIVFA (inhibitor of pro- σ^K processing), SpoIVFB (enzyme that cleaves the prosequence from pro- σ^K) and BofA (another inhibitor of pro- σ^K processing)

(Cutting et al., 1991b; Ricca et al., 1992). SpoIVFA brings SpoIVFB and BofA to the prespore outer membrane where SpoIVFB cleaves the prosequence from the pro- σ^K. The cleavage process is negativelly regulated by both, SpoIVFA and BofA (Rudner and Losick, 2001, 2002).

Active σ^K is responsible for expression of genes involved in the spore coat formation (14 *cot* genes) and spore maturation genes (*spoVD, spoVK*) (Daniel et al., 1994; Fan et al., 1992; Henriques and Moran, 2000).

The spore cortex and coat need to become highly resistant in order to protect the genetic material. The spore coat of *B. subtilis* spores consists of two layers; the thinner inner layer and the thicker outher layer. High resistance of the coat is reached by synthesizing low-molecular-weight proteins to coat the DNA molecule inside the spore. Proteins that are rich in tyrosine and cysteine represent the large majority of coat components, but there are also minor amounts of carbohydrates and lipids. All the components are added to the coat in a multistep assembly process which then results in a complex structure of the coat (Hiragi, 1972; Warth et al., 1963). Many of the proteins undergo later modifications, such as various cross-linking. Proper assembly and cross-links play an important role later in germination of the spore (Aronson and Fitz-James, 1976). The coat, consisting of Cot proteins, is attached to the spore membrane via SpoIVA and SpoVID proteins (Driks et al., 1994).

After completion of the spore coat, the mother cell lyses and the spore is released. The coat protects spore, but there are also other mechanisms of protection. Resistance to heat has not much to do with the protective coat, but more with dehydrated state of the spore core (Popham et al., 1996). Again, also chromosome resistance against UV

depends more on small acid soluble proteins that are bound to DNA molecule (Setlow, 1995)

Important feature of the spore coat is the ability to alow penetration of small molecules such as sugars or amino acids. This is crucial for the initiation of germination, so that the spore can sense nutrients in the environment (Moir, 1981; Moir et al., 1994).

Aims

The aims of this study were to confirm and understand more the chromosome trapping defect that can be observed in *minD* null mutants during the early stage of sporulation.

Polar attachment of the chromosomes during the early stage of sporulation involves many different proteins. To understand the function of MinD, we wanted to study interactions between those proteins that are involved in this process, to identify interacting partners that work together with MinD in chromosome segregation during sporulation.

Chapter 2: Methods

2.1. Lists of strains, oligonucleotides and plasmids used

Table 2: List of strains used in this study

Strain	Relevant genotype	Source/Construction
***Bacillus subtilis* strains**		
168	*trpC2*	(Burkholder and Giles, 1947)
1272	*trpC2*Δ*racA*::erm	L Wu, unpublished
1273	*trpC2*Δ*racA*::spec	(Wu and Errington, 2003)
1274	Δ*divIVA::catΩ(yoaVW::spoIIQ-lacZ tet) chr::pSG1850 (divIVA13 tet) (N99D)*	(Wu and Errington, 2003)
1901	*trpC2* Ω(*minD::ermC*)1901	(Edwards and Errington, 1997)
1920	*trpC2 amyE Ω(minD::ermC)1901 Ω(divIVA::tet)1042*	(Marston et al., 1998)
2640	*trpC2* Δ*spo0J::spec*	(Autret et al., 2001)
2641	*trpC2spo0J-gfpmut1-neo*	(Autret et al., 2001)
36.3	*trpC2 spoIIIE36*	(Piggot, 1973)
3309	*trpC2* Δ*minCD*::kan	L Hamoen, unpublished
3381	*trpC2* P_{minC} Δ*minC minD ΩKanR*	L Hamoen, unpublished
HM31	*trpC2* Δ*soj*Δ*spo0J::*tet	(Murray and Errington, 2008)
HM36	*trpC2 sojD40A*::neo	(Murray and Errington, 2008)
HM40	*trpC2* s*ojG12V*::neo	(Murray and Errington, 2008)
HM41	*trpC2* Δ*spo0J*::neo	(Murray and Errington, 2008)
HM161	*trpC2* Δ*soj*::neo	(Murray and Errington, 2008)

HM302	*trpC2 Δsoj::neo (dnaA(S326L)*P_{spac}*-dnaN)::erm*	(Murray and Errington, 2008)
HM336	*trpC2 Δsoj::neo amyE::spec(*P_{xyl}*-soj)*	(Murray and Errington, 2008)
JWV017	*amyE*::P_{spoIIA}-*mCherry*-Chl, P_{dnaX}-*dnaX*-*yfp*-spec	(Veening et al., 2009)
JWV128	Δ*sda*::tet	(Veening et al., 2009)
KS32	Δ*lacA*::chl	K Surdova, unpublished
RD021	Δ*minJ*::tet (Δ*yvjD*::tet)	(Bramkamp et al., 2008)
4732	*trpC2 spoIIIE36* P_{qpr} - *lacZ*-chl at *amyE*	(Wu and Errington, 2003)
4733	*trpC2 spoIIIE36* P_{qpr} - *lacZ*-chl at *jag*	(Wu and Errington, 2003)
4734	*trpC2 spoIIIE36* P_{qpr} - *lacZ*-chl at *spoIID*	(Wu and Errington, 2003)
4735	*trpC2 spoIIIE36* P_{qpr} - *lacZ*-chl at *yxaM*	(Wu and Errington, 2003)
RL 1	*trpC2 spoIIIE36* P_{qpr} - *lacZ*-chl at *amyE*, Δ*minD*::erm	Δ*minD*::erm from 1901 transformed into 4732
RL 3	*trpC2 spoIIIE36* P_{qpr} - *lacZ*-chl at *jag*, Δ*minD*::erm	Δ*minD*::erm from 1901 transformed into 4733
RL 4	*trpC2 spoIIIE36* P_{qpr} - *lacZ*-chl at *spoIID*, Δ*minD*::erm	Δ*minD*::erm from 1901 transformed into 4734
RL 5	*trpC2 spoIIIE36* P_{qpr} - *lacZ*-chl at *yxaM*, Δ*minD*::erm	Δ*minD*::erm from 1901 transformed into 4735
RL 6	*trpC2 spoIIIE36* P_{qpr} - *lacZ*-chl at *amyE*, Δ*minCD*::kan	Δ*minCD*::kan from 3309 transformed into 4732
RL 8	*trpC2 spoIIIE36* P_{qpr} - *lacZ*-chl at *jag*, Δ*minCD*::kan	Δ*minCD*::kan from 3309 transformed into 4733
RL 9	*trpC2 spoIIIE36* P_{qpr} - *lacZ*-chl at *spoIID*, Δ*minCD*::kan	Δ*minCD*::kan from 3309 transformed into 4734
RL 10	*trpC2 spoIIIE36* P_{qpr} - *lacZ*-chl at *yxaM*, Δ*minCD*::kan	Δ*minCD*::kan from 3309 transformed into 4735
RL 11	*trpC2 spoIIIE36* P_{qpr} - *lacZ*-chl at *amyE*, Δ*minC*::kan	Δ*minC*::kan from 3381 transformed into 4732
RL 13	*trpC2 spoIIIE36* P_{qpr} - *lacZ*-chl at *jag*, Δ*minC*::kan	Δ*minC*::kan from 3381 transformed into 4733

RL 14	*trpC2 spoIIIE36* P_{qpr} - *lacZ*-chl at *spoIID*, Δ*minC*::kan	Δ*minC*::kan from 3381 transformed into 4734
RL 15	*trpC2 spoIIIE36* P_{qpr} - *lacZ*-chl at *yxaM*, Δ*minC*::kan	Δ*minC*::kan from 3381 transformed into 4735
RL 16	*trpC2 spoIIIE36* P_{qpr} - *lacZ*-chl at *amyE*, Δ*racA*::erm	Δ*racA*::erm from 1272 transformed into 4732
RL 18	*trpC2 spoIIIE36* P_{qpr} - *lacZ*-chl at *jag*, Δ*racA*::erm	Δ*racA*::erm from 1272 transformed into 4733
RL 19	*trpC2 spoIIIE36* P_{qpr} - *lacZ*-chl at *spoIID*, Δ*racA*::erm	Δ*racA*::erm from 1272 transformed into 4734
RL 20	*trpC2 spoIIIE36* P_{qpr} - *lacZ*-chl at *yxaM*, Δ*racA*::erm	Δ*racA*::erm from 1272 transformed into 4735
RL 21	*trpC2 spoIIIE36* P_{qpr} - *lacZ*-chl at *amyE*, Δ*divIVA*::tet	*Ω(divIVA::tet)1042* from 1920 transformed into 4732
RL 23	*trpC2 spoIIIE36* P_{qpr} - *lacZ*-chl at *jag*, Δ*divIVA*::tet	*Ω(divIVA::tet)1042* from 1920 transformed into 4733
RL 24	*trpC2 spoIIIE36* P_{qpr} - *lacZ*-chl at *spoIID*, Δ*divIVA*::tet	*Ω(divIVA::tet)1042* from 1920 transformed into 4734
RL 25	*trpC2 spoIIIE36* P_{qpr} - *lacZ*-chl at *yxaM*, Δ*divIVA*::tet	*Ω(divIVA::tet)1042* from 1920 transformed into 4735
RL 26	*trpC2 spoIIIE36* P_{qpr} - *lacZ*-chl at *amyE*, Δ*(soj-spo0J)*::tet	Δ*(soj-spo0J)*::tet from HM31 transformed into 4732
RL 28	*trpC2 spoIIIE36* P_{qpr} - *lacZ*-chl at *jag*, Δ*(soj-spo0J)*::tet	Δ*(soj-spo0J)*::tet from HM31 transformed into 4733
RL 29	*trpC2 spoIIIE36* P_{qpr} - *lacZ*-chl at *spoIID*, Δ*(soj-spo0J)*::tet	Δ*(soj-spo0J)*::tet from HM31 transformed into 4734

RL 30	*trpC2 spoIIIE36* P_{qpr} - *lacZ*-chl at *yxaM*, Δ*(soj-spo0J)*::tet	Δ*(soj-spo0J)*::tet from HM31 transformed into 4735
RL 33	*trpC2* Δ*minCD*::tet	complete knock out, tetracyclin cassette inserted
RL 56	*trpC2 spoIIIE36, spo0J-gfp*-neo, Δ*minD*::erm	Δ*minD*::erm from 1901 transformed into RL 57
RL 57	*trpC2 spoIIIE36, spo0J-gfp*-neo	*spo0J-gfp*-neo from 2641 transformed into 36.3
RL 58	*trpC2* Δ*minCD*::tet, Δ*lacA*::chl	Δ*lacA*::chl from KS32 transformed into RL 33
RL 59	*trpC2* Δ*minCD*::tet, Δ*lacA*::chl, pLOSS::*minCD*	pLOSS::*minCD* transformed into RL 58
RL 60	*trpC2* Δ*minCD*::tet, Δ*lacA*::chl, pLOSS::*minCD*, pMAR-B	pMAR-B transformed into RL 59
RL 61	*trpC2 spoIIIE36, spo0J-gfp*-neo, *divIVA N99D*	*divIVA N99D* from 1274 transformed into RL 57
RL 62	*trpC2 spoIIIE36, spo0J-gfp*-spec	ECE141 transformed into RL 57
RL 64	*trpC2 spoIIIE36, spo0J-gfp*-neo, Δ*minC*::kan	Δ*minC*::kan from 3381 transformed into RL 57
RL 65	*trpC2*,*gfp-racA*-chl	168 transformed with pSG4916
RL 67	*trpC2*,*gfp-racA*-chl, Δ*minD*::erm	Δ*minD*::erm from 1901 transformed into RL 65
RL 104	*trpC2*,*gfp-racA*-chl, Δ*soj*::neo	Δ*soj*::neo from HM161 transformed into RL65
RL 111	*trpC2 spoIIIE36* P_{qpr} - *lacZ*-chl at *amyE*, Δ*soj*::neo	Δ*soj*::neo from HM161 transformed into 4732
RL 113	*trpC2 spoIIIE36* P_{qpr} - *lacZ*-chl at *jag*, Δ*soj*::neo	Δ*soj*::neo from HM161 transformed into 4733
RL 114	*trpC2 spoIIIE36* P_{qpr} - *lacZ*-chl at *spoIID*, Δ*soj*::neo	Δ*soj*::neo from HM161 transformed into 4734

RL 115	*trpC2 spoIIIE36* P_{qpr} - *lacZ*-chl at *yxaM*, Δ*soj*::neo	Δ*soj*::neo from HM161 transformed into 4735
RL 121	*trpC2,gfp-racA*-chl, Δ*divIVA*::tet	Δ*divIVA*::tet from 1920 transformed into RL 65
RL 123	*trpC2 spoIIIE36* P_{qpr} - *lacZ*-chl at *amyE*, Δ*soj*::neo, spec-P_{xyl}-*soj*	spec-P_{xyl}-*soj* from HM336 was transformed into RL 111
RL 125	*trpC2 spoIIIE36* P_{qpr} - *lacZ*-chl at *jag*, Δ*soj*::neo, spec-P_{xyl}-*soj*	spec-P_{xyl}-*soj* from HM336 was transformed into RL 113
RL 126	*trpC2 spoIIIE36* P_{qpr} - *lacZ*-chl at *spoIID*, Δ*soj*::neo, spec-P_{xyl}-*soj*	spec-P_{xyl}-*soj* from HM336 was transformed into RL 114
RL 127	*trpC2 spoIIIE36* P_{qpr} - *lacZ*-chl at *yxaM*, Δ*soj*::neo, spec-P_{xyl}-*soj*	spec-P_{xyl}-*soj* from HM336 was transformed into RL 115
RL 131	*trpC2 spoIIIE36* P_{qpr} - *lacZ*-chl at *amyE*, Δ*soj*::neo, spec-P_{xyl}-*soj*, Δ*minD*::erm	Δ*minD*::erm from 1901 transformed into RL 123
RL 133	*trpC2 spoIIIE36* P_{qpr} - *lacZ*-chl at *jag*, Δ*soj*::neo, spec-P_{xyl}-*soj*, Δ*minD*::erm	Δ*minD*::erm from 1901 transformed into RL 125
RL 134	*trpC2 spoIIIE36* P_{qpr} - *lacZ*-chl at *spoIID*, Δ*soj*::neo, spec-P_{xyl}-*soj*, Δ*minD*::erm	Δ*minD*::erm from 1901 transformed into RL 126
RL 135	*trpC2 spoIIIE36* P_{qpr} - *lacZ*-chl at *yxaM*, Δ*soj*::neo, spec-P_{xyl}-*soj*, Δ*minD*::erm	Δ*minD*::erm from 1901 transformed into RL 127
RL 136	*trpC2 spoIIIE36* P_{qpr} - *lacZ*-chl at *amyE*, Δ*soj*::neo, Δ*minD*::erm	Δ*minD*::erm from 1901 transformed into RL 111
RL 138	*trpC2 spoIIIE36* P_{qpr} - *lacZ*-chl at *jag*, Δ*soj*::neo, Δ*minD*::erm	Δ*minD*::erm from 1901 transformed into RL 113
RL 139	*trpC2 spoIIIE36* P_{qpr} - *lacZ*-chl at *spoIID*, Δ*soj*::neo, Δ*minD*::erm	Δ*minD*::erm from 1901 transformed into RL 114
RL 140	*trpC2 spoIIIE36* P_{qpr} - *lacZ*-chl at *yxaM*, Δ*soj*::neo, Δ*minD*::erm	Δ*minD*::erm from 1901 transformed into RL 115
RL 141	Δ*minD::*erm, Δ*soj*::neo	Δ*soj*::neo from HM161

		transformed into 1901
RL 162	*trpC,* P_{dnaX}-*dnaX-yfp*-spec	P_{dnaX}-*dnaX-yfp*-spec from JWV017 transformed into 168
RL 163	*trpC, dnaX-yfp*-spec, Δ*minD*::ery	Δ*minD*::ery from 1901 transformed into RL 162
RL 168	*trpC2 spoIIIE36* P_{qpr} – *lacZ*-chl at *amyE, soj G12V*-neo	*soj G12V*-neo from HM40 transformed into 4732
RL 169	*trpC2 spoIIIE36* P_{qpr} - *lacZ*-chl at *jag, soj G12V*-neo	*soj G12V*-neo from HM40 transformed into 4733
RL 170	*trpC2 spoIIIE36* P_{qpr} - *lacZ*-chl at *spoIID, soj G12V*-neo	*soj G12V*-neo from HM40 transformed into 4734
RL 171	*trpC2 spoIIIE36* P_{qpr} - *lacZ*-chl at *yxaM, soj G12V*-neo	*soj G12V*-neo from HM40 transformed into 4735
RL 172	*trpC2 spoIIIE36* P_{qpr} - *lacZ*-chl at *amyE, soj D40A*-neo	*soj D40A*-neo from HM36 transformed into 4732
RL 173	*trpC2 spoIIIE36* P_{qpr} - *lacZ*-chl at *jag, soj D40A*-neo	*soj D40A*-neo from HM36 transformed into 4733
RL 174	*trpC2 spoIIIE36* P_{qpr} - *lacZ*-chl at *spoIID, soj D40A*-neo	*soj D40A*-neo from HM36 transformed into 4734
RL 175	*trpC2 spoIIIE36* P_{qpr} - *lacZ*-chl at *yxaM, soj D40A*-neo	*soj D40A*-neo from HM36 transformed into 4735
RL 176	*trpC2 spoIIIE36* P_{qpr} – *lacZ*-chl at *amyE, soj G12V*-neo, Δ*minD*::erm	Δ*minD*::erm from 1901transformed into RL 168
RL 177	*trpC2 spoIIIE36* P_{qpr} - *lacZ*-chl at *jag, soj G12V*-neo, Δ*minD*::erm	Δ*minD*::erm from 1901transformed into RL 169
RL 178	*trpC2 spoIIIE36* P_{qpr} - *lacZ*-chl at *spoIID, soj G12V*-neo, Δ*minD*::erm	Δ*minD*::erm from 1901transformed into RL 170
RL 179	*trpC2 spoIIIE36* P_{qpr} - *lacZ*-chl at *yxaM, soj G12V*-neo, Δ*minD*::erm	Δ*minD*::erm from 1901transformed into RL

		171
RL 180	*trpC2 spoIIIE36* P_{qpr} - *lacZ*-chl at *amyE*, *soj D40A*-neo, Δ*minD*::erm	Δ*minD*::erm from 1901transformed into RL 172
RL 181	*trpC2 spoIIIE36* P_{qpr} - *lacZ*-chl at *jag*, *soj D40A*-neo, Δ*minD*::erm	Δ*minD*::erm from 1901transformed into RL 173
RL 182	*trpC2 spoIIIE36* P_{qpr} - *lacZ*-chl at *spoIID*, *soj D40A*-neo, Δ*minD*::erm	Δ*minD*::erm from 1901transformed into RL 174
RL 183	*trpC2 spoIIIE36* P_{qpr} - *lacZ*-chl at *yxaM*, *soj D40A*-neo, Δ*minD*::erm	Δ*minD*::erm from 1901transformed into RL 175
RL 184	*trpC*, P_{dnaX}-*dnaX-yfp*-spec, P_{spoIIA}-*mCherry*-chl	P_{spoIIA}-*mCherry*-chl from JWV017 transformed into RL 162
RL 185	*trpC*, P_{dnaX}-*dnaX-yfp*-spec, P_{spoIIA}-*mCherry*-chl, Δ*minD*::erm	Δ*minD*::erm from 1901 transformed into RL 184
RL 200	*trpC2 spoIIIE36* P_{qpr} - *lacZ*-chl at *amyE*, Δ*yabA*::phl	Δ*yabA*::phl (Noirot-Gros et al., 2002) transformed into 4732
RL 201	*trpC2 spoIIIE36* P_{qpr} - *lacZ*-chl at *jag*, Δ*yabA*::phl	Δ*yabA*::phl (Noirot-Gros et al., 2002) transformed into 4733
RL 202	*trpC2 spoIIIE36* P_{qpr} - *lacZ*-chl at *spoIID*, Δ*yabA*::phl	Δ*yabA*::phl (Noirot-Gros et al., 2002) transformed into 4734
RL 203	*trpC2 spoIIIE36* P_{qpr} - *lacZ*-chl at *yxaM*, Δ*yabA*::phl	Δ*yabA*::phl (Noirot-Gros et al., 2002) transformed into 4735
RL 205	*trpC2* Δ*minD*::spec	ECE79 transformed into 1901
RL 207	*trpC2* Δ*minD*::neo	ECE77 transformed into

		1901
RL 211	*trpC2 spoIIIE36* P_{qpr} - *lacZ*-chl at *amyE*, Δ*yabA*::phl, Δ*minD*::erm	Δ*minD*::erm from 1901 transformed into RL 200
RL 212	*trpC2 spoIIIE36* P_{qpr} - *lacZ*-chl at *jag*, Δ*yabA*::phl, Δ*minD*::erm	Δ*minD*::erm from 1901 transformed into RL 201
RL 213	*trpC2 spoIIIE36* P_{qpr} - *lacZ*-chl at *spoIID*, Δ*yabA*::phl, Δ*minD*::erm	Δ*minD*::erm from 1901 transformed into RL 202
RL 214	*trpC2 spoIIIE36* P_{qpr} - *lacZ*-chl at *yxaM*, Δ*yabA*::phl, Δ*minD*::erm	Δ*minD*::erm from 1901 transformed into RL 203
RL 215	*trpC2 spoIIIE36* P_{qpr} - *lacZ*-chl at *amyE*, Δ*sda*::tet, Δ*minCD*::kan	Δ*minCD*::kan from 3309 transformed into RL 219
RL 216	*trpC2 spoIIIE36* P_{qpr} - *lacZ*-chl at *jag*, Δ*sda*::tet, Δ*minCD*::kan	Δ*minCD*::kan from 3309 transformed into RL 220
RL 217	*trpC2 spoIIIE36* P_{qpr} - *lacZ*-chl at *spoIID*, Δ*sda*::tet, Δ*minCD*::kan	Δ*minCD*::kan from 3309 transformed into RL 221
RL 218	*trpC2 spoIIIE36* P_{qpr} - *lacZ*-chl at *yxaM*, Δ*sda*::tet, Δ*minCD*::kan	Δ*minCD*::kan from 3309 transformed into RL 222
RL 219	*trpC2 spoIIIE36* P_{qpr} - *lacZ*-chl at *amyE*, Δ*sda*::tet	Δ*sda*::tet from JWV128 transformed into 4732
RL 220	*trpC2 spoIIIE36* P_{qpr} - *lacZ*-chl at *jag*, Δ*sda*::tet	Δ*sda*::tet from JWV128 transformed into 4733
RL 221	*trpC2 spoIIIE36* P_{qpr} - *lacZ*-chl at *spoIID*, Δ*sda*::tet	Δ*sda*::tet from JWV128 transformed into 4734
RL 222	*trpC2 spoIIIE36* P_{qpr} - *lacZ*-chl at *yxaM*, Δ*sda*::tet	Δ*sda*::tet from JWV128 transformed into 4735
RL 230	*trpC2 spoIIIE36* P_{qpr} - *lacZ*-chl at *amyE*, Δ*sda*::tet, *dnaA S326L*-ery, Δ*minCD*::kan	Δ*minCD*::kan from 3309 transformed into RL 234
RL 231	*trpC2 spoIIIE36* P_{qpr} - *lacZ*-chl at *jag*, Δ*sda*::tet, *dnaA S326L*-ery, Δ*minCD*::kan	Δ*minCD*::kan from 3309 transformed into RL 235
RL 232	*trpC2 spoIIIE36* P_{qpr} - *lacZ*-chl at *spoIID*, Δ*sda*::tet, *dnaA S326L*-ery, Δ*minCD*::kan	Δ*minCD*::kan from 3309 transformed into RL 236
RL 233	*trpC2 spoIIIE36* P_{qpr} - *lacZ*-chl at *yxaM*, Δ*sda*::tet, *dnaA S326L*-ery, Δ*minCD*::kan	Δ*minCD*::kan from 3309 transformed into RL 237

RL 234	*trpC2 spoIIIE36* P_{qpr} - *lacZ*-chl at *amyE*, Δ*sda*::tet, *dnaA S326L*-erm	*dnaA S326L*-erm from HM302 transformed into RL 219
RL 235	*trpC2 spoIIIE36* P_{qpr} - *lacZ*-chl at *jag*, Δ*sda*::tet, *dnaA S326L*-erm	*dnaA S326L*-erm from HM302 transformed into RL 220
RL 236	*trpC2 spoIIIE36* P_{qpr} - *lacZ*-chl at *spoIID*, Δ*sda*::tet, *dnaA S326L*-erm	*dnaA S326L*-erm from HM302 transformed into RL 221
RL 237	*trpC2 spoIIIE36* P_{qpr} - *lacZ*-chl at *yxaM*, Δ*sda*::tet, *dnaA S326L*-erm	*dnaA S326L*-erm from HM302 transformed into RL 222
RL 252	*trpC2 spoIIIE36* P_{qpr} - *lacZ*-chl at *amyE*, Δ*minJ*::tet	Δ*minJ*::tet from RD021 transformed into 4732
RL 253	*trpC2 spoIIIE36* P_{qpr} - *lacZ*-chl at *jag*, Δ*minJ*::tet	Δ*minJ*::tet from RD021 transformed into 4733
RL 254	*trpC2 spoIIIE36* P_{qpr} - *lacZ*-chl at *spoIID*, Δ*minJ*::tet	Δ*minJ*::tet from RD021 transformed into 4734
RL 255	*trpC2 spoIIIE36* P_{qpr} - *lacZ*-chl at *yxaM*, Δ*minJ*::tet	Δ*minJ*::tet from RD021 transformed into 4735
RL 258	*trpC2, spo0J-gfp-spec,* Δ*soj::neo*	Δ*soj::neo* from HM161 transformed into RL 62
RL 277	*trpC2 spoIIIE36* P_{qpr} - *lacZ*-chl at *amyE*, Δ*racA*::erm, Δ*minD*::spec	Δ*minD*::spec from RL 205 transformed into RL 16
RL 278	*trpC2 spoIIIE36* P_{qpr} - *lacZ*-chl at *jag*, Δ*racA*::erm, Δ*minD*::spec	Δ*minD*::spec from RL 205 transformed into RL 18
RL 279	*trpC2 spoIIIE36* P_{qpr} - *lacZ*-chl at *spoIID*, Δ*racA*::erm, Δ*minD*::spec	Δ*minD*::spec from RL 205 transformed into RL 19
RL 280	*trpC2 spoIIIE36* P_{qpr} - *lacZ*-chl at *yxaM*, Δ*racA*::erm, Δ*minD*::spec	Δ*minD*::spec from RL 205 transformed into RL 20
RL 281	*trpC2 spoIIIE36* P_{qpr} - *lacZ*-chl at *amyE*, Δ*racA*::erm, Δ*minD*::spec, Δ*soj*:neo	Δ*soj*:neo from HM161 transformed into RL 277
RL 282	*trpC2 spoIIIE36* P_{qpr} - *lacZ*-chl at *jag*,	Δ*soj*:neo from HM161

	Δ*racA*::erm, Δ*minD*::spec, Δ*soj*:neo	transformed into RL 278
RL 283	*trpC2 spoIIIE36* P_{qpr} - *lacZ*-chl at *spoIID*,	Δ*soj*:neo from HM161
	Δ*racA*::erm, Δ*minD*::spec, Δ*soj*:neo	transformed into RL 279
RL 284	*trpC2 spoIIIE36* P_{qpr} - *lacZ*-chl at *yxaM*,	Δ*soj*:neo from HM161
	Δ*racA*::erm, Δ*minD*::spec, Δ*soj*:neo	transformed into RL 280
RL 301	*trpC2 spoIIIE36* P_{qpr} - *yfp*-phl at -7°, P_{qpr}	36.3 co-transformed with
	- *cfp*-chl at +28°	pNS051 and pNS007
RL 302	*trpC2 spoIIIE36* P_{qpr} - *yfp*-phl at -7°, P_{qpr}	Δ*minD*::erm from 1901
	- *cfp*-chl at +28°, Δ*minD*::erm	transformed into RL 301
RL 303	*trpC2 spoIIIE36* P_{qpr} - *yfp*-phl at -7°, P_{qpr}	Δ*soj*::neo from HM161
	- *cfp*-chl at +28°, Δ*soj*::neo	transformed into RL 302
RL 304	*trpC2 spoIIIE36* P_{qpr} - *yfp*-phl at -7°, P_{qpr}	Δ*minC*::kan from 3381
	- *cfp*-chl at +28°, Δ*minC*::kan	transformed into RL 301
RL 305	*trpC2 spoIIIE36* P_{qpr} - *yfp*-phl at -7°, P_{qpr}	Δ*soj*::neo from HM161
	- *cfp*-chl at +28°, Δ*minD*::erm, Δ*soj*::neo	transformed into RL 302
RL 321	*trpC2 spoIIIE36* P_{qpr} - *lacZ*-chl at *amyE*,	Δ*racA*::spec from 1273 and
	Δ*racA*::spec, Δ*soj*::neo	Δ*soj*::neo from HM161
		transformed into 4732
RL 322	*trpC2 spoIIIE36* P_{qpr} - *lacZ*-chl at *jag*,	Δ*racA*::spec from 1273 and
	Δ*racA*::spec, Δ*soj*::neo	Δ*soj*::neo from HM161
		transformed into 4733
RL 323	*trpC2 spoIIIE36* P_{qpr} - *lacZ*-chl at *spoIID*,	Δ*racA*::spec from 1273 and
	Δ*racA*::spec, Δ*soj*-neo	Δ*soj*::neo from HM161
		transformed into 4734
RL 324	*trpC2 spoIIIE36* P_{qpr} - *lacZ*-chl at *yxaM*,	Δ*racA*::spec from 1273 and
	Δ*racA*::spec, Δ*soj*-neo	Δ*soj*::neo from HM161
		transformed into 4735
RL 334	*trpC2 spoIIIE36* P_{qpr} - *lacZ*-chl at *amyE*,	Δ*racA*::erm from 1272
	Δ*(soj-spo0J)*::tet, Δ*racA*::erm	transformed into RL 26
RL 335	*trpC2 spoIIIE36* P_{qpr} - *lacZ*-chl at *jag*,	Δ*racA*::erm from 1272
	Δ*(soj-spo0J)*::tet, Δ*racA*::erm	transformed into RL 28
RL 336	*trpC2 spoIIIE36* P_{qpr} - *lacZ*-chl at *spoIID*,	Δ*racA*::erm from 1272
	Δ*(soj-spo0J)*::tet, Δ*racA*::erm	transformed into RL 29

RL 337	*trpC2 spoIIIE36* P_{qpr} - *lacZ*-chl at *yxaM*, Δ*(soj-spo0J)*::tet, Δ*racA*::erm	Δ*racA*::erm from 1272 transformed into RL 30
RL 339	*trpC2 spoIIIE36* P_{qpr} - *yfp*-phl at -7°, P_{qpr} - *cfp*-chl at +28°, Δ*racA*::spec	Δ*racA*::spec from 1273 transformed into RL 301
RL 340	*trpC2 spoIIIE36* P_{qpr} - *yfp*-phl at -7°, P_{qpr} - *cfp*-chl at +28°, Δ*racA*::spec, Δ*minD*::erm	Δ*minD*::erm from 1901 transformed into RL 339
RL 341	*trpC2 spoIIIE36* P_{qpr} - *yfp*-phl at -7°, P_{qpr} - *cfp*-chl at +28°, Δ*racA*::spec, Δ*soj*::neo	Δ*soj*::neo from HM161 transformed into RL 339
RL 344	*trpC2 spoIIIE36* P_{qpr} - *lacZ*-chl at *amyE*, Δ*(soj-spo0J)*::tet, Δ*racA*::spec	Δ*racA*::spec from 1273 transformed into RL 26
RL 345	*trpC2 spoIIIE36* P_{qpr} - *lacZ*-chl at *jag*, Δ*(soj-spo0J)*::tet, Δ*racA*::spec	Δ*racA*::spec from 1273 transformed into RL 28
RL 346	*trpC2 spoIIIE36* P_{qpr} - *lacZ*-chl at *spoIID*, Δ*(soj-spo0J)*::tet, Δ*racA*::spec	Δ*racA*::spec from 1273 transformed into RL 29
RL 347	*trpC2 spoIIIE36* P_{qpr} - *lacZ*-chl at *yxaM*, Δ*(soj-spo0J)*::tet, Δ*racA*::spec	Δ*racA*::spec from 1273 transformed into RL 30
RL 352	*trpC2 spoIIIE36* P_{qpr} - *lacZ*-chl at *amyE*, Δ*(soj-spo0J)*::tet, Δ*minD*::erm	Δ*minD*::erm from 1901 transformed into RL 26
RL 353	*trpC2 spoIIIE36* P_{qpr} - *lacZ*-chl at *jag*, Δ*(soj-spo0J)*::tet, Δ*minD*::erm	Δ*minD*::erm from 1901 transformed into RL 28
RL 354	*trpC2 spoIIIE36* P_{qpr} - *lacZ*-chl at *spoIID*, Δ*(soj-spo0J)*::tet, Δ*minD*::erm	Δ*minD*::erm from 1901 transformed into RL 29
RL 355	*trpC2 spoIIIE36* P_{qpr} - *lacZ*-chl at *yxaM*, Δ*(soj-spo0J)*::tet, Δ*minD*::erm	Δ*minD*::erm from 1901 transformed into RL 30
RL 360	*trpC2 spoIIIE36* P_{qpr} - *lacZ*-chl at *amyE*, Δ*(soj-spo0J)*::tet, Δ*racA*::erm , Δ*minD*::neo	Δ*minD*::neo from RL 207 transformed into RL 334
RL 361	*trpC2 spoIIIE36* P_{qpr} - *lacZ*-chl at *jag*, Δ*(soj-spo0J)*::tet, Δ*racA*::erm, Δ*minD*::neo	Δ*minD*::neo from RL 207 transformed into RL 335
RL 362	*trpC2 spoIIIE36* P_{qpr} - *lacZ*-chl at *spoIID*, Δ*(soj-spo0J)*::tet, Δ*racA*::erm,	Δ*minD*::neo from RL 207 transformed into RL 336

	Δ*minD*::neo	
RL 363	*trpC2 spoIIIE36* P_{qpr} - *lacZ*-chl at *yxaM*, Δ*(soj-spo0J)*::tet, Δ*racA*::erm, Δ*minD*::neo	Δ*minD*::neo from RL 207 transformed into RL 337
RL 368	*trpC2 spoIIIE36* P_{qpr} - *yfp*-phl at -7°, P_{qpr} - *cfp*-chl at +28°, Δ*(soj-spo0J)*::tet, Δ*racA*::spec	Δ*racA*::spec from 1273 transformed into RL 369
RL 369	*trpC2 spoIIIE36* P_{qpr} - *yfp*-phl at -7°, P_{qpr} - *cfp*-chl at +28°, Δ*(soj-spo0J)*::tet	Δ*(soj-spo0J)*::tet from HM31 transformed into RL 301
RL 376	*trpC2 spoIIIE36* P_{qpr} - *lacZ*-chl at *amyE*, Δ*sda*::tet, Δ*spo0J*::spec	Δ*spo0J*::spec from 2640 transformed into RL 219
RL 377	*trpC2 spoIIIE36* P_{qpr} - *lacZ*-chl at *jag*, Δ*sda*::tet, Δ*spo0J*::spec	Δ*spo0J*::spec from 2640 transformed into RL 220
RL 378	*trpC2 spoIIIE36* P_{qpr} - *lacZ*-chl at *spoIID*, Δ*sda*::tet, Δ*spo0J*::spec	Δ*spo0J*::spec from 2640 transformed into RL 221
RL 379	*trpC2 spoIIIE36* P_{qpr} - *lacZ*-chl at *yxaM*, Δ*sda*::tet, Δ*spo0J*::spec	Δ*spo0J*::spec from 2640 transformed into RL 222
RL 392	*trpC2 spoIIIE36* P_{qpr} - *lacZ*-chl at *amyE*, Δ*spo0J*::spec, Δ*sda*::tet, Δ*minD*::neo	Δ*minD*::neo from RL 207 transformed into RL 376
RL 393	*trpC2 spoIIIE36* P_{qpr} - *lacZ*-chl at *jag*, Δ*spo0J*::spec, Δ*sda*::tet, Δ*minD*::neo	Δ*minD*::neo from RL 207 transformed into RL 377
RL 394	*trpC2 spoIIIE36* P_{qpr} - *lacZ*-chl at *spoIID*, Δ*spo0J*::spec, Δ*sda*::tet, Δ*minD*::neo	Δ*minD*::neo from RL 207 transformed into RL 378
RL 395	*trpC2 spoIIIE36* P_{qpr} - *lacZ*-chl at *yxaM*, Δ*spo0J*::spec, Δ*sda*::tet, Δ*minD*::neo	Δ*minD*::neo from RL 207 transformed into RL 379
RL 396	*trpC2 spoIIIE36* P_{qpr} - *yfp*-phl at -7°, P_{qpr} - *cfp*-chl at +28°, Δ*(soj-spo0J)*::tet, Δ*racA*::spec, Δ*minD*::erm	Δ*minD*::erm from 1901 transformed into RL 368
RL 397	*trpC2 spoIIIE36* P_{qpr} - *yfp*-phl at -7°, P_{qpr} - *cfp*-chl at +28°, Δ*(soj-spo0J)*::tet, Δ*minD*::erm	Δ*minD*::erm from 1901 transformed into RL 369

RL 408	*trpC2 spoIIIE36* P_{qpr} - *yfp*-phl at -7°, P_{qpr} - *cfp*-chl at +28°, Δ*minD*::erm, Δ*racA*::spec, Δ*soj*::neo,	Δ*soj*::neo from HM161 transformed into RL 340

***Escherichia coli* strains**

BL21(DE3)	F- ompT hsdSB(rB-mB-)gal dcm (DE3)	Novagen
BTH101	F^-, cya-99, araD139, galE15, galK16, rpsL1 (Str^r), hsdR2, mcrA1, mcrB1	(Karimova et al., 1998)
C41(DE3)	F – ompT hsdSB (rB- mB-) gal dcm (DE3)	Lucigen
DH5α	F^-φ80*lac*ZΔM15Δ(*lac*ZYA-*arg*F) U169 *rec*A1 *end*A1 *hsd*R17 (r_k-, m_k+) *gal*$^-$ *pho*A *sup*E44λ$^-$ *thi*$^-$1 *gyr*A96 *rel*A1	Invitrogen
MHD63	*ami::Cm amiBC::Km* Δ*slt*	(Heidrich et al., 2001)

Table 3: List of plasmids used in this study

Plasmid	Genotype	Reference
ECE77	(pErm::Neo) Ap Neo	(Steinmetz and Richter, 1994)
ECE79	(pErm::Spec) Ap Spec	(Steinmetz and Richter, 1994)
ECE141	bla, Neo::Spec	(Chary et al., 1997)
pMAL-c2x	*bla* P_{lac} *malE MCL*	New England Biolabs
pMarB	*bla erm* P_{ctc} *Himar 1 kan* (TnYLB-1)	(Le Breton et al., 2006)
pRL2	*bla spc* P_{spac} *minCD* P_{divIVA}*-lacZ lacI reppLS20*	This work
pRL10	*bla* P_{lac} *malE-racA*	This work
pRL44	*bla* P_{lac} *malE-minD*	This work

p25-N	*kan* P_{lac} *mcs-cyaA*$^{1-672}$	(Claessen et al., 2008)
pKT25	*kan* P_{lac} *cyaA*$^{1-672}$*-mcs*	(Karimova et al., 1998)
pUT18	*bla* P_{lac} *mcs-cyaA*$^{672-1197}$	(Karimova et al., 1998)
pUT18C	*bla* P_{lac} *cyaA*$^{672-1197}$*-mcs*	(Karimova et al., 1998)
pUT18C:Zip	*bla* P_{lac} *cyaA*$^{672-1197}$*-zip*	(Karimova et al., 1998)
pKT25:Zip	*kan* P_{lac} *cyaA*$^{1-672}$*-zip*	(Karimova et al., 1998)
pSG1612	*divIVA-gfp*	(Edwards et al., 2000)
pSG1154	*amyE* P_{xyl}*-gfpmut1 spc*	(Lewis and Marston, 1999)
pSG4916	*bla gfp-racA' cat*	(Wu and Errington, 2003)
pDG7	*amy::divIVA-GFP Sp*	(Lenarcic et al., 2009)
pBEST	*bla tet*	(Itaya, 1992)
pLOSS	*bla spc* P_{spac} *mcs* P_{divIVA}*-lacZ lacI reppLS20 (GA→CC)*	(Claessen et al., 2008)
pNS051	yycR::PspoIIQ-yfp-phl	(Sullivan et al., 2009)
pNS007	amyE::PspoIIQ-cfp-chl	(Sullivan et al., 2009)

Table 4: List of oligonucleotides used in this study

Name	Restr. site	Sequence (5'-3')	Reference/ comment
LH126	/	5'AACAATAACAACAACCTCGGGATCGAGGGAAGGATGGGTGAGGCTATCGTAATA3'	L. Hamoen
LH 127	/	5'GTAAAACGACGGCCAGTGCCAAGCTTGC CTTTAAGATCTTACTCCGAAAAATG3'	L. Hamoen
RL 5	/	5'GGGCGGTACGACAGAAGTTG3'	This work

RL 6	BamHI	5'ACTGGATCCCACCTCAACAACATACTC AT 3'	This work
RL 7	BamHI	5'ACTGGATCCTACGTCTGCCCTCATTAT TG3'	This work
RL 8	KpnI	5'ATTCGAGCTCGGTACCCTTG3'	This work
RL 9	KpnI	5'ACTGGTACCGAATCTGACAAAGCATA TGC 3'	This work
RL 10	/	5'CTCTGCAC CTCCTATTAGAC3'	This work
RL 12	BamHI	5'ACTGGATCCTAGTCAAGAACAAAGCA GGC3'	This work
RL 15	NotI	5'ACTGCGGCCGCATGAGTATGTTGTTGA GGTG3'	This work
RL 25	XbaI	5'ACTTCTAGAAAGGAGGTATGGGATCA TGA3'	This work
RL 26	KpnI	5'ACTGGTACCGGGAGCTTTTTGCTTTAG GTTTG3'	This work
RL 27		5'ACTGGTACCGGGAGCTTTTTGCTTTCG GTTTG3'	This work
RL 28	SalI	5'ACTGTCGACGTGAATGGGGTGAGGCT ATC3'	This work
RL 29	EcoRI	5'ACTGAATTCCATTGAGATCTTACTCCG AA3'	This work
RL 43	/	5'AACAATAACAACAACCTCGGGATCGA GGGAAGGATGAATACAAATATGGTAGC AAG 3'	This work
RL 44	/	5'GTAAAACGACGGCCAGTGCCAAGCTT GCCTTTAGGTTTGAAATTTGAACAGTG 3'	This work
ipcr1	/	5’GCTTGTAAATTCTATCATAATTG3’	(Le Breton et al., 2006)
ipcr2	/	5'AGGGAATCATTTGAAGGTTGG3'	(Le Breton et al., 2006)
ipcr3	/	5'GCATTTAATACTAGCGACGCC3'	(Le Breton et

			al., 2006)
ori1	/	5’GATCAATCGGGGAAAGTGTG3’	(Murray and Errington, 2008)
ori2	/	5’GTAGGGCCTGTGGATTTGTG3’	(Murray and Errington, 2008)
ter3	/	5’TCCATATCCTCGCTCCTACG3’	(Murray and Errington, 2008)
ter4	/	5’ATTCTGCTGATGTGCAATGG3’	(Murray and Errington, 2008)

2.2. Transformation methods

2.2.1. Transformation of *E. Coli*

2.2.1.1. Preparing competent *E. coli* cells

10 ml PAB (see appendix ‘Growth media’) was inoculated with 100 µl overnight culture of *E. coli* and was allowed to grow for about 2 h at 37°C with shaking, to reach OD_{600} = 0.3. The culture was then centrifuged for 5 min at 5000 rpm and the pellet was resuspended in 5 ml 0.1 M ice cold $CaCl_2$ followed by incubation on ice for 30 min. After centrifugation for 5 min at 5000 rpm, the pellet was resuspended in 500 µl 0.1 M ice cold $CaCl_2$. Cells were at this stage competent. Aliquots were freezed in liquid nitrogen and kept at -80°C.

2.2.1.2. Transformation

An aliquot of frozen competent cells was thawed on ice before adding 1-10 µl plasmid DNA (the amount differed depending on plasmid concentration) and mixed gently. Competent cells with DNA were incubated on ice for 45 min followed by a heat shock at 43°C for 90 seconds. To allow recovering cells, 400 µl LB (see appendix 'Growth media') was added and the cells were incubated for 1 h at 37°C with shaking. Transformants were then plated on selection agar plates. As a control, competent cells without DNA were used, following exactly the same procedure.

2.2.2. Transformation of *B. subtilis*

We prepared MM competence medium (see appendix 'Growth media) to grow cells and Starvation medium to make cells competent.

The day before the transformation we inoculated 10 ml MM competence medium with the relevant *B. subtilis* strain and grew it with shaking overnight at 37°C. The next morning we inoculated fresh 10 ml MM competence medium with 0.6 ml overnight culture and continued to grow cells at 37°C. After 3 h we added 10 ml prewarmed Starvation medium (see appendix 'Growth media') and continued to grow for another 2 h. We mixed 0.4 ml competent cells with 10 – 100 µl DNA (the amount of DNA differed according to DNA concentration) and the mixture was incubated for 1 h at 37°C with shaking. Transformants were then plated on selective agar plates.

2.3. DNA methods

2.3.1. Oligonucleotides

Oligonucleotides were designed using Clone Manager software and were purchased from Eurogentec. They were stored in aliquots at -20°C in a concentration of 10 µM.

2.3.2. Polymerase chain reaction (PCR)

All PCR reactions were performed according to the supplier's recommendations. For PCR reactions confirming constructs, we used GoTaq polymerase (Promega); for creating new genetic constructs, Pfu Turbo (Stratagene) or Phusion (NEB) polymerases were used.

2.3.2.1. *E. coli* colony PCR

To screen for the correct clones, colony PCR using *E. coli* colonies was performed. A colony was resuspended in 50 µl dH_2O and the suspension was incubated on 100°C for 10 min to lyse the cells. 10 µl of the boiled cell suspension was used as a DNA template to perform a standard PCR reaction by using GoTaq polymerase (Promega).

2.3.2.2. Q-PCR

Strains were sampled at different stages of growth/sporulation; V1 (vegetative growth at OD = 0.4 in CH medium), S0 (sporulation time 0 in sporulation medium; at the time of resuspension), S30 (sporulation time 30 min in sporulation medium; 30 min after resuspension), S60 (sporulation time 60 min in sporulation medium; 60 min after resuspension), S90 (sporulation time 90 min in sporulation medium; 90 min after

resuspension). From 2 ml of culture, DNA was isolated as described in 2.3.12. The concentration of isolated DNA was measured using NanoDrop Spectrophotometer ND-1000 (Labtech) and diluted to 2.5 pg/µl, which was then used for Q-PCR reactions. All samples were mixed in PCR reaction in duplicates, both with 'ter' primer mix (ter3 and ter4 primers) and 'ori' primer mix (ori1 and ori2 primers). The reaction contains: 10 µl of Master mix (Cyber Green 2x), 2 µl of 3 uM primer mix, 8 µl of diluted DNA (2.5 pg/µl). PCR reactions were mixed in a microtiter plate, and reactions were performed in a Roche LightCycler 480 Instrument (Roche, Inc.) using LightCycler Software version 4.0 (Roche, Inc.). As a negative control, PCR reaction mixture without DNA was used and as a calibrator, spore DNA was used. Calibrator is used to compare the efficiency of the primer mixes and also to standardize the *ori:ter* ratio. After PCR reactions, the amount of product amplified with 'ori' primer mix was compared to the amount of product amplified with 'ter' primer mix, divided by the ratio of spore DNA.

2.3.3. Purification of PCR products

PCR products were purified according to manufacturer's instructions using QIAquick PCR purification kit (Qiagen) or PureLink PCR purification kit (Invitrogen).

2.3.4. Plasmid purifications

Plasmids were purified according to manufacturer's instructions by QIA miniprep (Qiagen) or PureLink Mini Plasmid DNA purification (Invitrogen) kits.

2.3.5. Agarose gel electrophoresis

Agarose gel electrophoresis of DNA fragments was performed using 1 % agarose gels in 1x TAE buffer, containing 0.5 mg/ml ethidium bromide. Prior to loading on the gel, DNA samples were mixed with loading dye. The voltage used for electrophoresis was 100 V. After electrophoresis, bands were visualised by using UV transilluminator and photographed using a Lumenera USB 2.0 camera.

2.3.6. Extraction of DNA fragments from an agarose gel

DNA fragments were cut out of an ethidium bromide stained agarose gel when necessary. DNA was purified according to manufacturer's instructions using QIAquick extraction kit (Qiagen) or PureLink extraction kit (Invitrogen).

2.3.7. Restriction endonuclease digestions of DNA fragments

DNA was digested according to supplier's instructions in buffers provided with the used restriction endonuclease, usually for 1-3 hours. To remove the enzyme after reaction, DNA was purified using QIAquick PCR purification kit (Qiagen) or PureLink PCR purification kit (Invitrogen).

2.3.8. Dephosphorylation reactions

When required, linearised vectors were dephosphorylated to prevent self-ligation using alkaline phosphatase. After digestion with restriction endonuclease, 1 unit of alkaline phosphathase (Roche) was added to the reaction mixture. The enzyme was removed after 1 hour incubation at 37°C.

2.3.9. Ligation of DNA fragments

DNA fragments were ligated using 0.2 unit T4 DNA ligase (Roche) in the buffer provided by the supplier. The reaction volume was 20 µl, incubated overnight at 4°C in a bucket filled with water of room temperature.

2.3.10. DNA sequencing

New constructs and plasmids were sequenced using the sequencing service of the University of Dundee in Scotland.

2.3.11. Isolation of genomic DNA of *B. subtilis* for transformation

B. subtilis genomic DNA used for transformation was prepared using a quick isolation method described by Ward and Zahler (Ward and Zahler, 1973). 4 ml PAB was inoculated from a fresh overnight culture and grown at 37°C until dense. The culture was then pelleted and washed with 1 ml SSC solution before resuspended in 1 ml SSC solution. After adding 10 µl lysozyme solution (10 mg/ml), the mixture was incubated at 37°C until lysed. After cell lysed, 1 ml 4 M NaCl was added and then mixture was filtered through 0.45 µm pore filter. Around 80 µl of DNA was then used for transformation procedure.

2.3.12. Isolation of genomic DNA for PCR

Pellet of 2 ml of the overnight *B. subtilis* strain was resuspended in 100 µl 50 mM EDTA with 10 µl lysozyme and 3 µl RNase. Sample was incubated at 37°C for 60

min before adding 500 µl Nuclei Lysis Solution (Promega). To lyse the cells, sample was incubated at 80°C fot 5 min and then cooled to room temperature. Next, we added 200 µl Protein Precipitation Solution to the cell lysate before vortexing vigorously at high speed for 20 seconds, followed by incubation on ice for 10 min and centrifugation at 13.000 g for 10 min. Supernatant with DNA was then transferred to 600 µl isopropanol and after mixing gently when DNA strands formed a visible mass, DNA was centrifuged at 13.000 g for 10 min. After centrifugation, we washed DNA pellet in 70 % ethanol and air dried and the pellet before resuspending it in TE.

2.4. Protein methods

2.4.1. Purification of MinD and biochemical experiments

2.4.1.1. Cloning and purification of MinD

minD gene was amplified from *B. subtilis* chromosomal DNA using primers LH126 and LH127, and cloned into pMAL-C2x using the restriction free cloning method (van den Ent and Lowe, 2006) resulting in plasmid pRL44.

MinD was purified as a MBP-MinD fusion. pRL44 containing MBP-minD fusion was transformed into *E. coli* strain C41(DE3). Expression of MBP-RacA was induced with IPTG when the culture reached an OD_{600} ~ 0.4. After shaking for 2 h at 37°C cells were harvested and washed in cold Column buffer M, followed by cell disruption using French press. After the addition of 200 µl 100 mM PMSF, 2 mini protease inhibitor tablets, 20 µl bensoaze and 20 µl RNAse, supernatant was centrifuged at 20.000 rpm for 30 min, filtered and loaded onto an amylase column

(New England BioLabs). The column was then washed with Buffer M1, Buffer M2, and Buffer M3, followed by elution with Buffer M3 containing 10 mM maltose. Cleavage of MBP was performed in 1 mM $CaCl_2$ and 0.3 % factor Xa protease at 4ºC overnight. Protein fractions were analysed with SDS-PAGE, and protein concentrations were determined with Bradford assays or spectrophotometrically (A_{260}). Purified protein fractions were aliquoted, freezed in liquid N_2 and stored at -80°C.

2.4.1.2. Testing DNA binding activity of MinD

Different amounts of purified MinD (46.8 µg, 23.4 µg, 11.7 µg and 0 µg) were added to the reaction mixture containing purified PCR product from *B. subtilis* wild type chromosome. Reaction mixtures were allowed to incubate for 10 min at 30ºC in Binding buffer DM prior to loading on 1 % agarose gel. After electrophoresis at 100 V, the gel was stained with ethidium bromide and visualised by camera.

2.4.1.3. Membrane binding activity of MinD

To test the affinity of MinD for membranes, we mixed purified MinD protein with or without lipid vesicles and ATP (final concentration 1 mM). Lipid vesicles were prepared as described in 2.8.2.1. using 0.4 µm pore filter in Binding buffer BM to a final concentration of 1 mg/ml. Reaction mixtures were incubated at 30°C for 10 min and then centrifuged for 10 min at 80.000 rpm and 30ºC. After centrifugation, the supernatant was carefully removed. 40 µl of supernatant and the pellet for each reaction mixture were mixed with 40 µl SDS sample buffer and ran on SDS-PAGE gel, followed by western blotting using antibodies against MinD.

2.4.1.4. Testing interaction between MinD and DivIVA

To test direct interaction between MinD and DivIVA *in vitro*, we mixed purified MinD protein with or without purified DivIVA, with or without lipid vesicles and with of without ATP (final concentration 1 mM). Lipid vesicles were prepared as described in 2.8.2.1. using 0.4 μm pore filter in Binding buffer BM to a final concentration of 1 mg/ml. Reaction mixtures with purified DivIVA and lipid vesicles were preincubated at room tempereature for 10 min (to allow DivIVA to bind to lipids) and then MinD was added. After incubation at room temperature for another 15 min, samples were centrifuged for 10 min at 80.000 rpm at 30ºC. After centrifugation, supernatant was carefully removed. 40 μl of supernatant and pellet for each reaction mixture were mixed with 40 μl SDS sample buffer and ran on SDS-PAGE gel, followed by western blotting using antibodies against MinD.

2.4.2. RacA purification and biochemical experiments

2.4.2.1. Cloning of RacA

racA gene was amplified from *B. subtilis* chromosomal DNA using primers RL43 and RL44, and cloned into the over-expression vector pMAL-c2x using the restriction free cloning method (van den Ent and Lowe, 2006) resulting in pRL10 plasmid.

2.4.2.2. RacA purification

RacA was purified as a MBP-RacA fusion. pRL10 carrying MBP-racA fusion was transformed in an *E. coli* strain BL21. Expression of MBP-RacA was induced with

1mM IPTG when the culture reached an OD_{600} of ~ 0.5. After 2 h cells were harvested, followed by sonication and centrifugation. The supernatant was filtered and loaded onto an amylase column (New England BioLabs). The column was washed with Buffer R1, Buffer R2, and Buffer R3, followed by elution with Buffer R3 containing maltose. Protein fractions were analysed with SDS-PAGE, and protein concentrations were determined with Bradford assay or spectrophotometrically (A_{260}). Purified protein fractions were aliquoted, freezed in liquid N_2 and stored at -80°C.

2.4.2.3. RacA pull down with lipids and DivIVA

To test interaction between RacA and DivIVA, density gradient flotation was used. MBP-RacA was mixed with or without liposomes and DivIVA in the presence of 0.5 mg/ml BSA and 20 % sucrose in Binding buffer BR. Before adding MBP-RacA, the mixtures were preincubated at room temperature for 15 min. After incubation for 1 h at room temperature, the solutions were loaded into the bottom of 0.8 ml centrifuge tubes (5 x 41 mm). Then 100 µl of each 15 % sucrose, 10 % sucrose, 5 % sucrose and 0 % sucrose in the buffer was loaded. Gradients were centrifuged at 25000 r.p.m. at 30ºC for 2 h in a Beckman Optima MAX Ultracentrifuge using a MLS 50 rotor. After centrifugation, the gradients were sampled in five fractions, which were analysed by western blotting using RacA-specific antibodies.

2.4.3. SDS-Polyacrylamide gel electrophoresis

Proteins were separated on NuPAGE Novex Bis-Tris SDS-PAGE Midi Gels (Invitrogen) using MOPS SDS Running Buffer and the protocol suggested by Invitrogen.

2.4.4. Comassie staining

Gel was dropped in Staining solution A (50 % methanol and 10 % acetic acid) and left for 10 min on the shaker. After fixative removal it was dipped into 75 ml Staining solution B (8 % NH_4SO_4 and 1.6 % phosphoric acid) with 20 ml ethanol and left on the shaker for another 10 min before adding 5 ml Staining solution C (0.8 g CBB-G in 50 ml water). Gel was stained for 3 h then destained with water.

2.4.5. Western blotting

After running SDS-PAGE gel, proteins were transferred to the PVDF transfer membrane (Hybond). The transfer membrane was cut to the size of the gel (13 cm x 7.5 cm), pre-wetted in methanol and dipped in destiled water. To assemble the tank cassette, scotch brit was pre-wetted in Transfer buffer followed by 2 layers of Wattman papers slightly bigger than the SDS-PAGE gel and pre-wetted in Transfer buffer, followed by membrane, gel, 2 Wattman papers pre-wetted in Transfer buffer and another scotch brit pre-wet in Transfer buffer. The tank cassette with gel and PVDF transfer membrane was put into the tank filled with Transfer buffer (0.5 x buffer SDS, 20 % ethanol in destiled water), with membrane on the positive side. Transfer was run overnight on 25 mA.

The next morning, the membrane was washed with PBST (PBS with 0.1 % Tween), dipped into a dish with 10 ml blocking buffer (PBST with 5 % milk powder) and left on shaker for 1 h at room temperature. After 1 h first antibodies were added and were allowed to bind to proteins with shaking at room temperature for 1 h. The membrane was washed 3 x with PBST and left for 10 min in fresh PBST inbetween washes. Washed membrane was dipped into fresh 10 ml blocking buffer with secondary

antibodies and allowed to be shaked at room temperature for 1 h. The following washing procedure was the same as above.

For detection, ECL Plus Western Blotting Detection System solution (GE Healthcare) was added to the protein side of the membrane for 2 min and the excess liquid was drained. High performance chemiluminescence film (Amersham Hyperfilm^{TM} ECL from GE Healthcare) was exposed to the membrane for about 5 min (depending on signal strength).

2.5. Chromosome trapping assays

2.5.1. Localisation of *oriC* by Spo0J-GFP and light fluorescence microscopy

Investigated strains were grown in CH medium (see appendix 'Growth media') overnight at 30ºC. The next morning, cultures were diluted in fresh CH medium to an OD_{600} of 0.1, transferred to 37°C and allowed to grow for about 2 h to reach an OD_{600} = 0.7. Cells were then collected by centrifugation for 5 min and resuspended in prewarmed (37°C) sporulation medium (see appendix 'Growth media') and allowed to induce sporulation at 37ºC by shaking. After 3 h, 2 µl of a colony was mounted onto microscope slides coated with a thin layer of 1.5 % agarose. Samples were allowed to dry briefly and were then examined by fluorescence light microscopy. Images were taken with a Zeiss Axiovert 200M coupled to a CoolsnapHQ CCD camera and using Metamorph imaging software (Universal Imaging).

2.5.2. Trapping observation by using *lacZ* reporter gene

To observe in more detail which part of DNA is trapped in the prespore and which not, we constructed 4 parental strains, each had a *lacZ* reporter gene that was integrated at different location on the chromosome around *oriC* region as shown on Figure 2.2. The *lacZ* reporter genes were preceded by a σ^F promoter. All parental strains also had a point mutation in SpoIIIE DNA exporter (*spoIIIE36*), making this DNA translocase inactive (Figure 2.1) and so allowing us to observe trapping pattern specifically at the early stage of sporulation.

2.5.3. Reporter gene *lacZ*

The *lacZ* reporter gene is preceded by a prespore-specific σ^F promoter (Figure 2.1), which is the first sigma factor being active and only in the prespore (King et al., 1999). This means, that if a specific part of the chromosome carrying the reporter gene is trapped in the prespore, the *lacZ* gene will be expressed giving blue colonies on nutrient agar plate containing X-gal. If this part of chromosome is in the mother cell, the *lacZ* gene will not be expressed and the colonies on nutrient agar plates containing X-gal remain white.

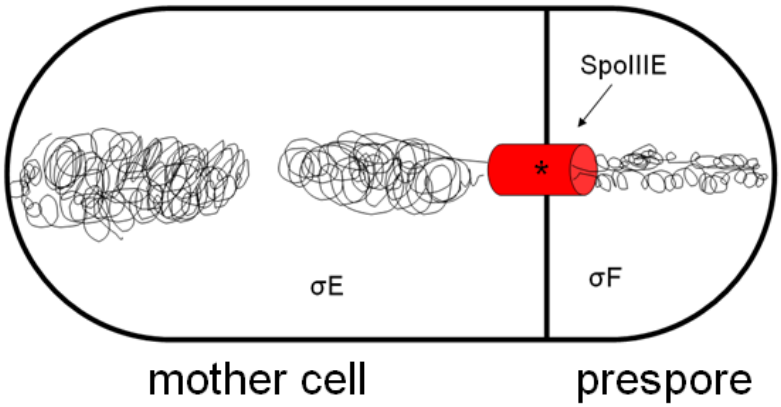

Figure 2.1: SpoIIIE point mutation.
SpoIIIE point mutation allows the chromosomal region entering the prespore upon completion of septation to be mapped. All strains used to study trapping had the *spoIIIE*36 mutation to prevent transfer of chromosomal DNA into the prespore after asymmetric septation.

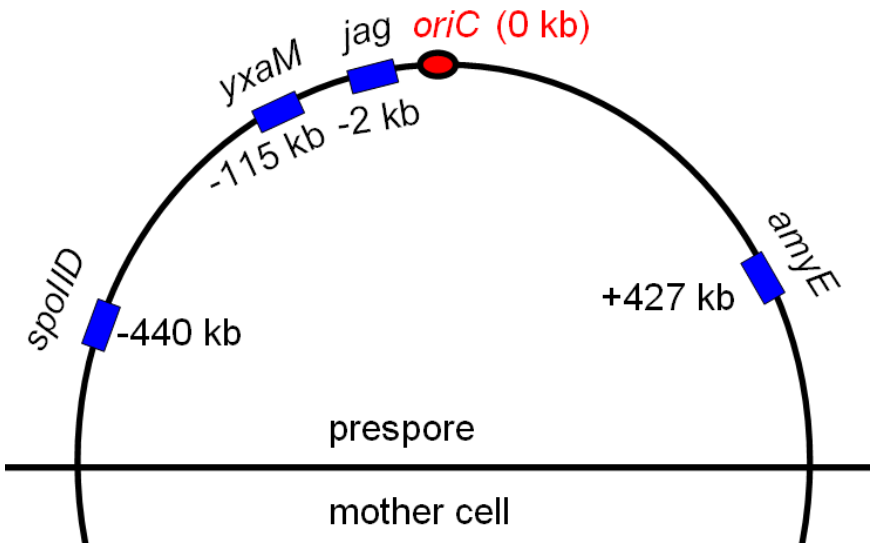

Figure 2.2: Locations of the *lacZ* reporter on the chromosome.
Positions of the *lacZ* reporter gene (blue) on the chromosome around *oriC* (red). Reporter gene locations are marked by their distance to *oriC* and by the name of the gene where the reporter is integrated on *B. subtilis* 168 chromosome.

2.5.4. Constructing strains

To test effects of different mutations on trapping efficiency, we transformed chromosomal DNA of mutants of interest into the 4 parental strains, each of them carrying *lacZ* reporter at a different position as presented on Figure 2.2. The transformants were restreaked to single colonies several times, then tested for resistance to various antibiotics to ensure that no mutations have been lost during strain construction.

2.5.5. Plating and growth of strains

Strains were then inoculated on nutrient agar plate containing X-gal, which is a substrate for β-galactosidase; the product of *lacZ*. Production of β-galactosidase gives blue colonies on X-gal plates. Strains were incubated at 37°C for 2 days (one day to allow colonies to grow and one day to allow cells to start sporulating) when the colour of colonies was checked for blue or white.

2.5.6. Trapping in liquid media

To determine in more detail the percentage of cells that trap *oriC* and the ones that do not trap it, the trapping experiment was repeated in liquid media. Cells were induced to sporulate in sporulation medium with various concentrations of Mg^{2+}. Samples were taken every 15 minutes: 200 μl for β-galactosidase assay (to quantify expression of *lacZ* reporter gene) and 750 μl for alkaline phosphatase assay (indication of sporulation efficiency). Both samples were freezed in liquid nitrogen and stored at -80ºC.

2.5.7. β-galactosidase assay

Frozen samples were defrosted and warmed up to 30ºC in water bath. 400 µl lysis solution (200 µg/ml lysozyme, 100 µg/ml DNaseI, 1.25 % Triton-X) was added to the samples and the mixture was incubated for 10 min at 37ºC to lyse the cells. The reaction was started when 200 µl of ONPG (4 mg/ml, dissolved in Z-buffer) was added to lysed cells. When the yellow colour developed, reaction was stopped by adding 400 µl of 1 M Na_2CO_3 and time was noted. After spinning down the samples on full speed in microfuge for 5 min, A_{420} was read against blank of ONPG in Z-buffer only. Measurement of A_{420} of 400 µl Z-buffer + 200 µl ONPG + 400 µl sodium carbonate solution was substracted from all readings. Miller units were calculated with using formula: $(A_{420} * 6 * 1000)/(\text{reaction time} * OD_{600})$.

2.5.8. Alkaline phosphatase assays

Alkaline phosphatase assay was based on that of Glenn & Mandelstam, 1971 and Errington & Mandelstam, 1983 (Errington and Mandelstam, 1983; Glenn and Mandelstam, 1971). Frozen samples were thawed and warmed to 30ºC before the addition of 0.5 ml para-nitrophenyl phosphate. Reaction was stopped after 1 h by adding 0.5 ml 2 N NaOH. OD_{410} was measured against water blank (with same reagents) after centrifugation. Units (one unit of enzyme is the amount that hydrolases 1 nmol para-nitrophenyl phosphate in 1 min at 30ºC) per ml of culture were calculated using formula: $(OD_{410} * 101 * 2.33)/(\text{incubation time})$.

2.6. Phase contrast and fluorescence microscopy

Cells (1 µl) were added onto microscopy slides covered by a thin layer of 1 % agarose, if requred in medium (Glaser et al., 1997). To stain cell membrane, 1 µl of Nile Red (Molecular Probe) solution (12.5 mg/ml) was added to 800 µl of agarose solution. When staining nucleoids, 2 µl of DAPI (Sigma) solution (1 mg/ml in 50 % glycerol) was mixed with 8 µl of cell suspention prior to mounting onto agarose covered microscopy slide. Images were aquired with a Sony CoolSnap HQ cooled CCD camera (Roper Scientific) camera attached to a Zeiss Axiovert 200M microscope.

2.6.1. Studying trapping by using fluorescent reporter genes

We confirmed results obtained by *lacZ* reporter gene using YFP at -7º and CFP at +28°, the system that has been previously reported (Sullivan et al., 2009). Both reporters were under the σ^F promoter (Figure 2.1). We constructed parental strain carrying the *spoIIIE36* mutation and harbouring both fluorescent reporters, each of them on different location close to the *oriC* region (Figure 2.3). Mutations of interest were then introduced into the parental strain and examined by fluorescence microscopy. The number of cells containing only CFP signal or YFP or both in the prespore were compared.

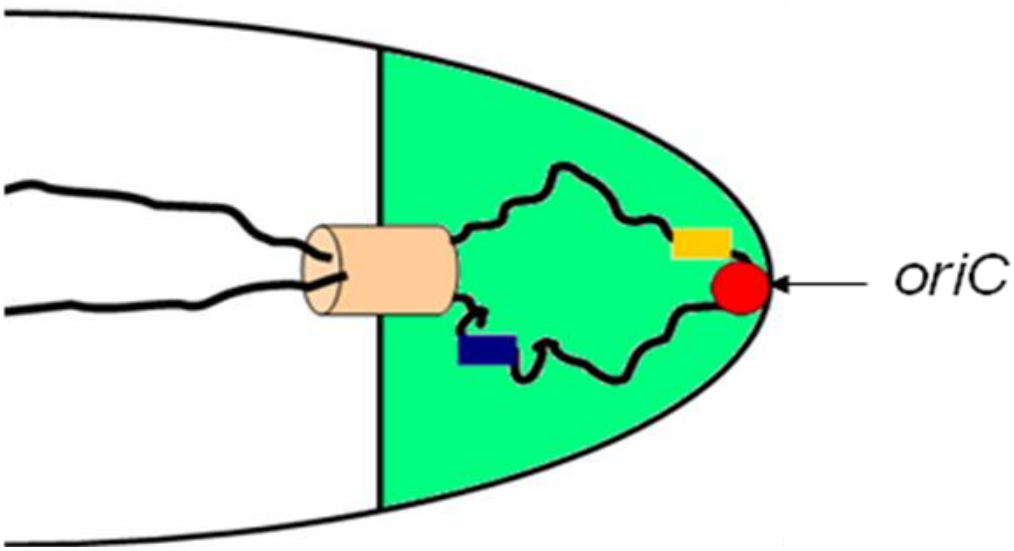

Figure 2.3: Position of fluorescent reporter genes on the chromosome of *B. subtilis*.
YFP (yellow square) is positioned 7º left of *oriC* (red circle) CFP (blue square) is positioned 28º right of *oriC*. When both genes are trapped in the prespore compartment, we can observe both, YFP and CFP signal in the prespore.

2.6.2. Fluorescence microscopy of strains harbouring YFP at -7º and CFP at 28°

The strains were induced to sporulate grown in CH medium (see appendix 'Growth media') overnight at 30ºC. The next morning, cultures were resuspended in fresh CH medium to OD_{600} = 0.1, transferred to 37°C and allowed to grow for about 2 h to reach an OD_{600} = 0.7. Cells were then collected by centrifugation for 5 min and resuspended in prewarmed (37°C) sporulation medium (see appendix 'Growth media') containing 5 mM Mg^{2+} and allowed to induce sporulation at 37ºC by shaking. After 3 h, 2 µl of a cells was mounted onto microscope slides coated with a thin layer of 1.5 % agarose. Samples were allowed to dry and were then investigated by fluorescence light microscopy. Images were taken with a Zeiss Axiovert 200M coupled to a CoolsnapHQ CCD camera and using Metamorph imaging software (Universal Imaging).

2.7. Bacterial two hybrid screens

Bacterial two hybrid analyses were carried out as described by Daniel *et al*. (Daniel et al., 2006) using a method based on Karimova *et al*. (Karimova et al., 1998). This test is based on production of adenylate cyclase and consequently blue colonies on plates containing X-gal, if the two proteins interact.

2.7.1. Cloning

2.7.1.1. RacA

The coding sequence of *racA* was amplified by PCR using primers RL25 and RL26/RL27 and cloned into p25-N (low-copy plasmid for C-terminal adenylate cyclase T25 fragment fusion), pKT25 (low-copy plasmid for N-terminal adenylate cyclase T25 fragment fusion), pUT18 (high-copy plasmid for C-terminal adenylate cyclase T18 fragment fusion) and pUT18C (high-copy plasmid for N-terminal adenylate cyclase T18 fragment fusion) vectors using XbaI and KpnI restriction sites. Clones were checked by PCR and sequencing.

2.7.1.2. MinD

The coding sequence of *minD* was amplified by PCR and cloned into p25-N (low-copy plasmid for C-terminal adenylate cyclase T25 fragment fusion), pUT18 (high-copy plasmid for C-terminal adenylate cyclase T18 fragment fusion) vectors using SalI and EcoRI restriction sites. Clones were checked by PCR and sequencing. Fusion of *minD* in pKT25 (low-copy plasmid for N-terminal adenylate cyclase T25 fragment fusion) and pUT18C (high-copy plasmid for N-terminal adenylate cyclase T18 fragment fusion) we got from Robyn Emmins (Bramkamp, 2008).

2.7.2. Transformations

Constructs were co-transformed into *E. coli* strain BTH101, which was made competent using standard protocol. For each combination of plasmids tested, 15 µl competent cells BTH101 were mixed with 1 µl of each plasmid. After incubation on ice for 20 min, cells were heat shocked at 42°C for 2 min and recovered on ice for 5

min followed by addition of 80 µl LB. Cells were then incubated at 30°C for 3 h and 10 µl of cells was then spotted onto plates containing X-gal and incubated at 30°C for around 36 hours. As a control, empty plasmids without any cloned gene were used and as a positive control, pUT18C:Zip and pKT25:Zip were used.

2.7.3. List of plasmids and constructs used in Bacterial two-hybrid screening

p25-N (low-copy plasmid for C-terminal adenylate cyclase T25 fragment fusion)

pKT25 (low-copy plasmid for N-terminal adenylate cyclase T25 fragment fusion)

pUT18 (high-copy plasmid for C-terminal adenylate cyclase T18 fragment fusion)

pUT18C (high-copy plasmid for N-terminal adenylate cyclase T18 fragment fusion)

Table 5: List of constructs used in Bacterial two-hybrid screen

pUT18::DivIVA	p25N::DivIVA
pUT18C::DivIVA	pKT25::DivIVA
pUT18C::DivIB	pKT25::DivIB
pUT18C::MinC	pKT25::MinC
pUT18::MinD	p25N::MinD
pUT18C::MinD	pKT25::MinD
pUT18C::MreB	pKT25::MreB
pUT18C::MreC	pKT25::MreC
pUT18C::MreD	pKT25::MreD
pUT18::Soj	p25N::Soj
pUT18C::Soj	pKT25::Soj
pUT18::Spo0J	p25N::Spo0J
pUT18C::Spo0J	pKT25::Spo0J
pUT18::RacA	p25N::RacA
pUT18C::RacA	pKT25::RacA
pUT18C::ZIP	pKT25::ZIP

2.7.4. Plating transformants

Transformants were plated on LB agar and minimal media agar plates, both with 4 % X-gal. Colonies were allowed to grow at 30°C for 2 days to develope blue colour.

Minimal media plates:

For 1 litre we mixed 10 g of agar, 1 ml Solution A, 10 ml Solution B and destiled water. After autoclaving we added:

- 20 ml Glucose to final concentration 0.08 %
- 20 ml CAA to final concentration 0.4 %
- 1 ml X-gal to final concentration 0.004 %
- 1 ml Kanamycin stock to final concentration 25 μg/ml
- 2 ml Ampicilin stock to final concentration 100 μg/ml
- 200 μl Thiamine to final concentration 3 μM
- 100 μl IPTG stock to final concentration 0.1 mM

2.8. Localization of DivIVA

2.8.1. DivIVA localization in *E. coli*

For fluorescence microscopy, the *divIVA-gfp* region of plasmid pSG1612 (Edwards et al., 2000) was isolated (XhoI x SpeI) and subcloned into pSG1154, resulting in plasmid pDG7. This plasmid can replicate in *E. coli* and the *divIVA* region includes its promoter that is active also in *E. coli. E. coli* cells (wild type K12 or MHD63 strain) carrying pDG7 plasmid were grown in PAB media (see appendix 'Growth media') at 30°C. Samples were taken at exponential growth and mounted into microscope slides

coated with a thin layer of 1.5 % agarose for microscopy. The exposure time for DivIVA-GFP fusion was 1000 ms. Images were taken with a Zeiss Axiovert 200M coupled to a CoolsnapHQ CCD camera and using Metamorph imaging software (Universal Imaging).

2.8.2. DivIVA membrane localization

The affinity of DivIVA for lipid vesicles was shown *in vitro* by using lipid vesicles (of different diameter) and that proteins localizes to the cell membranes was shown by fluorescence microscopy *in vivo* in *S.pombe* and in *E.coli*.

2.8.2.1. Lipid vesicles preparation

Liposomes were prepared as described by Avanti Polar Lipids. *E. coli* polar lipid extract (Avanti Polar Lipids) dissolved in chloroform was desiccated in a rotary evaporator, followed by vacuum excitation (4 h). Lipids were resuspended in 50 mM Tris-acetate (pH 7.5) by vigorous vortexing (20 min) and sonication (2 x 5 min) in a bath sonicator. Aliquots were covered with Argon and stored at -80°C. Liposomes were then mixed with the specified buffer and freeze-thawed several times followed by extrusion through a 0.1 or 0.4 μm filter (Avanti Polar Lipids).

2.8.2.2. DivIVA lipid binding

DivIVA lipid binding experiment was performed in Binding buffer BD. Liposomes of different diameters were prepared by extrusion through 0.1 μm, 0.4 μm or 5.0 μm

pore filters. Liposomes (0.5 mg/ml) were mixed in binding buffer prior to the addition of different concentrations of purified DivIVA. After 20 min incubation at room temperature samples were centrifuged (Beckman TL-100 rotor, 80000 rpm, 30 Min, 30°C) and pellet fractions were analysed by SDS-PAGE and Comassie staining. The intensities of DivIVA bands were measured by scanning the stained gels using EPSON Perfection V700 Photo Scanner.

2.9. Synthetic lethal screen

2.9.1. Constructing mutant and unstable plasmid

To construct a *minCD* complete knockout, we amplified by PCR a 2007 bp long DNA upstream of *minCD* using RL 5 and RL 6 primers, and a 1937 bp long downstream regions from the *minCD* genes using RL 9 and RL 10 primers. Upstream and downstream regions were ligated with tetracycline resistance marker inbetween, which was amplified by PCR from pBEST39 plasmid using RL 7 and RL 8 primers. Ligated PCR products with tetracycline resistance cassette were transformed in *B. subtilis* wild type and colonies were selected for tetracycline resistance. The phenotype of the resulting strain RL 33 was confirmed by light microscopy. High proportion of cells producing minicells confirmed lack of the Min system in the constructed strain.

In the same strain we also deleted the *lacA* gene to prevent false positive colonies during the screen.

The *minCD* genes were cloned into the unstable plasmid pLOSS using primers RL 15 with NotI restriction site and RL 12 with BamH1 restriction site. Genes were cloned into the plasmid with their native promoter and the resulting plasmid pRL2 was transformed into RL 33 (the *minCD* deletion strain) to test complementation. Light microscopy confirmed wild type-like phenotype with no minicells, suggesting that the genes cloned into pLOSS completely complemented *minCD* deletion on the chromosome.

2.9.2. Screening

While maintaining selection for pRL2 we transformed pMarB plasmid with the mariner transposon in RL 59. The resulting strain RL 60 was plated with keeping selection for pRL2 and incubated at 50°C allowing transposition of the transposon to occur. The next day, the library was collected and plated on big nutrient agar plates containing X-gal. Plates were incubated at 50ºC for 8 h to push the instability of pRL2 further and then they were transferred to 37°C for overnight incubation. The next day, blue colonies were patched on X-gal plate again and incubated at 50ºC for a few hours before transferred to 37ºC. In this step we got rid of residual plasmid that was still present. Colonies that were sensitive to erythromycin, but resistant to spectinomycin and blue on X-gal plate were potentially synthetic lethal mutants of MinCD (see plasmid descriptions in Table 3). To confirm this, DNA from the potential synthetic lethal mutant was backcrossed into the initial strain RL 59. The resulting strain showed small white colonies that were without pLOSS plasmid and healthy blue colonies with pLOSS plasmid. This confirmed the discovered mutant as ‘synthetic lethal’.

To identify the position of insertion of the transposon, we isolated DNA from the synthetic lethal mutant. DNA was digested with TaqI and purified with PCR purification kit. TaqI digested DNA fragments were ligated with T4 ligase as described above and again purified with PCR purification kit prior to performing inverted PCR reaction. iPCR was performed using Phusion polymerase as suggested by manufacturer. We used primers ipcr1 and ipcr2. To identify the position of the transposon insertion, the products of iPCR were sequenced using ipcr3 primer (see Table 4 for primer list).

Chapter 3: Deletion of *minD* causes a defect in chromosome trapping in prespore during sporulation

3.1. Introduction

Soon after initiation of *B. subtilis* sporulation the two newly replicated chromosomes adopt a new structure called the axial filament. This structure of the bacterial chromosomes stretches from one end of the cell to the other (Figure 1.3), with the *oriC* region of the chromosome attached to the cell pole (Ben-Yehuda et al., 2003). This is partly due to the activity of RacA protein, expressed about 1 h after the initiation of sporulation; it acts to remodel the chromosomes and also to attach the chromosomes to the cell poles (Ben-Yehuda et al., 2005; Ben-Yehuda et al., 2003; Wu and Errington, 2003), and partly due to the action of Spo0J and DivIVA (Perry and Edwards, 2006). This is followed by the formation of an asymmetric septum near one of the cell poles (Errington, 1991). It has been shown that the MinCD complex blocks the formation of the septum at the midcell position during the sporulation; in the absence of MinCD complex, a thin septum can be formed at the midcell position (Barak et al., 1998). The asymmetric septum is formed such that it traps about 30 % of one chromosome in the prespore (Figure 1.4), the smaller compartment of the sporulating cell (Errington, 2003). The remaining 70 % of the chromosome is later transported into the prespore by the SpoIIIE protein (Bath et al., 2000; Wu and Errington, 1994). The other copy of the chromosome remains in the mother cell: the bigger compartment of the sporulating cell. Therefore the prespore and the mother cell each contains one intact chromosome, but activate the expression of different sets of genes in each of the two compartments; different sigma factors control gene expression in the prespore and in the mothercell (Illing and Errington, 1991a; Partridge et al., 1991).

During the early stage of sporulation it is very important to anchor the chromosome to the cell poles, because one copy is destined for the prespore. After chromosomes are anchored to the cell poles, the most important and crucial morphological event is formation of an asymmetric septum and consequently establishment of asymmetry in the sporulating cell. Compartmentalisation of the sporulating cell allows different programs of gene expression in each compartment (Errington, 2003).

To anchor the chromosome to the cell pole, joint action of a number of proteins is needed (Figure 1.4); with RacA, Soj, Spo0J and DivIVA being the most important players (Lee et al., 2003; Sharpe and Errington, 1996; Thomaides et al., 2001; Wu and Errington, 2003). Soj and Spo0J act to condense the *oriC* region of the chromosome, while RacA binds to the chromosome close to the *oriC* and attaches it to the cell pole in a DivIVA dependent manner (Ben-Yehuda et al., 2003; Wu and Errington, 2003). Also DivIVA shows proximity to Spo0J during the sporulation (Perry and Edwards, 2006), suggesting that also this interaction helps to bring the chromosome to the cell pole. The absence of RacA or Soj alone has no significant affect on the trapping of the prespore chromosome, but when both proteins are absent, a dramatic defect of trapping can be observed (Wu and Errington, 2003): the *oriC* region of the chromosome is no longer present in the prespore as it is in wild type cells. Instead, *oriC* seems to remain in the mother cell. This phenotype is similar to that of a null mutant of *divIVA*, which lacks the membrane anchor for the chromosome (Wu and Errington, 2003).

During the vegetative growth DivIVA also acts as a cell pole determinant protein, recruiting Min proteins to the cell poles. The ‘Min’ system inhibits FtsZ

polymerization at the cell poles, but it also seems to act by other mechanism: MinD has been shown to colocalise with the lipid spirals observed in the cells of *B. subtilis* (Barak et al., 2008) which may allow MinD to form a gradient. The 'Min' system is composed of MinJ, MinD, MinC and DivIVA. Preliminary data showed that *minD* mutations, similar to *divIVA*, have a dramatic effect on trapping efficiency, such that the *oriC* is excluded from the prespore, but the regions left and right of *oriC* are trapped in the prespore. This suggests that cell division protein MinD also plays an important role in the establishment of polar attachment of the chromosomes during sporulation. In this chapter, the sporulation defect of the *minD* mutants were examined in detail and confirmed.

In our experiments we made use of the *lacZ* reporter system previously used to map the region of the chromosome trapped in the prespore (Wu and Errington, 2003), of which expression was under the prespore-specific sigma factor SigF. When *lacZ* reporter was trapped in the prespore, the colonies on plates containing X-gal were blue, and when *lacZ* reporter was excluded from the prespore, the colonies on plates containing X-gal were white.

Reporter gene *lacZ* was placed at different locations of the chromosome around the *oriC* region: at -440 kb, -115 kb, -2 kb and +427 kb (Figure 3.1). Growing the strains on agar containing X-gal revealed which parts of the chromosome are trapped into the prespore (blue colonies) and which parts of the chromosome remain in the mother cell (white colonies).

However, the method using *lacZ* reporter only gives information about the whole population of cells. To map the segment of chromosome trapped in the prespore in individual cells, we have also used a dual-reporter system based on fluorescence microscopy; instead of the *lacZ* reporter, prespore-dependent YFP and CFP fusions were placed in the same strain at different positions on the chromosome (Figure 2.3) allowing us to determine the region of the chromosome trapped in the prespore in individual cells (see also Chapter 4).

We have also used a Spo0J-GFP fusion to directly visualize the *oriC* reigon by fluorescence microscopy. Spo0J is a DNA binding protein with majority of its binding sites positioned around the *oriC* and therefore is used as a marker for the origin of replication (Lewis and Errington, 1997).

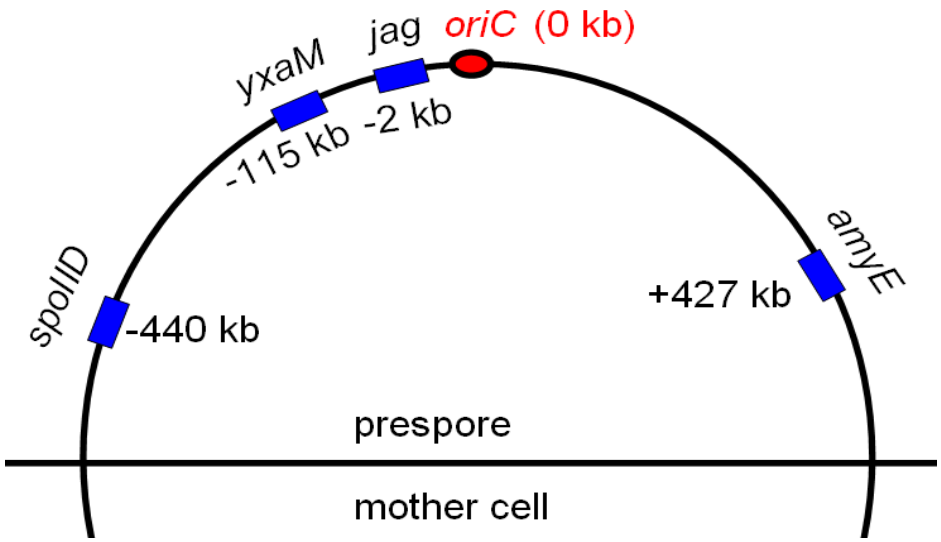

Figure 3.1: Positions of the *lacZ* reporter.
SigF-dependent *lacZ* is positioned at different tested locations around the *oriC* of the chromosome. All tested positions are part of the 30 % of the chromosome that normally is trapped in the prespore when the asymmetric septum is formed.

3.2. Results

3.2.1. Effect of mutations in Min system on the efficiency of prespore chromosome trapping during sporulation

3.2.1.1. **Deletion of *minD* caused a *divIVA*-like trapping defect**

We have noticed that null mutants of *minD* exhibit a Spo- phenotype. To test whether MinD is involved in the polar attachment of chromosomes at the early stages of sporulation, the trapping pattern of a *minD* null mutant was examined using the *lacZ* reporter system (Wu and Errington, 2003), and compared to those of the wild type and a *divIVA* mutant (strain 1920 described in table of strains). Strains carrying the various mutations and the prespore-specific, sigF-dependent lacZ reporter at -440 kb, -115 kb, -2 kb or +427 kb on the chromosome, were grown on plates containing X-gal. As reported previously, in the otherwise wild type background, all the strains produced blue colonies suggesting that parts of the chromosome where reporter genes were placed were trapped in the prespore. This is consistent with the knowledge that wild type cells of *B. subtilis* trap about 30 % of the chromosome in the prespore during the early stage of sporulation: this 30 % of the chromosome includes *oriC* region. Surprisingly, the *minD* mutant produced white colonies when the reporter gene is placed close to the *oriC* of the chromosome, suggesting that the *oriC* is not trapped in the prespore. The observed defect for the *minD* mutants was comparable to previously reported trapping defect of *divIVA* mutant: the region of the chromosomal loci immediately adjacent to *oriC* are not trapped in the prespore (Wu and Errington, 2003), but the flanking regions are trapped correctly. Our experiment confirmed this finding (Figure 3.2).

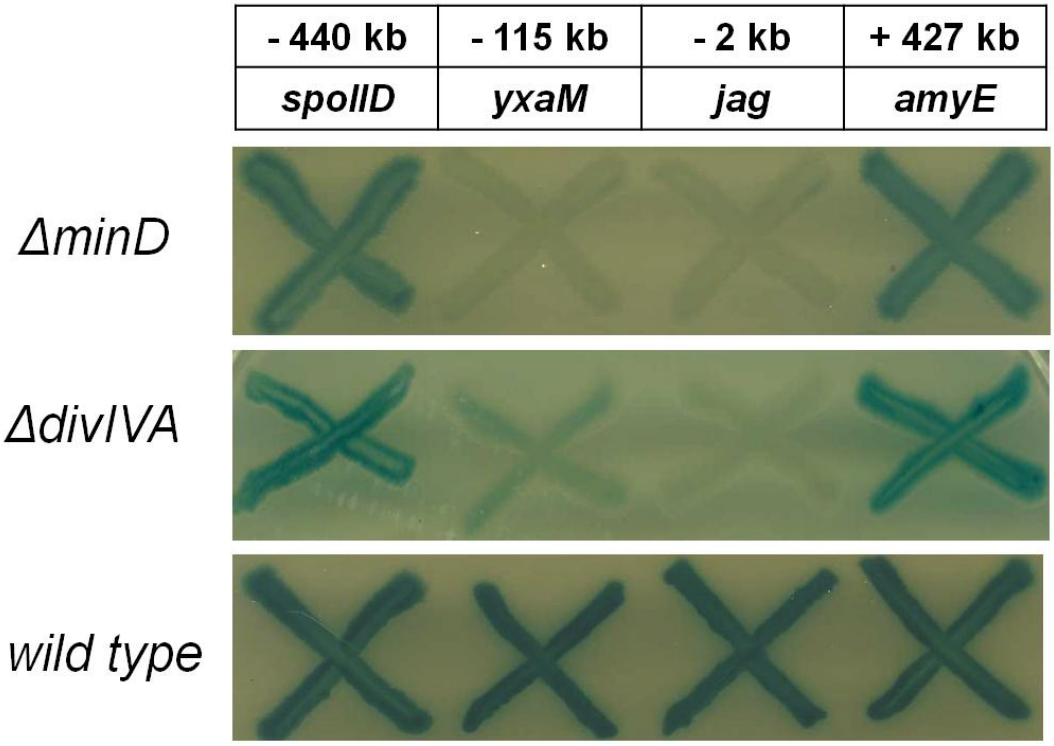

Figure 3.2: Trapping pattern of the *minD* null mutant compared to *divIVA* null mutant and wild type.
minD null mutant has an unexpected trapping phenotype such that the *oriC* is excluded from the prespore (the reporter gene positioned close to the *oriC* is not trapped in the prespore giving white colonies on X-gal plate; strains RL 3 and RL 5) but the flanking regions are trapped in the prespore (reporter gene positioned at *spoIID* or *amyE* location is trapped in the prespore giving blue colonies on X-gal plate; strains RL 1 and RL 4)
Similar to *minD* null mutant, *divIVA* null mutant (strains RL 21, RL 23, RL 24 and RL 25 carrying the *lacZ* reporter (each at different position as presented on Figure 3.1)) do not trap region of the chromosome around *oriC* into the prespore (white colonies), but flanking regions are (blue colonies). The *divIVA* deletion was amplified from the strain 1920 (see table of strains).
Wild type strain of *B. subtilis* traps about 30 % of the chromosome around *oriC* in the prespore. We tested strains 4732, 4733, 4734 and 4735. In our screen, reporter gene is positioned on locations that are trapped in the prespore during the early stage of sporulation (Figure 3.1). This gives blue colonies on the X-gal plate for strains with reporter gene at any position tested; it confirms that chromosomal loci close to the positions of reporter gene are all trapped in the prespore.

3.2.1.2. **MinJ**

MinJ (or MinP as sometimes named) has been shown to be the link between DivIVA at the cell pole and MinD (Bramkamp et al., 2008). Deletion of *minJ* in testing strains showed comparable trapping defect as observed in the *divIVA* null mutant, with the region of the chromosome containing *oriC* excluded from the prespore and the flanking regions trapped in the prespore correctly (Figure 3.3).

3.2.1.3. **MinC, MinD, MinCD**

MinC is the last localized protein in the chain of the Min system and the one that actually inhibits FtsZ polymerisation. It is brought to the location where its activity is needed by MinD, which is at the cell pole via an interaction with MinJ and DivIVA. It is extremely important to note that the Δ*minC* strain used in the majority of this work was derived from one containing a markerless deletion of *minC* that had been constructed using pMAD system, and was checked for retention of the *minC* promoter and expression of MinD. However, strain 3381 incorporated a linked antibiotic marker and despite it performing as expected, requires further characterization to confirm the expression of MinD is identical to the parent and the wild type 168. Testing *minC* deletion for trapping efficiency revealed that *minC* strain has trapping pattern undistinguishable from that of the wild type. Reporter genes at any location around the *oriC* region were correctly trapped in the prespore. In contrast to *minC*, *minD* mutant showed trapping defect similar to that observed for *minJ* and *divIVA* mutants. The region around *oriC* was not trapped in the prespore, but the flanking regions left and right or *oriC* were. Because the double mutant *minCD* showed exactly

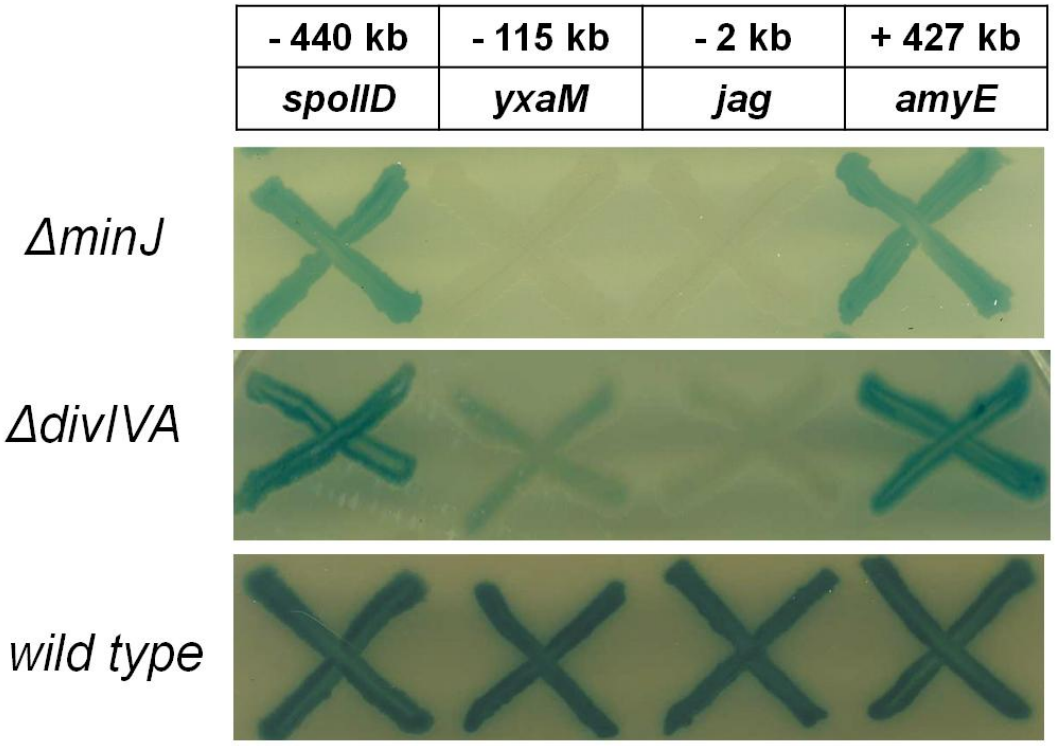

Figure 3.3: Trapping pattern of *minJ* null mutant.
Strains RL 252, RL 253, RL 254 and RL 255 harbouring *minJ* deletion and carrying *lacZ* reporter (each at different location as presented in Figure 8) were tested for trapping efficiency on X-gal plate. Region of the chromosome around *oriC* is not trapped in the prespore (white colonies), but flanking regions are (blue colonies). This is comparable to *divIVA* null mutant.

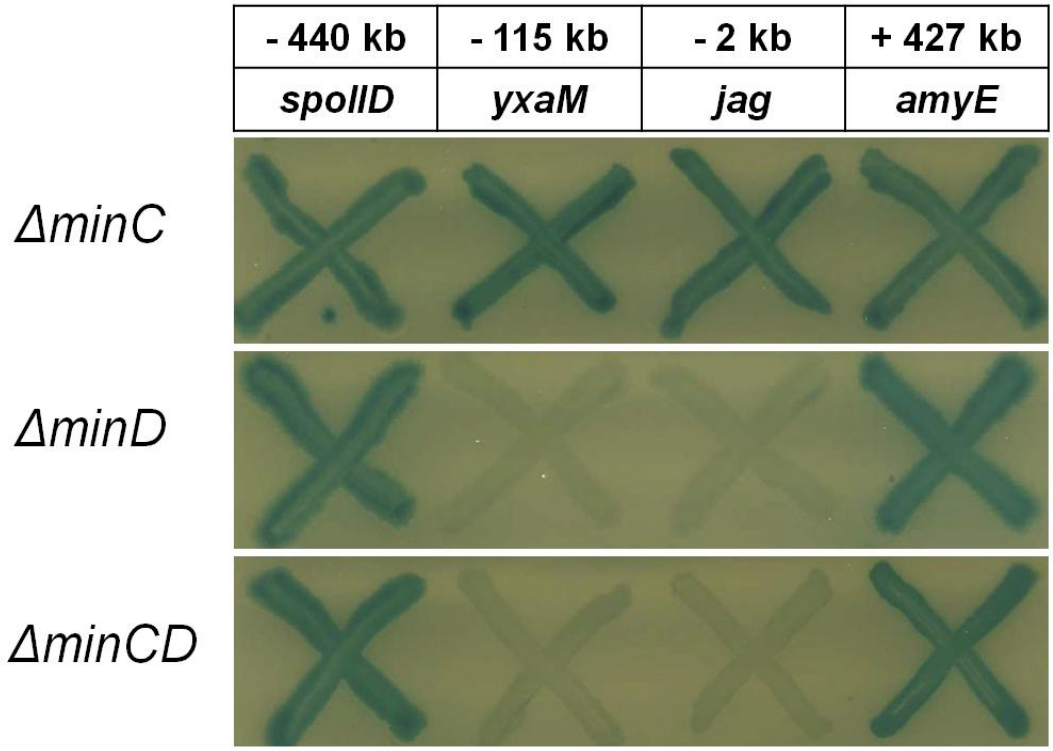

Figure 3.4: Trapping pattern of *minC* null mutant, *minD* null mutant and *minCD* double mutant.
minC single mutant carrying *lacZ* reporter showed trapping pattern undistinguished from the wild type trapping pattern (see Figure 3.2). Reporter gene at any tested position was trapped in the prespore (strains RL 11, RL 13, RL 14, RL 15).
minD null mutant has an unexpected trapping phenotype such that the *oriC* is excluded from the prespore (the reporter gene positioned close to the *oriC* is not trapped in the prespore giving white colonies on X-gal plate; strains RL 3 and RL 5) but the flanking regions are trapped in the prespore (reporter gene positioned at *spoIID* or *amyE* location is trapped in the prespore giving blue colonies on X-gal plate; strains RL 1 and RL 4)
minCD double mutant showed trapping pattern undistinguished from the *minD* null mutant; when reporter gene is positioned close to the *oriC*, it is not trapped in the prespore (RL 8, RL 10), but when positioned more distantly, it is trapped in the prespore (RL 6, RL 9). This suggests that the observed trapping defect is due to the absence of MinD in the cell.

the same trapping pattern as the *minD* null mutant, we suspect that this trapping defect is due to an absence of MinD in the cell and not due to the absence of MinC (Figure 3.4). This result clearly shows that the trapping defect of MinD is not due to the loss of the Min function, but due to the absence of MinD protein: strain lacking *minC* has a wild type-like trapping pattern although in this strain the function of the Min system is lost

3.2.2. The *oriC* region of the chromosome is excluded from the prespore in the absence of MinD

To be able to visualize the *oriC* region of the chromosome, we made use of a Spo0J-GFP fusion. Spo0J binds to 8 binding sites around *oriC* and marks the *oriC* region inside the cell. This also allowed us to quantify the number of prespores trapping the *oriC* region. To visualize the prespores, we used membrane stain. Wild type cells always contained two foci per cell, one close to the each cell pole: one in the prespore and another one in the mother cell. In contrast, in the strain lacking MinD we observed many prespores that contained no foci (the *oriC* of the chromosome was not trapped in the prespore). However, about 66 % of the sporulating cells of *ΔminD* strain (RL 56) still trapped the *oriC* region correctly. Interestingly, often *minD* cells contained more than 2 Spo0J-GFP foci, while in the wild type cells this occurs very rare (Figure 3.5).

We then examined strain lacking *minC* (RL 64) and were able to confirm that it behaved comparably to wild type (RL 57), because more than 90 % of sporulating cells were successful in trapping the *oriC* region of the chromosome during the early stage of sporulation (Figure 3.5 C). This result again confirmed that the trapping

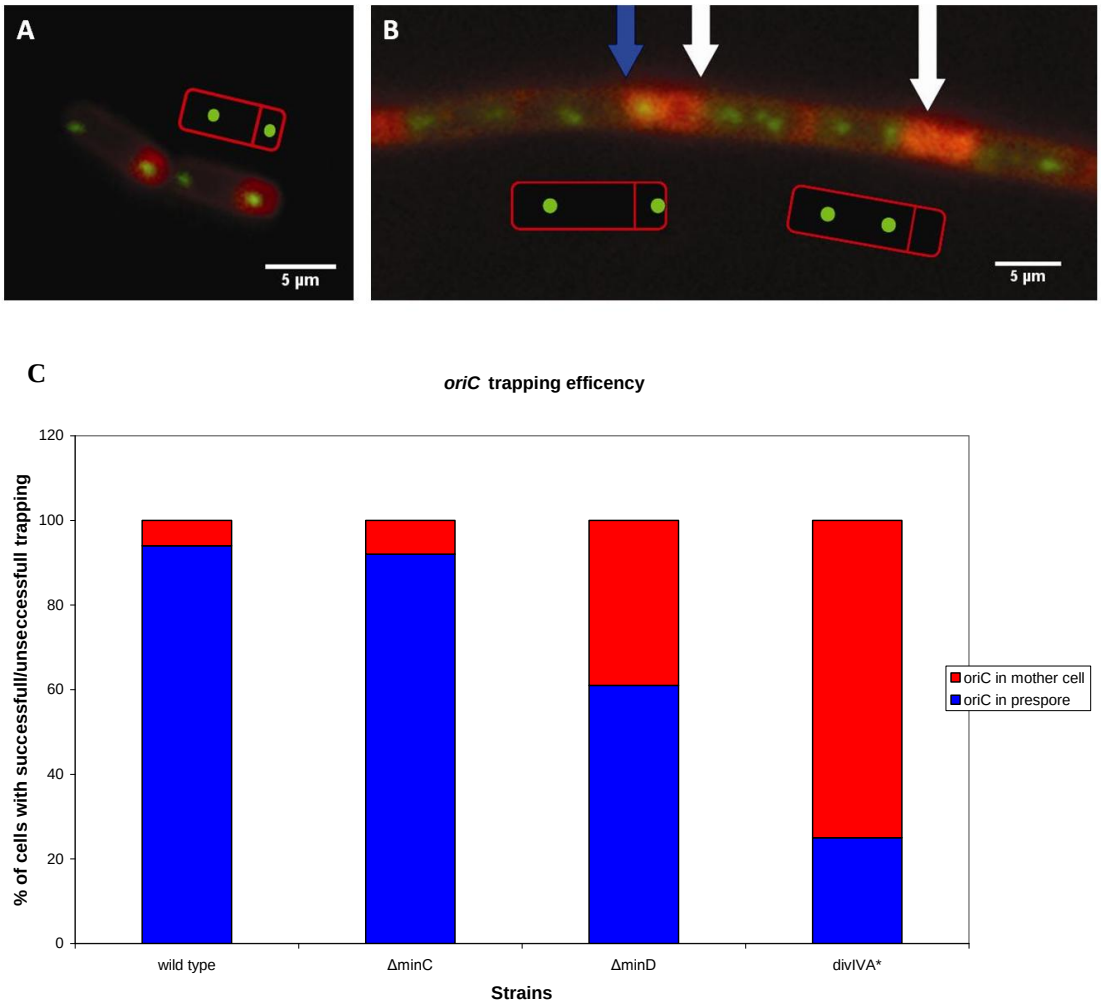

Figure 3.5: Spo0J-GFP localisation and trapping efficiency as determined using Spo0J-GFP comparison

Spo0J-GFP form foci at the *oriC*. Wild type cells always contain one *oriC* region in the mother cell and one in the prespore; green foci surrounded by red membranes (A) whereas *minD* null mutant often contains empty prespore and both *oriC* regions in the mother cell (white arrows) (B). However, some cells manage to trap the *oriC* in the prespore like the wild type (blue arrow) (B).

Comparing trapping efficiency of *minD* (RL 56), *minC* (RL 64) null mutants and *divIVA N99D* point mutant (RL 61) to wild type (RL 57) (C). The red colour represents proportion of the sporulating cell with 'empty' prespores (both copies of *oriC* were in the mother cell) and blue colour represents the proportion of the sporulating cells of which prespores contained *oriC*.

defect observed in strain lacking *minD* (RL 56) is only due to the absence of MinD rather than the loss of the Min function.

To compare the trapping defect caused by the absence of MinD and DivIVA, we have also examined the *divIVA N99D* point mutant (this mutant is not filamentous, and therefore easier to be exmined under the microscope, however, the function of DivIVA is lost) with the Spo0J-GFP fusion (RL 61). Consistent with the result obtained with the *lacZ* reporter, absence of active DivIVA caused a severe defect in the trapping of *oriC*, with only about a quarter of the cells managing to complete this process successfully (Figure 3.5 C).

3.2.3. Trapping defect of *minD* mutants is media-dependant

It has previously been noticed that although *minD* mutants often exhibit a severe Spo- phenotype when grown on nutrient agar plates, when grown in certain liquid media they seem to make spores more efficiently. We have looked into this in more detail and were able to confirm the observation. On nutrient agar plates the wild type and form thick colonies, whereas colonies of the *minD* mutant became lytic and translucent, characteristic of a sporulation defect. When examined using phase contrast microscope, colonies of the wild type were full of spores, but the minD mutant had many dead and lysed cells and only few spores (data not shown).

The resuspension method of Sterlini in Mandelstam (Sterlini and Mandelstam, 1969) was used to study sporulation in liquid medium, where cells were grown in rich medium (CH) until exponential phase then resuspended in sporulation medium to

induce sporulation. Heat-resistant spore counts at 6h after induction of sporulation revealed little difference between the mutants and the wild type (data not shown).

We also examined the trapping frequencies of different chromosomal loci using the strain carrying the prespore specific *lacZ* reporters, by measuring the β –galactosidase activity, produced from the *lacZ* reporter (Figure 3.1). As reported previously, the strains lacking *divIVA* (RL 23 or RL 25) showed reduced trapping efficiency for the reporter genes close to the *oriC* region of the chromosome, which is also in agreement with results obtained on X-gal agar plates (colonies remained white suggesting that reporter gene was not trapped into the prespore). In contrast to results obtained from X-gal plates, the strain lacking *minD* showed only slightly reduced trapping efficiency of the reporter genes close to the *oriC* region (data not shown).

3.2.4. *minD* trapping defect depends on Mg^{2+} concentration

Mg^{2+} ions has been shown to restore cell morphology and growth of mutants in cell shape morphology, such as *mreB* null mutant (Formstone and Errington, 2005). Mg^{2+} ions are also included in the sporulation medium to prevent lysis of sporulation mutants during sporulation. It is possible that the difference in sporulation defect observed for the *minD* mutants was due to different amounts of Mg^{2+} ions present in the media: sporulation medium used in the resuspension method has 40 mM Mg^{2+}. To test this and to identify the optimal concentration of Mg^{2+} required for observing sporulation defects of *minD* mutants, we tested trapping efficiency both on nutrient agar plates and in liquid media containing different concentrations of Mg^{2+}.

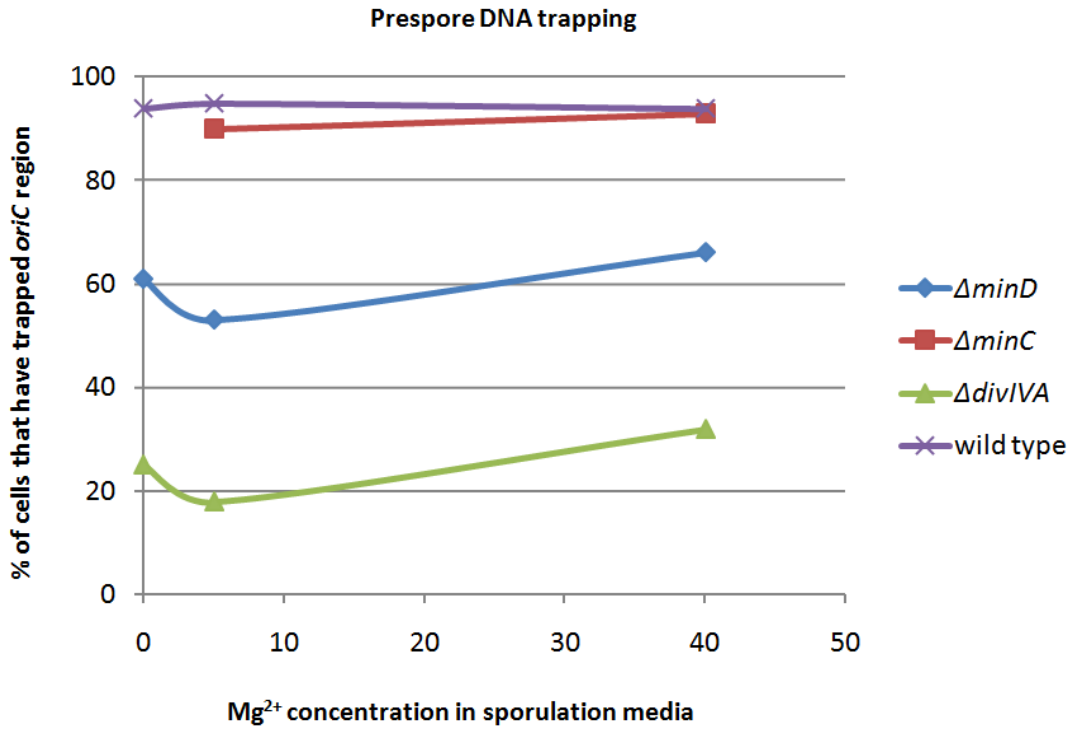

Figure 3.6: Trapping efficiency depends on Mg^{2+} concentration.
Fluorescence microscopy was performed using Spo0J-GFP fusion to localise *oriC* of the chromosome in the sporulating cells. Experiment was repeated in sporulation media containing different concentrations of Mg^{2+}. *minD* and *divIVA* null mutants had lowest trapping efficiency of *oriC* at 5 mM Mg^{2+} in sporulation media and best trapping efficiency of *oriC* at higher concentration of Mg^{2+} (40 mM).

When 40 mM Mg^{2+} was added to the nutrient agar plates with X-gal, trapping of the *oriC* region of the chromosome by the strain lacking *minD* improved (data not shown). Figure 3.6 shows the effect of Mg^{2+} concentration on the trapping defect of the *minD* mutant in liquid. Various concentrations of $MgSO_4$ (0 mM to 40 mM) were included in the sporulation medium and efficiency of *oriC* trapping using Spo0J-GFP fusion was examined under the microscope. The biggest trapping defect was observed for the *minD* null mutant when 5 mM $MgSO_4$ was used. At this concentration, the wild type strain sporulated normally. Therefore all microscopy examinations of trapping were carried out using sporulation medium with 5 mM $MgSO_4$. It is not yet clear why Mg^{2+} ions have an effect on the trapping pattern, however it could be linked to the MreB and cell shape.

3.3. Discussion

Formation of the asymmetric septum soon after the initiation of sporulation leads to the entrapment of part of the prespore chromosome in the prespore compartment. Wild type sporulating cells trap about 30% of the chromosome in the prespore, containing the *oriC* of the chromosome. Preliminary results showed that *minD* null mutants carrying prespore-specific *lacZ* reporters at different locations around the chromosome exhibited a severe trapping defect on plates containing X-gal. The region of the chromosome including the *oriC* is not trapped in the prespore while the flanking regions left and right of *oriC* are. We have confirmed our preliminary result using the same method; *lacZ* reporters at different locations on the chromosome as presented on Figure 3.1. The Δ*minD* trapping pattern and the observed defect on plates containing X-gal is comparable to previously discovered Δ*divIVA* trapping defect (Wu and Errington, 2003). DivIVA is part of a MinD/FtsZ complex during the vegetative growth and is responsible for proper localisation of MinD, but during the sporulation it is found exclusively at the cell poles (Thomaides et al., 2001), and is part of the complex with Spo0J (Perry and Edwards, 2006). During sporulation it may serve as a polar target for RacA and Spo0J to anchor the chromosome to the cell pole (Ben-Yehuda et al., 2003; Perry and Edwards, 2006).

However, it is not clear why *divIVA* mutants have such a severe trapping defect if its main role in sporulation is only to target RacA to the cell poles, as RacA mutants do not have such a severe trapping defect (see Chapter 4, (Wu and Errington, 2003). DivIVA also seems to bring Spo0J to the cell pole and helps to organise and relocate chromosome from the quarter position towards the cell pole (Perry and Edwards, 2006), but again, Spo0J mutant does not have such a severe trapping defect (see

Chapter 4). Moreover, DivIVA mutants that are no longer targeted to the cell pole are still capable of significant level of sporulation (Perry and Edwards, 2004). Results present here suggest that MinD also plays a role in the establishment of chromosome polar attachment. It is therefore most likely that the severe trapping defect of the *divIVA* mutants is partly contributed by the failure of MinD to be recruited to the cell poles.

To confirm the trapping defect we made use of a Spo0J-GFP fusion, which marks the *oriC* and enables us to visualize it in the cell. The results obtained by using Spo0J-GFP fusion in sporulating cells revealed that many cells of the *minD* single mutant during the early stage of sporulation indeed do not contain *oriC* in the prespore as is the case in the wild type cells. Instead, we can often see both *oriC* regions in the mother cell, and an empty prespore.

Cells without MinD are often double the size of the wild type cells due to the division near one of the cell poles. Therefore we initially thought that the trapping defect observed in the *minD* null mutant could be due to the abnormal cell length. To test this, we constructed strain harbouring a *minC* deletion and tested it in our systems. Like *minD* mutants, *minC* mutant cells often divide near one of the cell poles. However, the *minC* null mutant had a wild type-like trapping pattern, and the mutant sporulates efficiently. This demonstrated that the sporulation defect does not result from the loss of the Min function, and that MinD has a separate role in sporulation, acting to ensure that the *oriC* region of the chromosome is included in the prespore compartment.

Surprisingly, the trapping efficiency is medium-dependent, specially the concentration of Mg^{2+} ions in the growing/sporulating media. Testing trapping of the *minD* mutant in sporulation media with different concentrations of Mg^{2+} ions revealed that the trapping efficiency of the *oriC* region in the prespore is lowest at 5 mM Mg^{2+} ions. We do not know the reason for this effect and more experiments has to be done to understand this. Investigation of Mg^{2+} effect under the microscope would be beneficial.

Chapter 4: What is the reason for the *minD* trapping defect?

4.1. Introduction

In order to sporulate, the sporulating cell has to replicate chromosome precisely prior to initiation of the irreversible sporulation process. The key protein that initiates chromosome replication is DnaA (Murray and Errington, 2008). It binds to the region of the chromosome at the *oriC* and mediates open complex formation (Goranov et al., 2009). This is followed by the recruitment of other proteins to assemble into a replisome. There have to be exactly two copies of the genetic material in the sporulating cell and any following replication cycle needs to be inhibited. The most important protein that couples chromosome replication and sporulation initiation is Sda (Veening et al., 2009). It acts as a check point by inhibiting the histidine kinase KinA and consequently allowing Spo0A~P to reach the required level that can initiate sporulation (Burkholder, 2001).

Once chromosomes are replicated, RacA helps to remodel the chromosomes to form an elongated structure such that the *oriC* regions of each chromosome are positioned at the edges and can be anchored to the cell pole (Ben-Yehuda et al., 2003). To attach *oriC* of the chromosome to the pole, a joint action of several proteins is needed (Figure 1.4), including Soj, Spo0J, RacA and DivIVA. Soj and Spo0J, both DNA binding proteins belong to the *par* operon and help to condense the region of the chromosome around the *oriC*. RacA, another DNA binding protein that functions as a kinetochore, attaches the chromosomes to the cell poles in a DivIVA dependent manner (Ben-Yehuda et al., 2003; Lee and Grossman, 2006; Wu and Errington, 2003). It is possible that some of these proteins have redundant functions: both, RacA and Spo0J act together with DivIVA to attach the chromosome to the cell pole.

After chromosomes are attached to the cell poles, the asymmetric septum is formed near one cell pole so that it traps 30 % of one chromosome in the smaller compartment that is called the prespore (Errington, 1991). This 30 % of the chromosome includes the *oriC* region. The remaining 70% of the chromosome is soon transported in the prespore by SpoIIIE DNA exporter (Burton et al., 2007; Kaimer et al., 2009). The other chromosome remains in the bigger compartment of the sporulation cell that is called the mother cell.

In the previous chapter we show that MinD is involved in the establishment of chromosome polar attachment during sporulation; deletion of *minD* causes a trapping defect similar to that of the *divIVA* mutants: the *oriC* of the chromosome is excluded from the prespore while the flanking regions are trapped in the prespore as normally. Microscopy experiments using Spo0J-GFP to localise *oriC* of the chromosome showed that cells lacking MinD sometimes contain more than 2 Spo0J-GFP foci per cell, while cells of wild type contain only 2 Spo0J-GFP foci per cell prior to sporulation. This may suggest that strains lacking MinD have over-replicated chromosomes prior to sporulation, which could be the reason for the observed trapping defect. In this chapter we show that deletion of *minD* did not change the *oriC:ter* ratio significantly. Furthermore, mutants that over-initiate DNA replication did not show *minD*-like trapping defects.

MinD has been shown to help Soj to localise during the vegetative growth (Autret and Errington, 2003; Doubrovinski and Howard, 2005) and Soj helps to deliver chromosome to the cell pole prior to an asymmetric septum formation (Lee and Grossman, 2006). Moreover, very recent findings implicated Soj in the process that

couples chromosome replication and sporulation initiation; Soj has been shown to act as spatially regulated molecular switch that is able to activate or inhibit DNA replication initiation via a direct interaction with DnaA (Murray and Errington, 2008). In this chapter we show that the trapping defect of *minD* could be suppressed by deleting *soj*, suggesting that MinD affects chromosome trapping via Soj, but not due to over-initiation of DNA replication.

4.2 Results

4.2.1. Does *minD* null mutant over-replicate chromosomes prior to sporulation?

We used several different approaches to test whether *minD* mutant over-initiate DNA replication: counting the number of prespores containing *oriC* under fluorescence microscope, following chromosome replication at the onset of sporulation by time-lapse microscopy and measuring the *oriC:ter* ratio by qPCR.

Spo0J binds to 8 sites on the chromosome around the *oriC* (Breier and Grossman, 2007; Lee et al., 2003) so in cells carrying a *spo0J-gfp* fusion, the *oriC* can be seen under the microscope as a GFP foci. We firstly examined exponentially growing cells in CM medium (competence medium). As shown in Figure 4.1A, majority of the wild type cells (about 70 %) had 2 Spo0J-GFP foci per cell, suggesting that there are 2 origins in the cell. The remaining 30 % of the wild type cells had 3 or 4 Spo0J-GFP foci per cell. Similar pattern was observed for the *soj* null mutant (Figure 4.1A), even though *soj* null mutants have been shown to over-initiate DNA replication slightly (Murray and Errington, 2008). Surprisingly, *minD* null mutant showed very low proportion of cells with 2 Spo0J-GFP foci per cell (only about 15 %). The remaining group of the *minD* null mutant cells contained between 3 and 8 Spo0J-GFP foci per cell; mostly there were 4 (37 %) (Figure 4.1A).

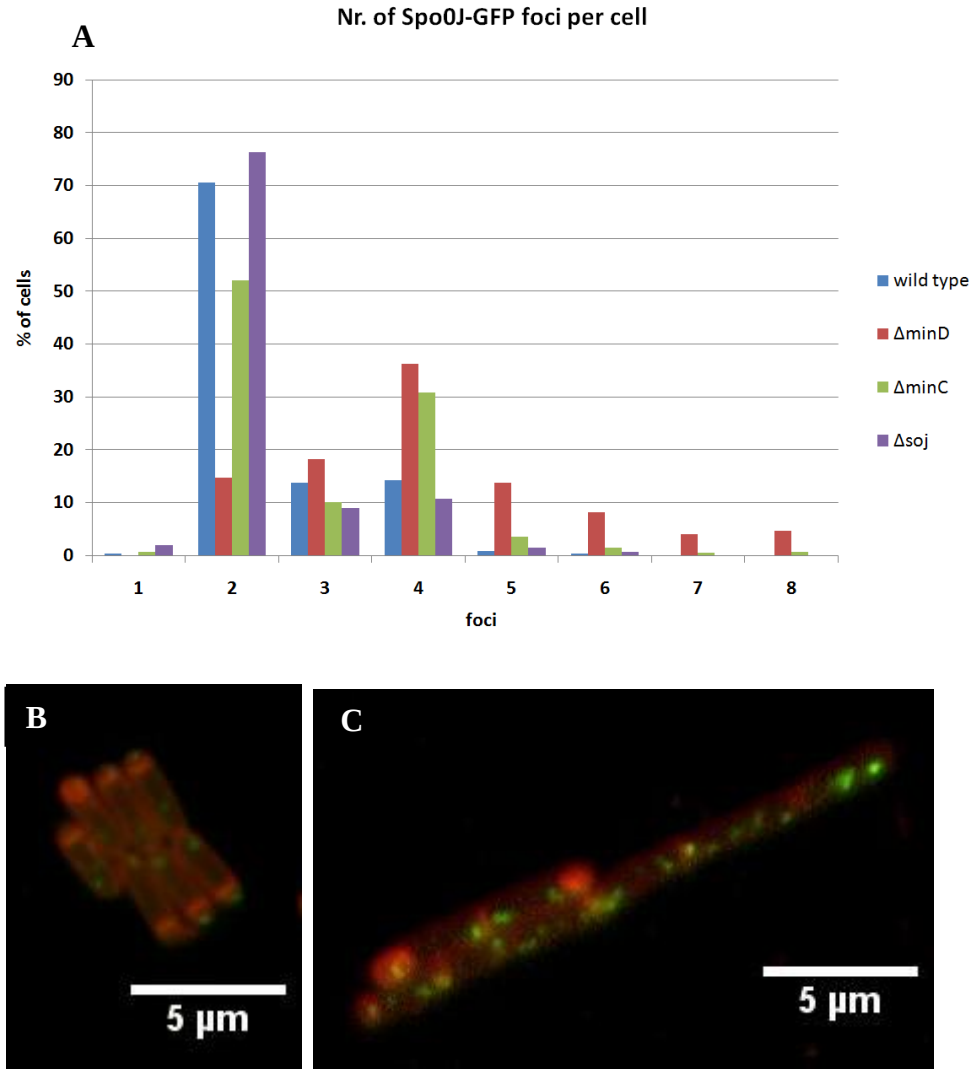

Figure 4.1: Counting Spo0J-GFP foci per cell.
Number of Spo0J-GFP foci per cell during exponential growth in minimal media (A). The strain that stands out from the pattern is *minD* null mutant. It has high proportion of cells with 4 or more Spo0J-GFP foci per cell compared to wild type, which mostly has 2 Spo0J-GFP foci per cell. Also *soj* and *minC* null mutants mostly have 2 Spo0J-GFP foci per cell, however, cells with 4 Spo0J-GFP foci per cell are also frequent in the *minC* null mutant (A). Example of Spo0J-GFP foci in wild type cells (B) and in *minD* null mutant (C).

One possible reason for the prespore trapping defect in *minD* mutants was that DNA replication somehow was able to continue during sporulation when MinD was absent. Consequently, the *oriC* region might be held at the quarter positions instead of being released to the poles, resulting in it being excluded from the prespore. We tested this possibility using a dual-labelling method with DnaX-YFP and SpoIIAA-mCherry. DnaX is part of the replisome and when fused to a YFP it forms visible foci when cells are replicating chromosomes. Foci then disappear once the replication process is finished. SpoIIAA-mCherry is expressed soon after sporulation is initiated and the signal is dispersed through the cell. In the wild type culture of *B. Subtilis* DnaX-YFP could be seen as foci soon after initiation of sporulation, when no SpoIIA-mCherry could be detected. The DnaX-YFP foci disappeared when SpoIIAA-mCherry signal became detectable, because DNA replication should have completed by the time SpoIIAA started to be expressed and no new rounds of replication should be initiated (Figure 4.2). Surprisingly, in *minD* null mutant we could observe cells with both, the DNAX-YFP foci and the SpoIIAA-mCherry signal (Figure 4.2) suggesting that chromosome replication is still ongoing some time after sporulation has been initiated. This result suggested that not all cells of *minD* null mutant stop chromosome replication prior to sporulation initiation. A more detailed figure is presented in Supplementary data of Appendix, showing a montage made of a movie obtained by a time lapse microscopy experiment (Figure A1).

A more reliable method that can give answer to the question of whether *minD* null mutant over-replicates chromosomes prior to sporulation is qPCR (quantitative PCR). By running 2 different PCR reactions with same template, it is possible to relatively compare the number of *ori* regions (origin of replication) to the number of *ter* regions

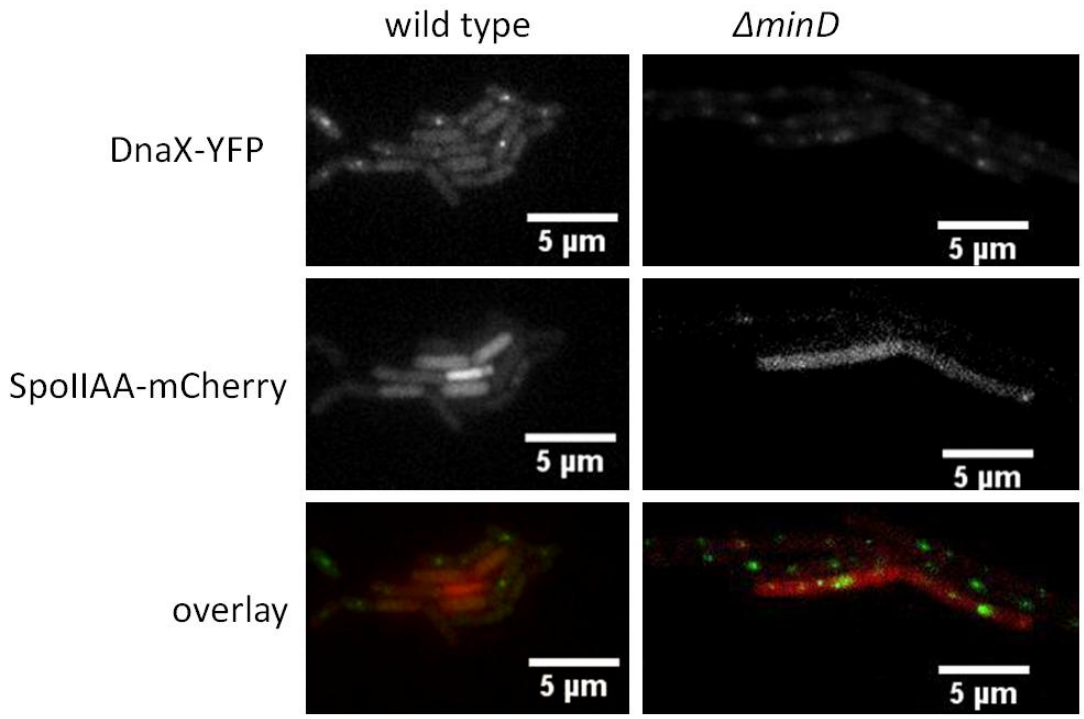

Figure 4.2: Chromosome replication and sporulation initiation.
DnaX-YFP forms foci when cells are replicating the chromosome (green channel), and SpoIIAA-mCherry signal (spread through the cell) indicates initiation of sporulation (red channel). Wild type cells (left figures) finish chromosome replication prior to sporulation initiation: cells expressing SpoIIAA-mCherry (red signal through the cell) do not contain green DnaX-YFP foci. In contrast to wild type cells, not all cells of strain lacking *minD* stop chromosome replication at the time when sporulation has been initiated: some cells contain both, red SpoIIAA-mCherry signal and green DnaX-YFP foci (right figures).

(terminus of replication) in the cell. The ratio *ori:ter* is 1:1 in dormant spores, where there is only one copy of the chromosome and there is no replication ongoing. Growing cells that are replicating chromosomes have a *ori:ter* ratio of more than 2:1.

The wild type and the various mutant strains (1901*(*Δ*minD*), HM161 *(*Δ*soj*) and RL 141*(*Δ*minD* Δ*soj*)) were grown in the rich CH medium and then induced to sporulate by the resuspension method. During vegetative growth, and at the time of induction of sporulation, the wild type strain had an *ori:ter* ratio of about 2.4 (Figure 4.3). The *soj* null mutant had a ratio of 3.2:1, consistent with the reported over-initiation phenotype. The *minD* single mutant, however, showed a comparable *ori:ter* ratio to that of the wild type strain. As sporulation progressed, the ratios of both the wild type and the *minD* mutant decreased to about 1.4:1 at 90 min after sporulation induction. The *ori:ter* ratio of the *soj* single mutant also dropped to about 1.5:1. The *minD soj* double mutant gave similar results to the *soj* single mutant (Figure 4.3).

4.2.2. Effect of DNA binding proteins on trapping efficiency during sporulation

4.2.2.1. Soj and Spo0J

It has previously been reported that deletion of *soj-spo0J* also affects the trapping efficiency of the prespore chromosome at asymmetric septation: the right arm of the chromosome right of *oriC* was trapped in the prespore with lower efficiency than the region of the chromosome left of the *oriC* (Figure 4.4). When only Soj is absent, the trapping pattern seems to be comparable to wild type (Wu and Errington, 2003).

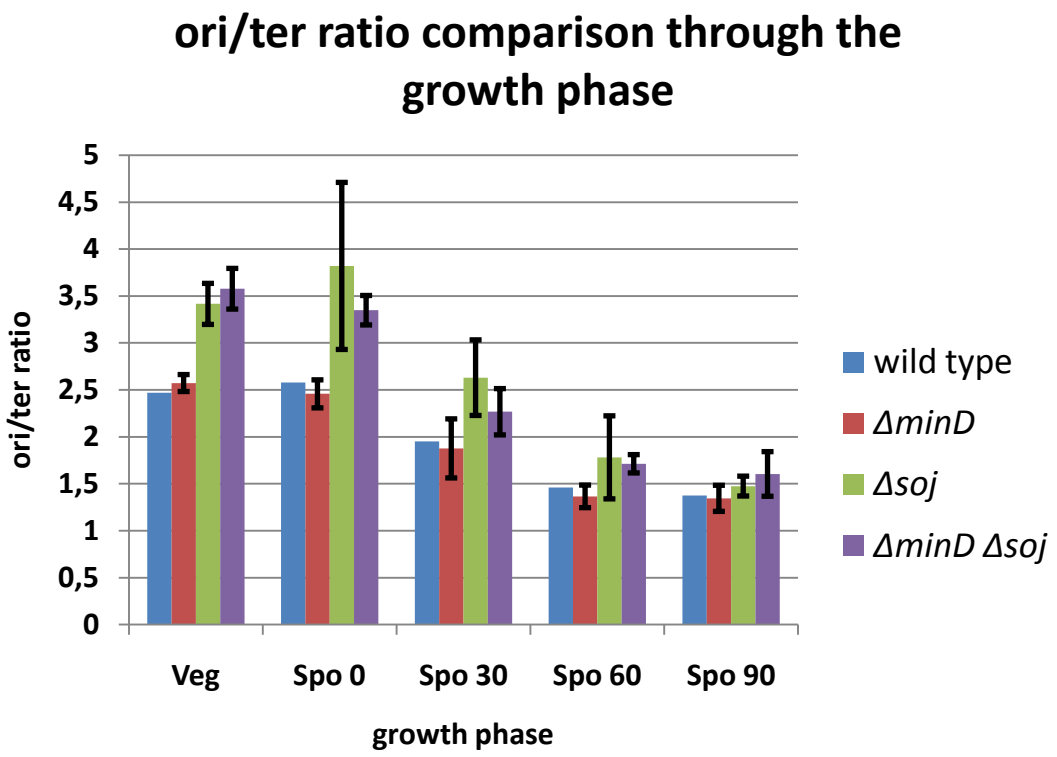

Figure 4.3: MinD mutants have a normal *ori:ter* ratio.
Comparison of *ori:ter* ratio of wild type, *minD* null mutant, *soj* null mutant and *minD soj* double mutant during different stages of growth (Veg; vegetative growth, exponential phase at OD_{600}=0.4, Spo 0; initiation of sporulation, at the time of resuspension, Spo 30; 30 min after resuspension, Spo 60; 60 min after resuspension, Spo 90; 90 min after resuspension. *minD* null mutant showed comparable pattern to the wild type, but *soj* null mutant (and also *minD soj* double mutant) showed slightly higher ratio; chromosomes are slightly over-replicated in strains lacking Soj. Presented data are averaged relative values of each of the three experiments, compared to the wild type.

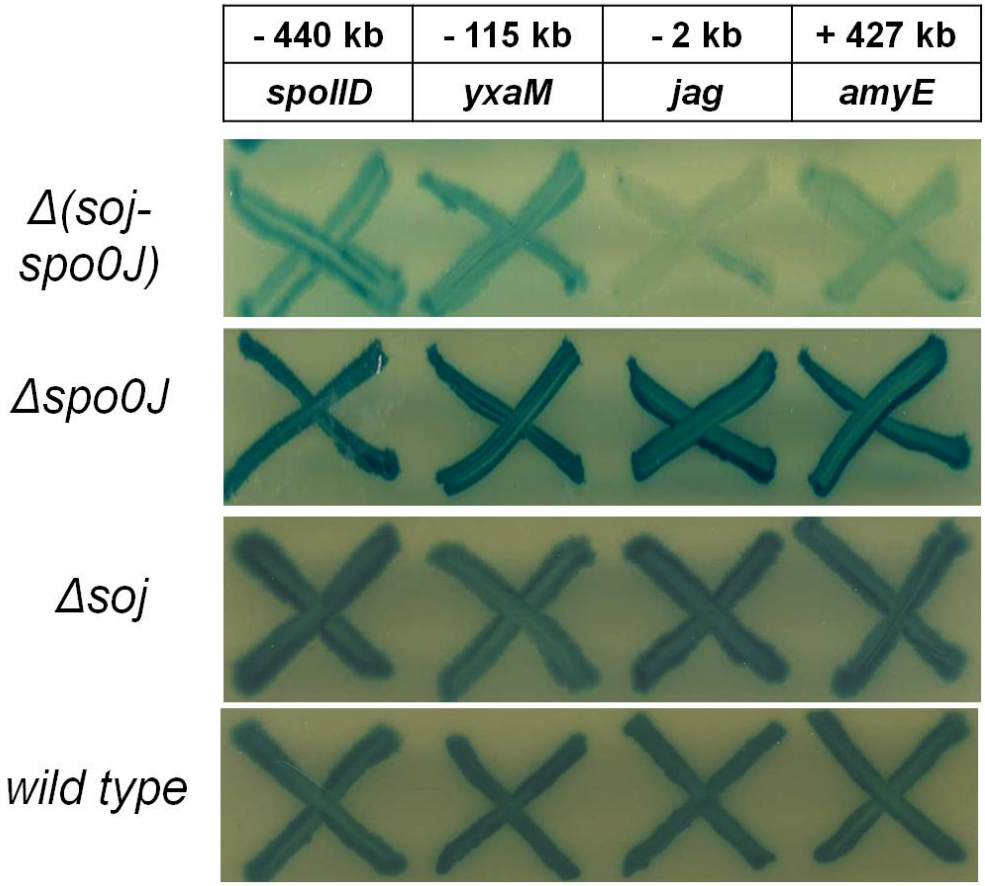

Figure 4.4: Trapping pattern of *soj-spo0J* double mutant and each single null mutant compared to the wild type trapping pattern.
soj-spo0J double mutant carrying *lacZ* reporter showed a trapping defect that was different to the trapping defect of *minD* null mutant. The region of the chromosome right of the *oriC* was trapped into the prespore (RL 29, RL 30) with lower efficiency than the region left of the *oriC* (RL 26, RL 28).
spo0J null mutant showed trapping pattern undistinguished from the wild type trapping pattern. Reporter gene on any tested position was trapped in the prespore. Strains RL 11, RL 13, RL 14, RL 15 were tested on X-gal plate.
Trapping pattern of *soj* null mutant on X-gal plate is undistinguishable from that of the wild type. Reporter gene at any location around the *oriC* region of the chromosome was trapped in the prespore (strains RL 111, RL 113, RL 114, RL 115). Wild type has been previously shown to trap reporter gene at any tested location.

However, the effect of *spo0J* null mutant has not been tested before because *spo0J* mutants are blocked at an early stage of sporulation. To overcome the inhibition to sporulation in *spo0J* mutants, an additional deletion of *sda* is needed, because this check point protein prevents sporulation of *spo0J* mutants. We constructed a *spo0J sda* double mutant, which sporulated normally. Surprisingly, the strain had a wild type-like trapping pattern, indicating that the absence of Spo0J did not affect the trapping of the *oriC* region in the prespore (Figure 4.4).

4.2.2.2. YabA, Sda, DnaA

If the trapping defect of the *minD* mutants is due to over-initiation of chromosome replication, mutations in genes that regulate chromosome replication would be expected to have similar trapping defects. To test this, we determined the trapping patterns of such mutants, including YabA, Sda and DnaA. YabA is a negative regulator of replication initiation by modulating the activity of DnaA (Goranov et al., 2009; Hayashi et al., 2005). Deletion of *yabA* therefore results in over-replicated chromosomes. Sda is a check point protein coupling chromosome replication and sporulation initiation (Veening et al., 2009). When Sda is absent, sporulation can be initiated also under the conditions of DNA replication stress. We first tested the single mutants of *yabA* and *sda*; both showed a wild type-like trapping pattern, suggesting that trapping is not affected by the absence of any of these two proteins (Figure 4.5). We also tested a DnaA point mutant (*dnaA S326L*) that causes over-replication of chromosomes (Murray and Errington, 2008). It should be noted that we could not test the trapping efficiency of the *dnaA* point mutant in the presence of Sda in the cell, so we had to delete *sda* to remove the check point. The trapping pattern of the

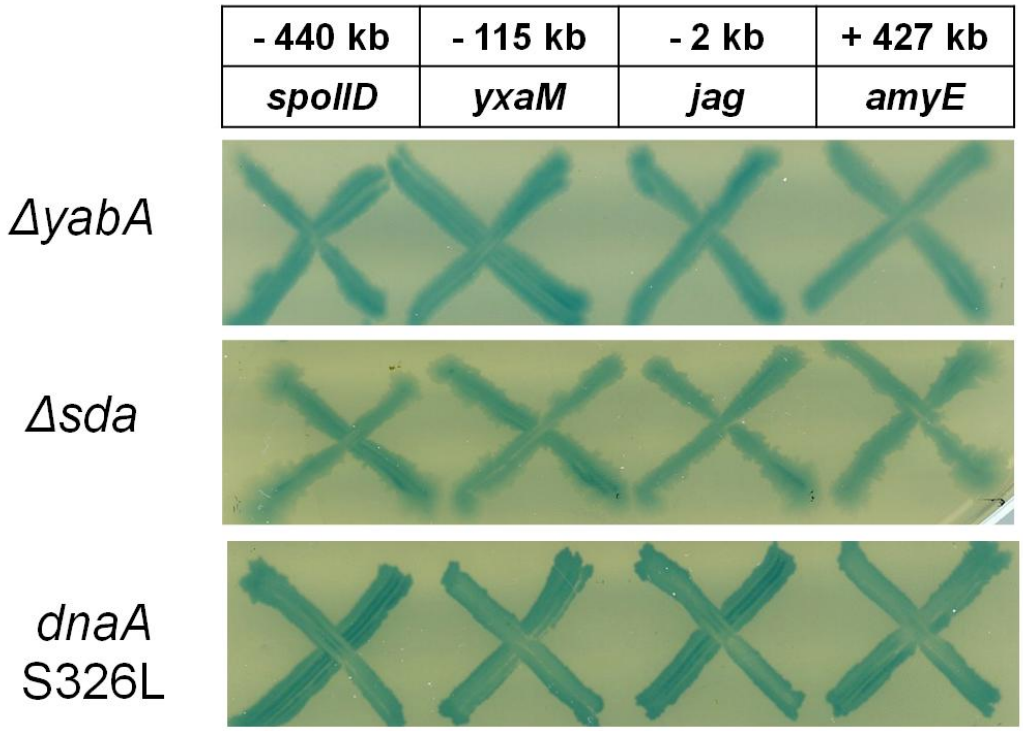

Figure 4.5: Trapping pattern of *yabA* null mutant, *sda* null mutant and *dnaA S326L* mutant

yabA null mutant carrying *lacZ* reporter did not show any trapping defect; *yabA* null mutant (strains RL 200, RL 201, RL 202, RL 203) had trapping pattern on X-gal plate comparable to that of the wild type.

Prespore trapping pattern of *sda* null mutant carrying *lacZ* reporter (strains RL 219, RL 220, RL 221, RL 222) also did not show any defect. Reporter genes at any location of the chromosome around *oriC* were trapped in the prespore as in the wild type.

dnaA S326L mutant with absent *sda* and carrying *lacZ* reporter over-replicates chromosomes (strains RL 234, RL 235, RL 236, RL 237). However, trapping pattern is not perturbed and is comparable to the wild type trapping pattern, with reporter gene being trapped in the prespore at any location around the *oriC*.

We first tested the single mutants of *yabA* and *sda*; both showed a wild type-like

sda dnaA SS326L double mutation was comparable to that of the wild type, again suggesting that chromosome over-replication under the conditions tested did not cause trapping defect (Figure 4.5).

4.2.3. Trapping pattern of the combined mutants

Previous results showed that *racA soj* double mutant lost trapping of *oriC* in the prespore, which is similar to what happens in *minD* single mutant, although all these proteins act at different stages of chromosome trapping. Therefore, we thought it would be interesting to investigate also combined mutants.

4.2.3.1. Δ*yabA* Δ*minD* and Δ*sda* Δ*minCD dnaS326L*

Strains lacking YabA over-replicate chromosomes. A null mutant showed a trapping pattern that was indistinguishable from the wild type. We then combined the *yabA* and the *minD* null mutants and examined the trapping pattern of the double mutant. The combined double mutant showed a trapping pattern typical of the *minD* single mutant (Figure 4.6).

To combine the *sda* null mutant with *minD*, we used a *minCD* double mutant because of the lack of antibiotic resistance markers available. The *minCD* double mutant has the same trapping defect as the *minD* single mutant (Figure 3.4). Again, the triple mutant showed a trapping pattern typical of the *minD* single mutant (Figure 4.7).
Surprisingly, a quadruple mutant *(*Δ*sda, dnaA326L,* Δ*minCD*) showed a wild type-like trapping pattern despite of the presence of the *minD* mutant (to test *dnaA326L*

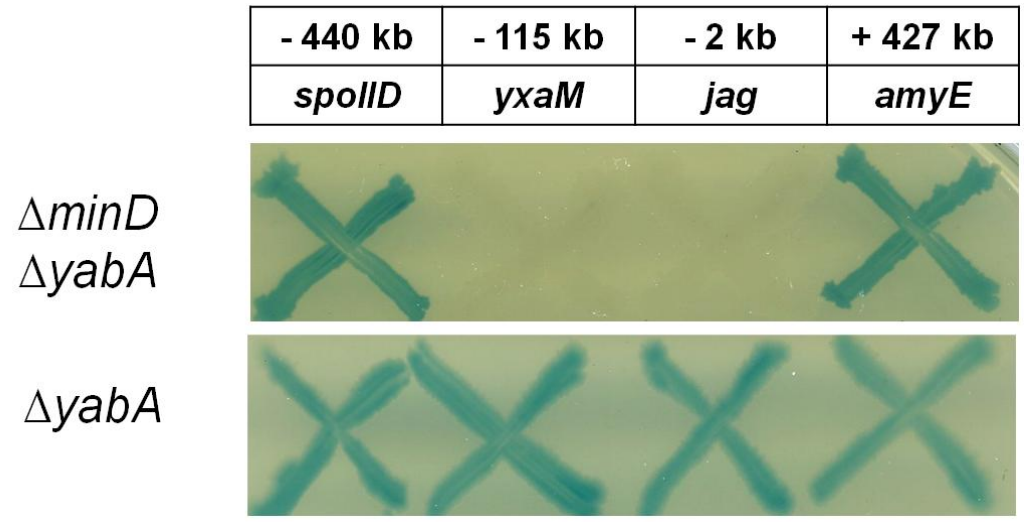

Figure 4.6: Trapping pattern of *yabA minD* double mutant compared to *yabA* single mutant
Double mutant *yabA minD* (strains RL 211, RL 212, RL 213, RL 214) carrying *lacZ* reporter. The region around the *oriC* is not trapped in the prespore, but the flanking regions are. Trapping pattern is undistinguishable from the *minD* null mutant trapping pattern (Figure 3.2). In contrast, *yabA* single mutant showed wild type-like trapping pattern.

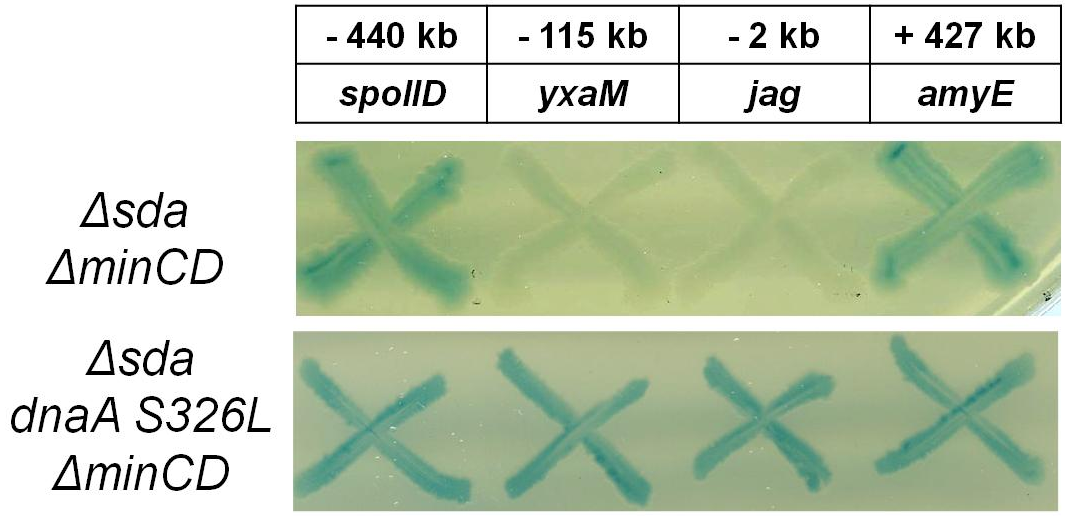

Figure 4.7: Trapping pattern of *sda minCD* triple mutant and *sda, dnaAS326L minCD* quadruple mutant.
sda minCD triple mutant carrying *lacZ* reporter (strains RL 215, RL 216, RL 217, RL 218) had trapping pattern comparable to *minD* null mutant (Figure 3.2), but *sda, dnaAS326L minCD* quadruple mutant carrying *lacZ* reporter (strains RL 230, RL 231, RL 232, RL 233) showed improved trapping efficiency when compared to *minD* null mutant.

Δ*minCD* mutant the *sda* check point had to be deleted in order to allow cells to initiate sporulation). In this case, over-replication of the chromosomes seemed to improve the trapping, with the region of the chromosome around *oriC* being present in the prespore more frequently than in the triple mutant.

4.2.3.2. Δ*racA,* Δ*minD* and Δ*racA,* Δ*soj*

RacA is a sporulation specific protein, expressed only during the early stage of sporulation (Ben-Yehuda et al., 2003). It reorganises chromosomes after replication to form an elongated structure called axial filament, which is then anchored to the cell pole via a direct interaction between RacA and DivIVA (see Chapter 6). Surprisingly, deletion of *racA* shows no defect on trapping pattern on X-gal plates (Figure 4.8) (Wu and Errington, 2003). This probably indicates that RacA is only involved in the latest stage of anchoring the chromosome to the cell pole, but not also in the organisation and relocation of the *oriC* from the quarter position of the cell. To achieve *oriC* relocation from the quarter position towards the cell pole, Spo0J, Soj, MinD and DivIVA are crucial (Perry and Edwards, 2006). Moreover, RacA is not the only protein that has been shown to help to anchor the chromosome to the cell pole. Spo0J and DivIVA form a complex during the early stage of sporulation (Perry and Edwards, 2006), which might be sufficient for the attachment of the chromosome to the cell pole.

When combining *racA* single mutant with *minD* single mutant, the *racA minD* double mutant showed a *minD*-like trapping pattern, though in general the trapping efficiency

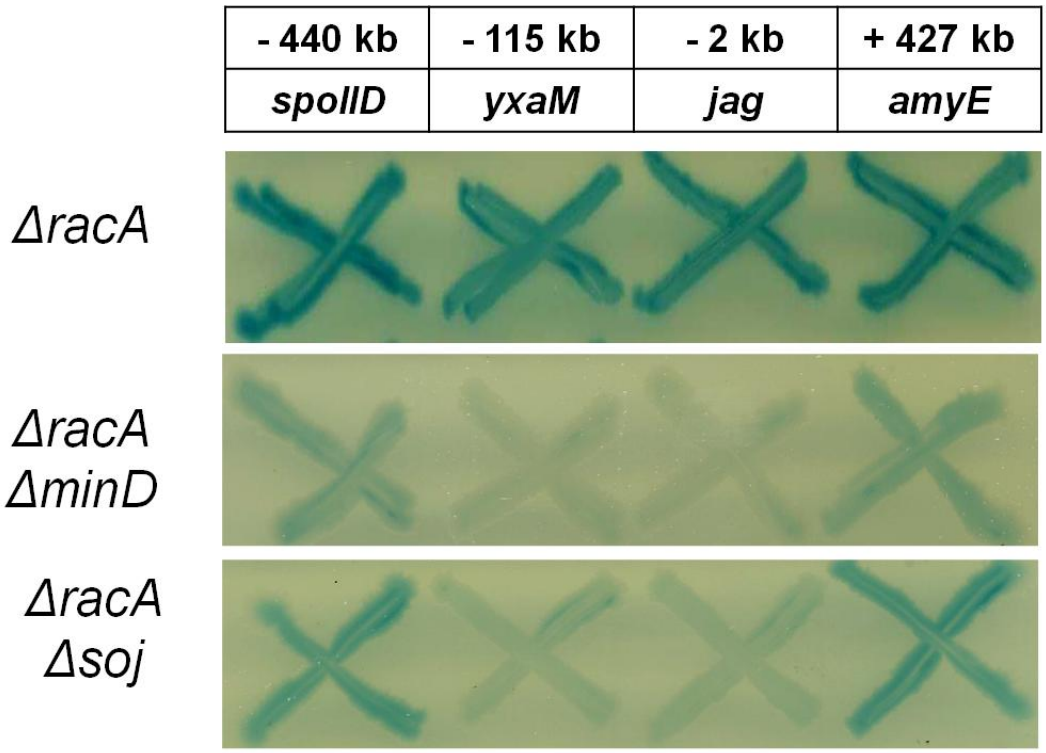

Figure 4.8: Trapping pattern of *racA minD* and *racA soj* double mutants compared to *racA* single mutant.
As it has been shown previously, *racA* single mutant carrying *lacZ* reporter showed no defect on trapping pattern on plate containing X-gal. Reporter gene *lacZ* was trapped in prespore comparably to wild type, not depending on the position (strains RL 16, RL 18, RL 19, RL 20).
racA minD double mutant carrying *lacZ* reporter (strains RL 277, RL 278, RL 279, RL 280) showed less effective prespore trapping ability when compared to each single mutant (Figure 3.2).
Also *racA soj* double mutant carrying *lacZ* reporter (strains RL 321, RL 322, RL 323, RL 324) showed reduced ability to trap *oriC* when compared to the wild type, as it had been reported previously. However, trapping efficiency is slightly better than the one of *racA minD* double mutant.

was lower (see Figure 4.8) when compared to the *minD* single mutant. This is probably because in the absence of RacA only about 50% of the prespores manage to capture DNA, and that the two proteins act at different steps of chromosome trapping. The *racA minD* double mutant also showed lower trapping efficiency than the *racA soj* double mutant. As previously reported, the *racA soj* double mutant had a trapping pattern similar to that of the *minD* mutant; colonies with reporter gene close to the *oriC* were almost white. This could indicate that some sporulating cells of double mutant *racA soj* are still able to trap *oriC* of the chromosome into the prespore, but with lower efficiency than the wild type (Figure 4.8).

4.2.3.3. Δ*racA,* Δ*minD,* Δ*soj*

The phenotypes of the *racA minD* and the *racA soj* double mutants suggested that *minD* and *soj* might have a comparable role in trapping process, so we constructed a *racA minD soj* triple mutant by introducing a *soj* null mutant into the *racA minD* double mutant. Interestingly, the triple mutant no longer had a *minD*-like trapping defect. Instead, all the markers showed similar frequency of trapping in the prespore, albeit at a reduced level compared to the wild type (Figure 4.9).

4.2.3.4. Δ*minD,* Δ*spo0J*

A *spo0J* null mutant (in order to allow *spo0J* null mutant to sporulate, *sda* check point was also deleted in these strains) showed no trapping defect although Spo0J has been implicated to play a role in chromosome attachment to the cell pole (Perry and Edwards, 2006). To investigate this further, we combined *spo0J* and *minD* null

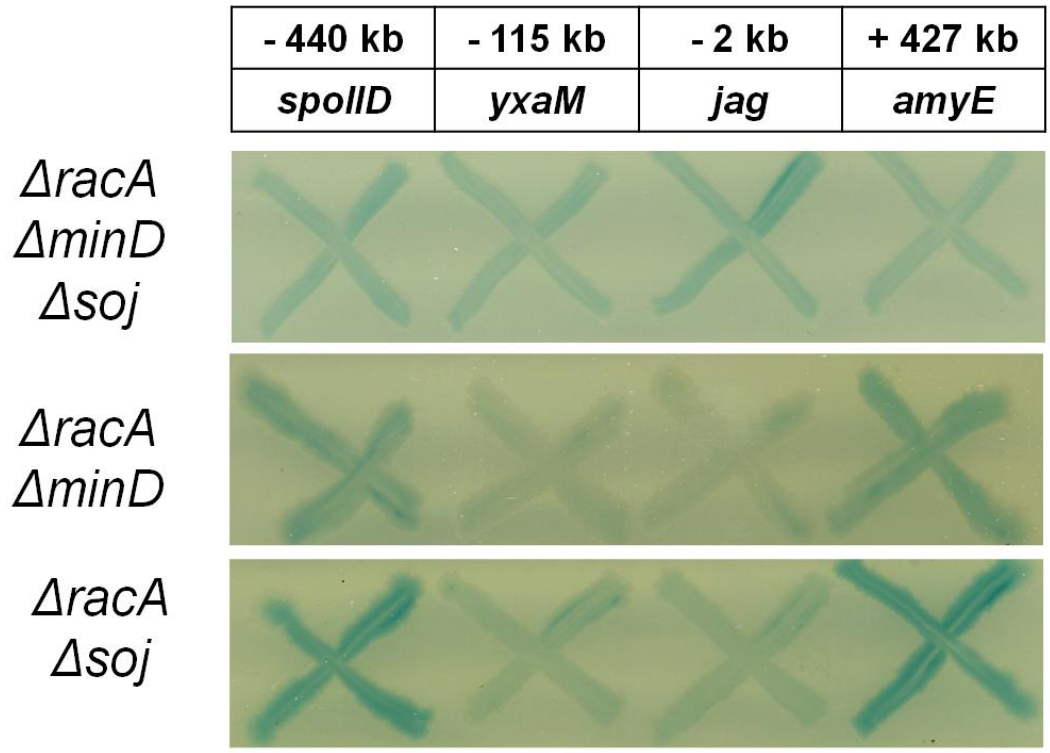

Figure 4.9: Trapping pattern of *racA minD soj* triple mutant, compared to *racA minD* and *racA soj* double mutants.
racA minD soj triple mutant carrying *lacZ* reporter (strains RL 281, RL 282, RL 283, RL 284) showed improved trapping efficiency compared to *racA minD* double mutant, probably because the absence of Soj suppresses the trapping defect caused by Δ*minD*. We could also no longer observe the trapping defect that is typical for *racA soj* double mutant.

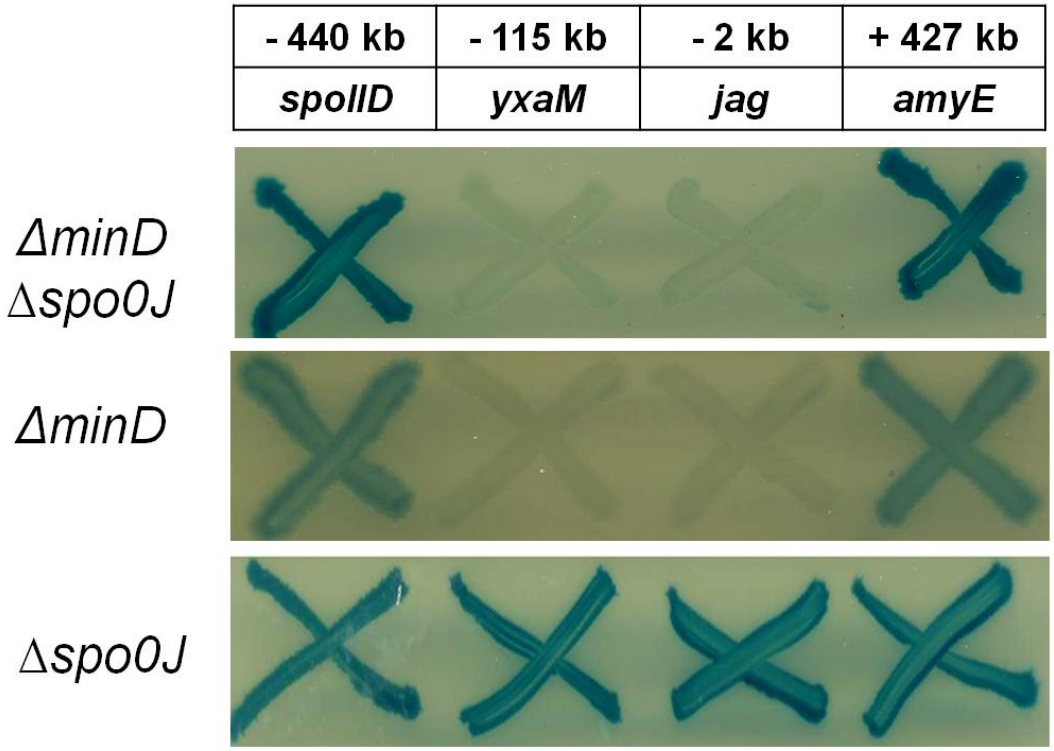

Figure 4.10: Trapping pattern of *minD spo0J* double mutant.
minD spo0J double mutant carrying *lacZ* reporter (strains RL 392, RL 393, RL 394, RL 395) had trapping defect comparable to Δ*minD* null mutant; the *oriC* of the chromosome is excluded from the prespore. In contrast, *spo0J* single mutant (RL 376, RL 377, RL 378, RL 379) had wild type-like trapping pattern.

mutations and then tested their effect on trapping. The double mutant gave a trapping pattern typical for *minD*: the *oriC* of the chromosome was excluded from the prespore.

4.2.3.5. Δ*minD,* Δ*(soj-spo0J)* compared to Δ*racA,* Δ*(soj-spo0J)*

Combining the *soj-spo0J* double deletion with the *minD* null mutant (Δ*minD* Δ*(soj-spo0J)* triple mutant) showed a significantly reduced trapping efficiency for the reporter genes at all the four locations tested (Figure 4.11). This is similar to a previous report on the *racA spo0J soj* triple mutant, which showed that prespores of triple mutant contain no or very little DNA. To confirm this, we have constructed a new *racA spo0J soj* triple mutant by using *spo0J-soj* double mutant with different marker. The new *racA spo0J soj* triple mutant had a similar trapping defect as reported. Therefore, although deletion of Spo0J has little effect on chromosome trapping when Soj is present, in the absence of Soj, Spo0J is required for the trapping of the chromosomal region flanking *oriC*. This is probably via previously reported DivIVA/Spo0J complexes (Perry and Edwards, 2006), which seem to be even more important in chromosome trapping process when Soj is absent.

4.2.3.6. Δ*minD* Δ*racA* Δ*(soj-spo0J)*

As expected, the quadruple mutant Δ*minD* Δ*racA* Δ*(soj-spo0J)* showed a severe trapping defect (strains RL 360, RL 361, RL 362, RL 363) similar to the triple mutant in 4.2.3.5.. Colonies with *lacZ* reporter gene at any location tested were white

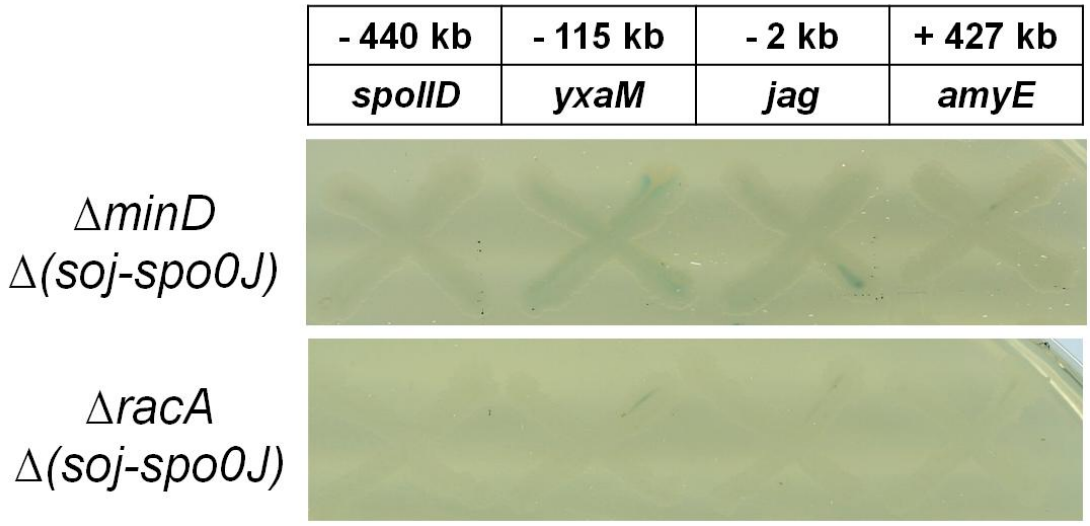

Figure 4.11: Trapping pattern of *minD (soj-spo0J)* and *racA (soj-spo0J)* triple mutants.
minD (soj-spo0J) triple mutant carrying *lacZ* reporter (strains RL 352, RL 353, RL 354 and RL 355). Due to the absence of 3 main actors helping to anchor the chromosome to the cell pole, trapping efficiency is significantly lower than the one of the wild type, but very few cells can still manage to trap some DNA
racA (soj-spo0J) triple mutant carrying *lacZ* reporter (strains RL 344, RL 345, RL 346, RL 347); the absence of these 3 proteins causes severe defect in trapping efficiency, such that prespores do not contain reporter gene at any location tested. This suggests that prespores contain very little or no DNA.

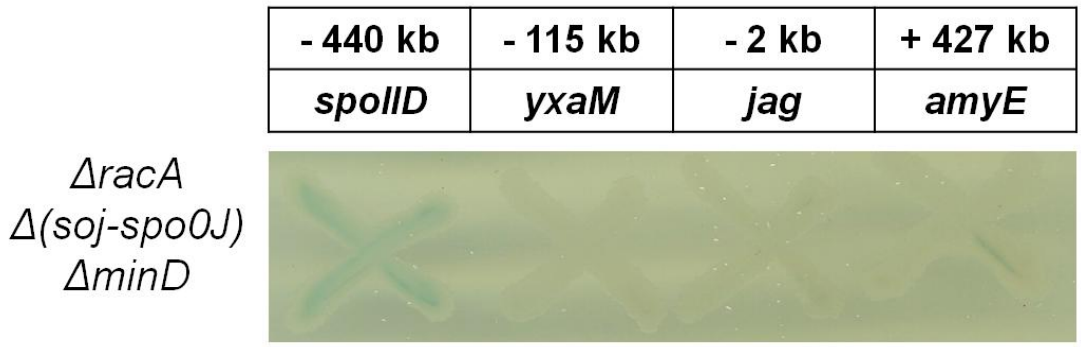

Figure 4.12: Trapping efficiency of *minD racA (soj-spo0J)* quadruple mutant.
minD racA (soj-spo0J) quadruple mutant carrying *lacZ* reporter (strains RL 360, RL 361, RL 362, RL 363); prespores of tested quadruple mutant most likely contain no DNA as they are severely defected in trapping ability; prespores do not trap reporter gene at any location tested.

(reporter not trapped in the prespore) (Figure 4.12). This confirmed the importance of these 4 proteins in trapping process.

4.2.4. Summary of the trapping patterns

Table 6: Trapping pattern summary of mutants

STRAIN	*spoIID*	*yxaM*	*jag4*	*amyE*
WT	X	X	X	X
ΔminD	X	X	X	X
ΔminC	X	X	X	X
ΔminCD	X	X	X	X
ΔminJ	X	X	X	X
ΔdivIVA	X	X	X	X
ΔracA	X	X	X	X
Δsoj	X	X	X	X
ΔminD Δsoj	X	X	X	X
sojG12V	X	X	X	X
ΔminD sojG12V	X	X	X	X
sojD40A	X	X	X	X
ΔminD sojD40A	X	X	X	X
ΔyabA	X	X	X	X
ΔminD ΔyabA	X	X	X	X
Δsda	X	X	X	X
Δsda Δspo0J	X	X	X	X

Δsda Δspo0J ΔMinD	X	X	X	X
Δsda DnaA S326L	X	X	X	X
Δsda DnaA S326L, ΔminCD	X	X	X	X
ΔminD ΔracA	X	X	X	X
ΔminD ΔracA Δsoj	X	X	X	X
ΔracA Δsoj	X	X	X	X
ΔminD Δ(soj-spo0J)	X	X	X	X
Δ(soj-spo0J)	X	X	X	X
ΔminD Δ(soj-spo0J) ΔracA	X	X	X	X
ΔracA Δ(soj-spo0J)	X	X	X	X

4.2.5. Suppressors of trapping defect

4.2.5.1. Deletion of *soj* suppresses the *minD* trapping defect

Because the localization of Soj has been reported to be dependent on MinD (Autret and Errington, 2003) and because *soj racA* double mutants have a *minD*-like trapping pattern, it was interesting to examine the trapping pattern of the *minD soj* double mutant.

Interestingly, combined *minD soj* double mutant had a wild type-like trapping pattern (Figure 4.13). This result suggested that deletion of *soj* was able to suppress the trapping defect of the *minD* null mutant.

To investigate this further, we also tested the trapping efficiency of the *minD soj* double mutant with a wild type copy of *soj* under the xylose inducible promoter to see the effects of different concentrations of Soj on trapping. In the absence of xylose (i.e. no or little Soj) the trapping pattern of the mutant was similar to that of the *minD soj* double mutant, and was comparable to the wild type. Increasing concentrations of xylose (increasing concentration of Soj) caused defects in the trapping of the *oriC* region that is more and more similar to the *minD* null mutant (Figure 4.14).

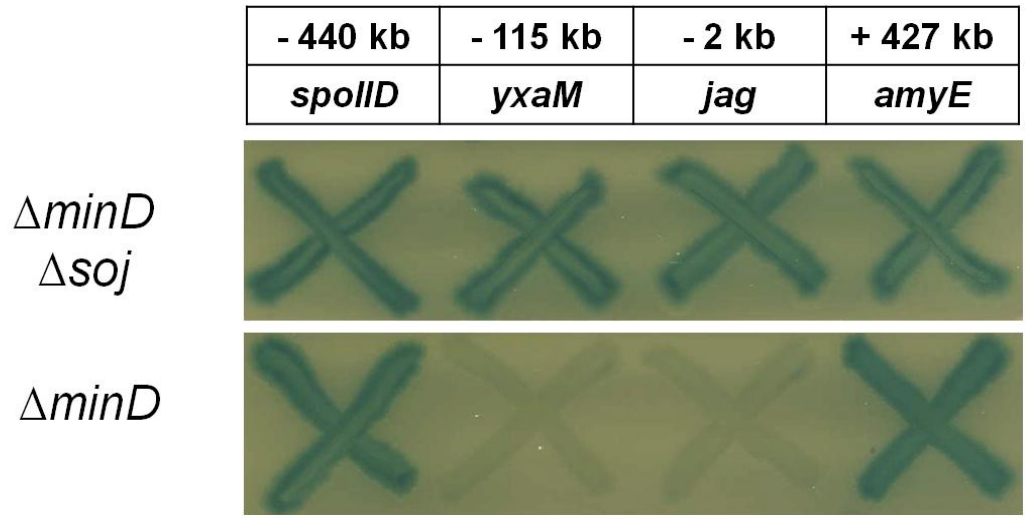

Figure 4.13: Trapping efficiency of *minD soj* double mutant.
In *minD soj* double mutant carrying *lacZ* reporter (strains RL 136, RL 138, RL 139, RL 140) we could not observe trapping defect typical for *minD* null mutant. *oriC* of the chromosome was trapped in the prespore.

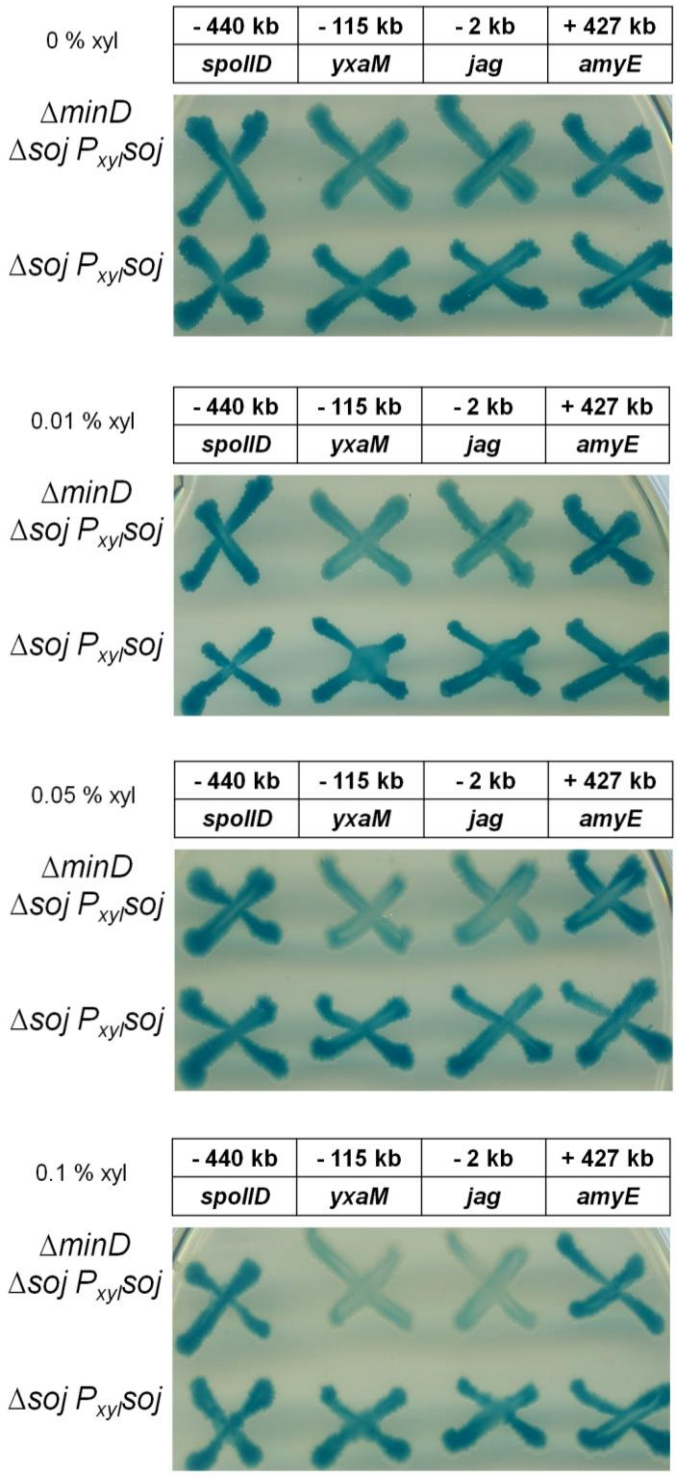

Figure 4.14: The effect of different amounts of Soj on trapping pattern.
Soj was expressed from the xylose inducible promoter on plates with different amounts of xylose as indicated at each figure. Strains with MinD (lower level: RL 123, RL 125, RL 126, RL 127) are compared to strains without MinD (upper level: RL 131, RL 133, RL 134, RL 135). In the absence of MinD, there is no trapping defect when Soj is absent (the top nutrient agar plate with no xylose). Increasing concentration of Soj causes increased trapping defect in the absence of MinD (upper level on each figure). However, when MinD is present in the cell, different concentrations of Soj have no effect on trapping pattern (lover levels on each figure).

4.2.5.2. Not all *soj* mutants can suppress the *minD* trapping defect

Soj has, beside condensing the chromosome, another important function; it controls chromosome replication through DnaA (Murray and Errington, 2008). This is important, as chromosome needs to be replicated prior to sporulation and at the same time, another round(s) of replication must be inhibited once sporulation proceeds. Suppression of the *minD* trapping defect by deletion of *soj* suggested that the defect was mediated through Soj. However, the fact that the *soj* null mutant and the *dnaA S326L* mutant, both over-initiate DNA replication, had a wild type-like pattern suggested that the *minD* defect was not a result of over-initiating DNA replication. To examine this further, we tested 2 *soj* mutants; *soj G12V* (lost DNA binding activity) and *soj D40A* (still able to bind DNA molecule but is trapped in a dimer form) with under-replicating and over-replicating effect on chromosome replication, respectively. To our surprise, both mutants behaved the same; the trapping pattern was wild type-like (Figure 4.15), suggesting that DNA replication itself has no effect on trapping.

We then combined these two point mutations with the *minD* null mutation. Interestingly, *soj G12* is able to suppress the *minD* trapping defect, but not *soj D40A* (Figure 4.16). This is again consistent with the idea that the trapping defect of *minD* is not due to over-initiation of DNA replication, because both, the *soj D40A* and the *soj* null mutants over-initiate replication, yet only the *soj* null mutant can suppress the *minD* trapping defect.

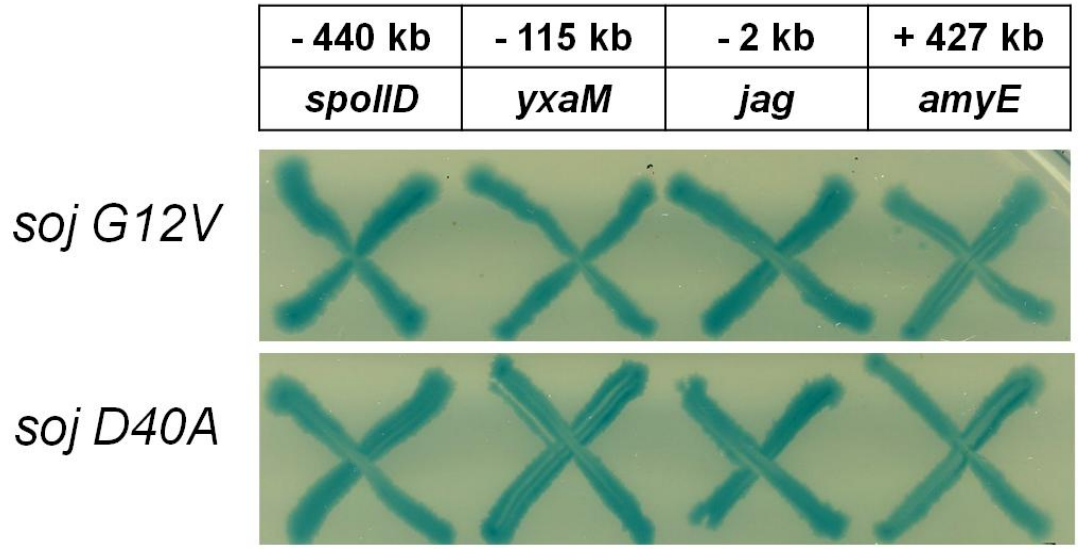

Figure 4.15: Trapping pattern of *soj* G12V and *soj* D40A mutants.
soj G12V (RL 168, RL 169, RL 170 and RL 171) and *soj* D40A (RL 172, RL 173, RL 174, RL 175) mutants carrying *lacZ*. Both mutants showed trapping pattern without any defects, comparable to *soj* null mutant or wild type. Reporter gene at any location around the *oriC* was trapped in the prespore.

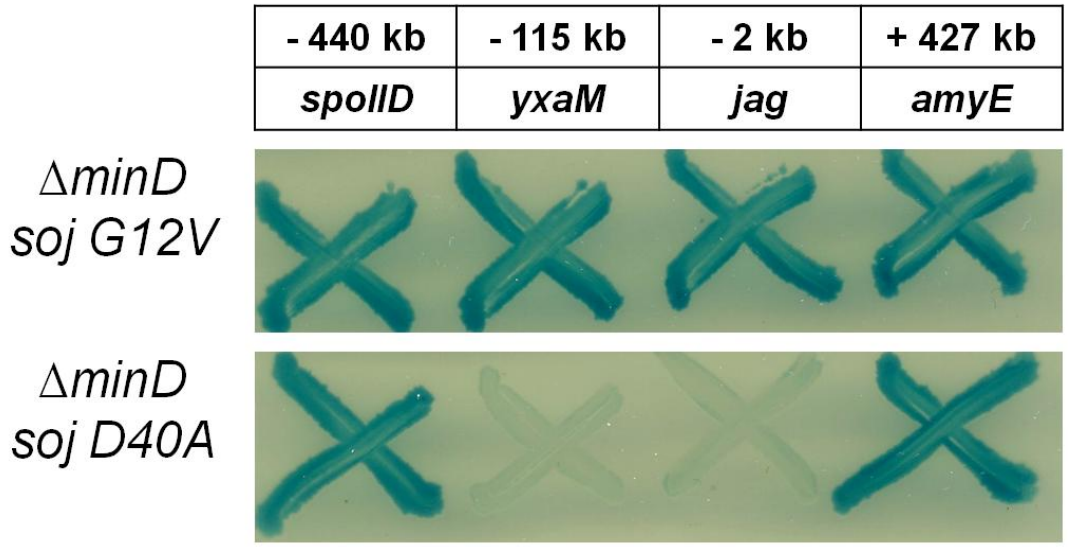

Figure 4.16: Trapping defect of Δ*minD* can be suppressed by *soj G12V* but not by *soj D40A*.
minD soj G12V double mutant carrying the *lacZ* reporter (strains RL 176, RL 177, RL 178, RL 179) compared to *minD soj D40A* double mutant carrying *lacZ* reporter (strains RL 180, RL 181, RL 182, RL 183) showed that *soj G12V* is able to suppress *minD* trapping defect while *soj D40A* cannot suppress the *minD* trapping defect; *oriC* of the chromosome is in *minD soj D40A* double mutant not trapped in the prespore.

4.2.5.3. Suppression of *minD* trapping defect by DnaA mutation

dnaA S326L mutant causes over-replication of DNA, but its prespores trap the *oriC* region of the chromosome efficiently. Since deletion of *soj* also causes over-initiation of DNA replication and can restore *minD* trapping pattern to the level of that of the wild type, we tested whether the *dnaA(S326L)* mutant could also suppress the *minD* mutation. Interestingly, when *dnaA S326L* mutant is combined with deletion of *minD*, the trapping defect was suppressed and the trapping pattern was comparable to that of the wild type (see 4.2.3.1.).

4.2.6. More precise mapping of trapping by light fluorescence microscopy

To investigate trapping patterns in more detail, we used a dual labelling method where a σ^F -dependent YFP fusion was placed at - 7° (- 4.1 kb) on the chromosome and a σ^F –dependent of CFP fusion was placed at + 28° (+ 427 kb) (Sullivan et al., 2009).

The parental strain RL 301 had the same *spoIIIE* point mutation that we used for plate trapping assay, to prevent any DNA transfer after formation of the asymmetric septum (Figure 2.1). Figure 4.17 shematicaly shows the possibilities that could have been observed under the microscope using this dual labelling method.

Using YFP and CFP reporter genes a number of mutants were tested for trapping efficiency. A summary of the results is presented in Table 7. Results obtained by this experiment are in general comparable to results obtained by other methods. Again, it shows that high proportion of wild type *B. subtilis* cells in strain RL 301 (91 %) traps *oriC* region of the chromosome in the prespore and there is only 8% empty prespores.

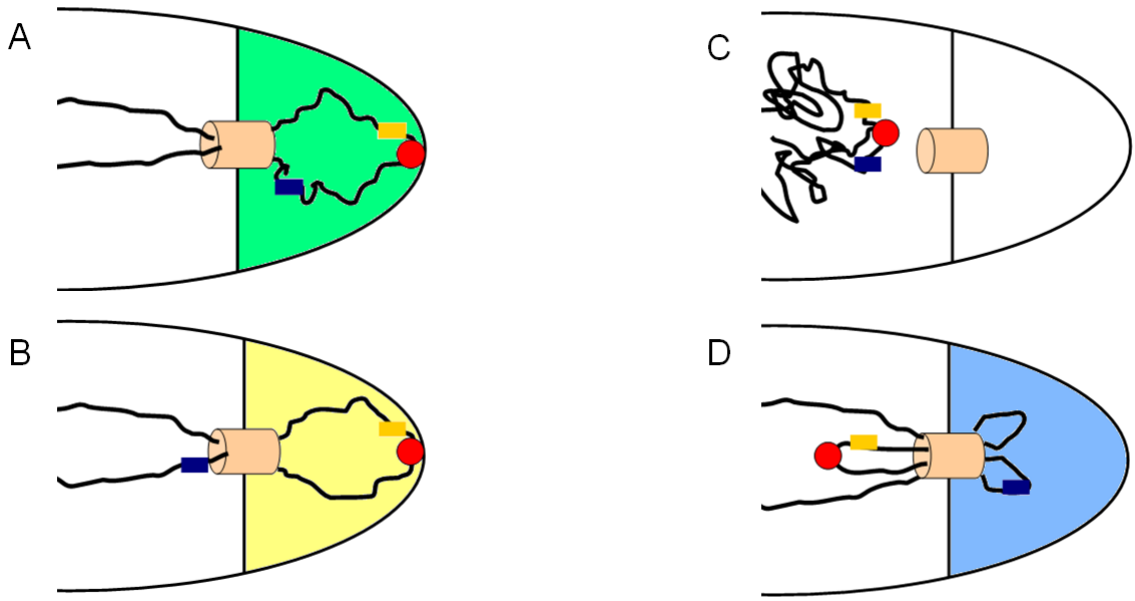

Figure 4.17: Shematic possibilities of trapping method using reporter genes YFP at - 7° and CFP at + 28°.
If both reporter genes are trapped in the prespore, there is CFP and YFP signal seen in the prespore (A). When there is only *oriC* region of the chromosome trapped in the prespore, only YFP signal can be observed in the prespore (B). Some spores contain no DNA at all; in this case, there is no signal expressed from any reporter gene observed in the prespore (C). When *oriC* is excluded from the prespore, but the flanking regions are trapped in the prespore, only CFP signal can be seen in the prespore (D).

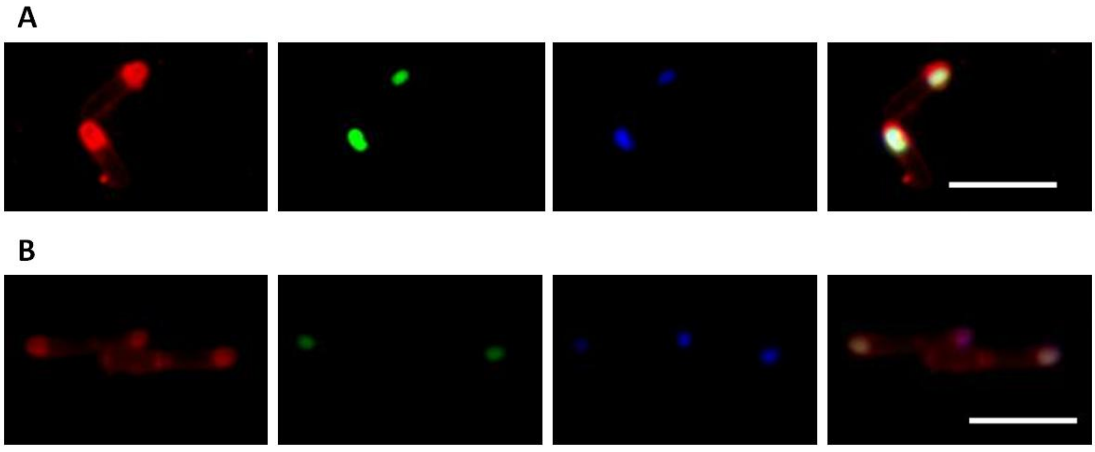

Figure 4.18: YFP and CFP reporters.
Comparing trapping of the chromosome by using YFP under the σ^F promoter on position - 7° and CFP under the σ^F promoter on position + 28°. Wild type strain cells (A) trap all 30 % of the chromosome around the *oriC* (prespore contains green and blue signal) while *ΔminD* strain (B) show cells that do not trap *oriC* (no green signal in the prespore), but they trap successfully the flanking regions (blue signal in the prespore). Scale bars (5 μm) apply to all the panels.

The reason for the empty prespore (besides the trapping defect) might be too weak signal of the reporter gene/s to be detected. This can happen when the prespore is too young to express detectable amount of reporter. However, only 29 % of *minD* null mutant prespores of strain RL 302 contained *oriC* of the chromosome and 41 % of the prespores were empty (example photograph is presented in figure 4.18). This result, when compared to the wild type and *minC* null mutant strain RL 304 (71 % prespores contained *oriC*, 17 % were empty), confirms specific *minD* trapping defect.

Using light fluorescence microscopy and reporter genes YFP and CFP revealed that *soj* null mutant strain RL 303 does not trap *oriC* with same efficiency as wild type. There is 62 % prespores that contain *oriC* and 18 % empty prespores; trapping efficiency is slightly worse than that of the wild type. Combining *soj* null mutant with *minD* null mutant improved trapping efficiency. Double mutant *soj minD* (strain RL 305) seemed to trap *oriC* better than each of single mutants; 65 % of all counted prespores contained *oriC*, but there was still 26 % empty prespores.

racA null mutant forms disporic cells; cells, that start to form prespore on both cell poles. For successful sporulation, only one prespore has to contain genetic material and the other copy has to stay in the mother cell. Consistent with the published results (Ben-Yehuda et al., 2003; Wu and Errington, 2003), strain RL 339 (Δ*racA*) showed many empty prespores (60 %) and 36 % of all prespores included *oriC* of the chromosome. Combining *racA* deletion with *minD* deletion (strain RL 340) caused increased trapping defect; 87 % of empty prespores and only 7 % prespores that managed to trap *oriC*. Again, combining *racA minD* double mutant with Δ*soj*

increased trapping efficiency (strain RL 408); 74 % of spores were empty and 19 % included *oriC* region.

Table 7: CFP/YFP trapping pattern

strain	*oriC* in the prespore			*oriC* in the mother cell	empty prespore
	+28°	-7°	-7°	+28°	/
wild type	78		13	1	8
	91				
Δ*minD*	24		5	30	41
	29				
Δ*minC*	58		13	12	17
	71				
Δ*soj*	54		8	20	18
	62				
Δ*minD* Δ*soj*	55		10	9	26
	65				
Δ*racA*	17		19	4	60
	36				
Δ*minD* Δ*racA*	3		4	6	87
	7				
Δ*minD* Δ*soj* Δ*racA*	9		10	7	74
	19				
Δ*racA* Δ*soj*	10		16	8	66
	26				
Δ*(soj-spo0J)*	12		31	15	42
	43				
Δ*(soj-spo0J)* Δ*racA*	1		4	9	86
	5				
Δ*(soj-spo0J)* Δ*minD*	12		14	16	58
	26				
Δ*(soj-spo0J)* Δ*racA* Δ*minD*	1		2	9	87
	3				

Combining *racA* and *soj* null mutants revealed that double mutant (RL 341) forms more empty prespores (66 %) than each of single mutants and also fewer prespores that contain *oriC* region of the chromosome (only 26 %). This is with an agreement with present knowledge about Soj and RacA as being two important players in trapping process (Figure 1.4).

Another protein helping to organise chromosome structure during the early stage of sporulation is Spo0J, in an operon together with *soj* (Lee and Grossman, 2006). Δ(*soj-spo0J*) double mutant in strain RL 369 therefore forms relatively high proportion of empty prespores (42 %). Despite their function, absence of Soj and Spo0J still allow 43 % of prespores to successfully trap the *oriC*. This efficiency lowers dramatically in the absence of RacA. Examining triple mutant (Δ*racA* Δ*(soj-spo0J)*) - strain RL 368, shows that only 5 % of prespores include *oriC* and there is 86 % empty prespores. When instead of RacA, MinD is absent (triple mutant Δ*minD* Δ*(soj-spo0J)* in strain RL 397, trapping efficiency is significantly improved; 26 % of prespores contain *oriC* and 58 % of prespores are empty. Moreover, quadruple mutant lacking all four proteins (RL 396; Δ*minD* Δ*racA* Δ*(soj-spo0J)*) has extremely low trapping efficiency with only 3 % of all prespores containing *oriC* and 87 % of all prespores containing no reporter gene; most likely containing no DNA.

4.3. Discussion

Surprisingly, the trapping defect of *minD* null mutant is much more severe than the trapping defect of any null mutant lacking DNA binding proteins that act on *oriC* attachment to the cell pole; Spo0J, Soj, RacA. Single mutants of all 3 proteins, Spo0J, Soj and RacA, showed no trapping defect on X-gal plates using *lacZ* reporter. However, when using more precise method: double labelling with CFP and YFP on different location on the chromosome, we can see a slight effect of absence of these proteins on trapping efficiency. The trapping defect of above mentioned single mutants is probably not that severe because they all have slightly redundant functions, which means that the absence of more than one DNA binding protein causes increased trapping defect.

When combining *minD* null mutant with other mutants, the trapping pattern is in most cases typical for *minD* null mutant. This is not the case when we combine Δ*soj* and Δ*minD*; the trapping defect is suppressed so that the *oriC* of the chromosome is trapped in the prespore more efficiently. We have confirmed this finding by using different methods. Using strain with deletion of *soj* and a copy of *soj* under the xylose inducible promoter allowed us to control the amount of Soj in the cell and compare it to the trapping pattern (Figure 4.14). When there was no Soj in the cells of Δ*minD* strain (agar plates with no xylose), the *minD* trapping defect was restored, but with more and more Soj in the sporulating cells of Δ*minD* strain, the more severe *minD* trapping defect can be observed (agar plates with higher concentrations of xylose).

Soj has some similarities to MinD and its localisation in the vegetative cells has been shown to be dependent on MinD (Autret and Errington, 2003). Recently it has also been shown to act on DnaA and control DNA replication (Murray and Errington, 2008). To understand better which Soj mutants can restore the *minD* trapping defect, we tested Soj mutant that causes over-replication of the chromosome and Soj mutant that causes under-replication of the chromosomes in the cell. Each of the single mutants had no effect on trapping pattern, but when we combined these 2 mutants with Δ*minD*, Soj mutant that causes under-replication of the chromosomes was able to suppress *minD* trapping defect, but Soj mutant causing chromosome over-replication was not able to suppress *minD* trapping defect (Figure 4.16).

This raised the question, whether the improper regulation of chromosome replication prior to sporulation can affect *oriC* trapping in the prespore. Although Soj mutants affect chromosome replication, the effect is not that dramatic. Deletion of *yabA* is known to cause a dramatic over-replication in the cells. Testing *yabA* single mutant for trapping efficiency showed noncomparable trapping pattern to that of the wild type and combining Δ*yabA* with Δ*minD* showed trapping pattern typical for Δ*minD* null mutant. This suggested that chromosome over-replication might not cause the trapping defect.

However, we have observed more Spo0J-GFP foci in *minD* null mutant strain than in the wild type (Figure 4.1). This result would suggest that in the absence of MinD, chromosomes are over-replicated and as already mentioned, this could be one possible reason for the trapping defect. Some following experiments confirmed this anticipation; we could see replication of the chromosomes going on in the cells that

have already initiated sporulation (Figure 4.2; DnaX-YFP foci that are indicating chromosome replication are present in the cells with SpoIIAA-mCherry signal which indicates that cells have already initiated sporulation).

We believe that chromosome replication during sporulation initiation cannot be the reason for the *minD* trapping defect, because *soj* null mutant over-replicates chromosomes and also *minD soj* double mutant, which has however restored trapping defect. Another experiment, arguing against chromosome replication during the sporulation initiation being the reason for trapping defect is qPCR experiment. It revealed that *ori:ter* (origin of replication: terminus of replication) ratio in *minD* single mutant does not differ from the one in wild type (Figure 4.3); although we could see more Spo0J-GFP foci in this strain, the chromosomes are not over-replicated. This might suggests that the absence of MinD somehow disrupts formation of Spo0J foci and therefore we see virtually more foci than there are *oriC* regions in the cell or MinD affects Spo0J localisation.

Taken together, those experiments lead us to a conclusion, that even if *minD* null mutant over-replicates chromosomes, this cannot be the reason for unsuccessful trapping of the *oriC* region of the chromosome into the prespore. Moreover, although Soj has an effect on chromosome replication, this function is probably distinct from its function in the trapping pattern.

Chapter 5: MinD activities and potential interactions with other proteins

5.1. Introduction

During vegetative growth, most bacteria form a division septum at the centre of the cell to give birth to two equal daughter cells. In order to achieve this, the positioning of the division septum is well regulated (Adams and Errington, 2009; Errington et al., 2003). The important system that spatially regulates assembly of the division machinery at the cell poles is the Min system (Harry, 2001; Kruse et al., 2007; Margolin, 2001). It was discovered when the so called minicells were observed in *E. coli*; small, round anucleate cells that are the product of a cell division close to the cell pole. The Min system in *E. coli* consists of three proteins: MinE, MinD and MinC. MinD recruits the cell division inhibitor MinC to the inner membrane (de Boer et al., 1991; Hu and Lutkenhaus, 1999; Hu et al., 2003), where it promotes disassembly of FtsZ polymers (Dajkovic et al., 2008; Hu et al., 1999; Levin et al., 1998) with its C-terminal part (Shiomi and Margolin, 2007). The Min proteins in *E. coli* have been shown to oscillate from one cell pole to the other. This oscillation is mediated by MinE protein and forms zones for MinCD activity (Ramirez-Arcos et al., 2002; Raskin and de Boer, 1999a, b; Rowland et al., 2000).

The Min system is well conserved among different bacterial species (Gregory et al., 2008; Szeto et al., 2002). However, in *B. subtilis*, MinE has a functional homologue: DivIVA, with the function of recruiting other Min proteins to the place of action (Harry and Lewis, 2003). Another difference between the *E. coli* and the *B. subtilis* Min systems is MinJ (sometimes called MinP); a protein that links MinD and DivIVA. MinJ interacts with both MinD and DivIVA and so it acts to localise MinD to the cell pole in *B. subtilis* (Bramkamp et al., 2008). MinJ has only been discovered very recently.

MinD is a member of the ParA superfamily of ATPases (de Boer et al., 1991; Hayashi et al., 2001), which has also been shown to interact with membranes in *E. coli* (Mazor et al., 2008a, b; Szeto et al., 2003; Zhou and Lutkenhaus, 2003). MinD – membrane interaction also plays a role in the oscillation of Min proteins in *E. coli* (Taghbalout et al., 2006).

To further understand the function of MinD, we have purified *B. subtilis* MinD to test its interaction with membranes and DNA. In order to find any partners of MinD in the trapping process, we also performed some Bacterial Two-hybrid tests and carried out a synthetic lethal screen for proteins that are functionally redundant with MinD.

5.2. Results

5.2.1. MinD does not bind DNA

MinD has some similarities to the DNA binding protein Soj, but apart from that there is no other evidence that would suggest DNA binding activity of MinD. The above described trapping defect indicates that MinD must somehow interact with DNA. This interaction could be direct or indirect via some other protein or proteins. To test whether this interaction is direct, we mixed purified MinD together with *B. subtilis* DNA (PCR product amplified from *B. subtilis* wild type genome). After incubation the mixture was loaded on agarose gel and electrophoresis was performed. Gel was afterwards stained with ethidium bromide. We expected to see DNA shift on agarose gel if there was MinD bound to it. Staining showed that there was no shift of DNA on the gel when purified MinD was mixed together with DNA. This preliminary data suggests that MinD has no DNA binding activity. However, the experiment needs to be repeated with positive and negative controls, and more importantly, the region of the chromosome around the *oriC* has to be tested instead of random DNA during our preliminary experiment. Moreover, MinD is an ATPase and it is not yet clear if ATPase activity is also needed for MinD to be able to bind the DNA molecule, which should also be tested in the future.

5.2.2. MinD binds to the membranes

To test if *B. subtilis* MinD has any affinity for liposomes, we mixed purified MinD with or without lipid vesicles in the presence or absence of ATP. After incubation we ultracentrifuged the samples to pellet lipid vesicles and analysed the pellets and supernatants by Westernblotting using MinD antibodies. The results showed that the addition of liposomes to the reaction mixture pulls down high proportion of the protein in mixture (Figure 5.1). Pellet fractions that contained lipid vesicles showed enriched signal of MinD compared to the fractions without lipid vesicles. In contrast to the pellet fractions, the supernatant fractions showed weaker signals when lipid vesicles were present in the reaction mixture and stronger signal when there was no lipid vesicles present (Figure 5.1).

The result also showed that the addition of ATP has no effect on MinD affinity/binding to the lipid vesicles, suggesting that this process is independent of ATP.

5.2.3. No direct interaction between MinD and DivIVA

Light fluorescence microscopy data have shown that the absence of DivIVA affects proper cell pole localization of MinD. Moreover, some experiments proved the existence of MinD and DivIVA in a complex with Spo0J during the sporulation as well as formation of a complex of DivIVA together with FtsZ and MinD during the vegetative growth (Perry and Edwards, 2004, 2006). This might suggest that there is a direct interaction between DivIVA and MinD. To test whether the interaction between MinD and DivIVA is direct, we made use of DivIVA ability to bind to lipid vesicles. We tried to pull down MinD from the reaction mixture when there were also purified DivIVA and lipid vesicles present in the reaction mixture.

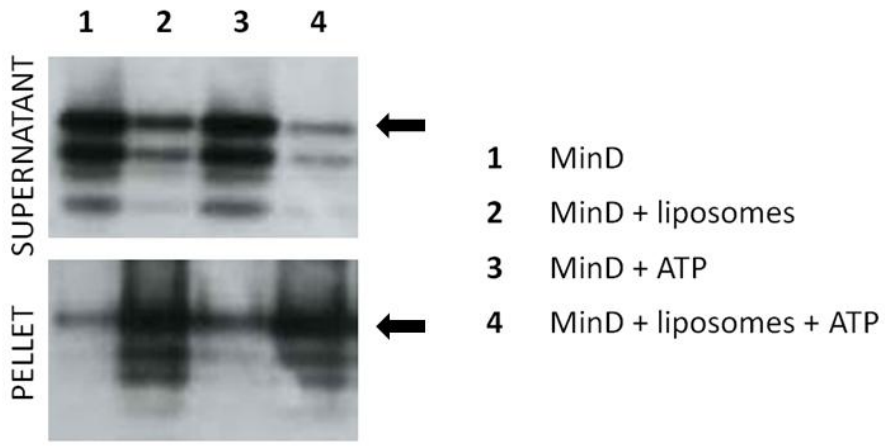

Figure 5.1: MinD affinity for liposomes.
The bottom western blot represents MinD signal in pellet fractions (the signal is blur due to the presence) and the upper western blot represents MinD signal in supernatant fractions after ultracentrugation of different reaction mixtures.The addition of liposomes to the reaction mixtures caused signal shift from supernatant to pellet fractions suggesting that majority of MinD was pulled down by lipid vesicles. Due to high instability of purified MinD protein, the degradation products of MinD can be detected by anti-MinD antibodies (multiple signals). The full length MinD is marked by arrows.

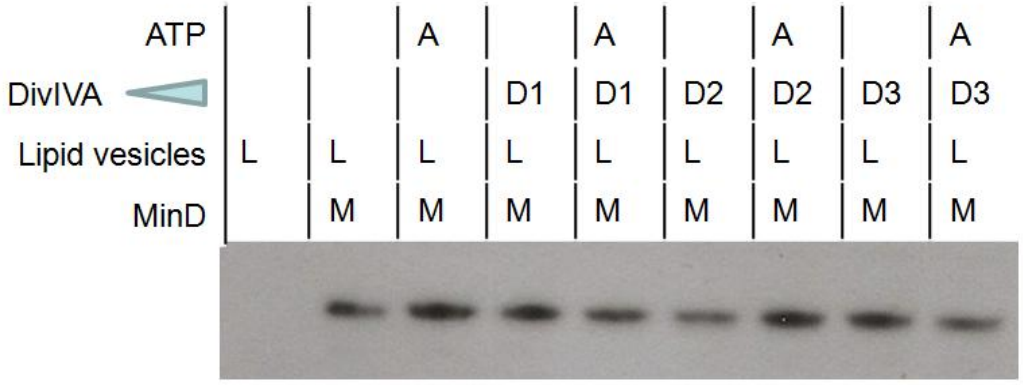

Figure 5.2: No MinD-DivIVA interaction could be detected.
MinD was mixed in reaction mixtures together with lipids, with or without DivIVA and with or without ATP as indicated above each reaction lane. The concentration of liposomes was 0.5 mg/ml, the concentration of MinD was 0.4 μM and the concentration of DivIVA was 0.2-2 μM (increasing concentrations D1-D3). Addition of DivIVA had no effect on MinD signal enrichment in the lipid fraction.

5.2.3.1. Testing MinD and DivIVA interaction by using lipid vesicles

DivIVA was mixed and pre-incubated with lipid vesicles (0.4 μm diameter) to allow the protein to bind to lipids. Purified MinD was then added to the reaction mixture, before centrifugation on high speed to pellet lipid vesicles. Pellets and supernatants were then analysed on the SDS-PAGE gel and Western blotting performed against MinD antibodies. As a control, we used reaction mixtures without DivIVA or without lipid vesicles. Comparison of the reaction mixtures showed that we could not pull down higher amount of MinD when there was DivIVA present in the reaction mixture, suggesting that there is no direct interaction *in vitro* between these two proteins (Figure 5.2).

5.2.3.2. Testing MinD and DivIVA interaction by using lipid coated beads

Ultracentrifugation of lipid vesicles with DivIVA and MinD did not reveal a positive interaction between the two proteins. To reduce background and prevent any protein precipitation that was possibly present in the reaction mixtures, we used lipid coated beads instead of lipid vesicles. Beads coated with lipid layer were mixed with both proteins and spinned down for a few seconds on full speed in a bench top centrifuge. Pellets were then analysed with Western blotting using antibodies against MinD. Again this method did not reveal a positive interaction between DivIVA and MinD. Results were comparable to the results obtained by previously described method (data not shown).

5.2.4. Bacterial two-hybrid screen

To identify interacting partners of MinD that help to anchor chromosome to the cell poles we performed a Bacterial two-hybrid screen using some constructs already available in the laboratory. We mainly tested proteins that are implicated in cell division (DivIVA, MinC, MinD), chromosome segregation (RacA, Soj, Spo0J) and cell shape (MreB, MreC, MreD, DivIB). The genes were cloned in 4 different vectors; p25N (low copy plasmid with C-terminal fusion of adenylate cyclase T25 fragment), pKT25 (low copy plasmid with N-terminal fusion of adenylate cyclase T25 fragment), pUT18 (high copy plasmid with C-terminal fusion of adenylate cyclase T18 fragment), pUT18C (high copy plasmid with N-terminal fusion of adenylate cyclase T18 fusion).

5.2.4.1. Bacterial two-hybrid screen with MinD

The screening did not reveal a positive interaction of MinD with any of the DNA-binding proteins tested (Spo0J, Soj, RacA) (Figure 5.3).

We found positive interaction of MinD with itself and with MinC (Figure 5.3), which has been shown previously for *E. coli* (de Boer et al., 1992). Positive interactions were also obtained with MreC and MreD, both are important in maintaining cell shape

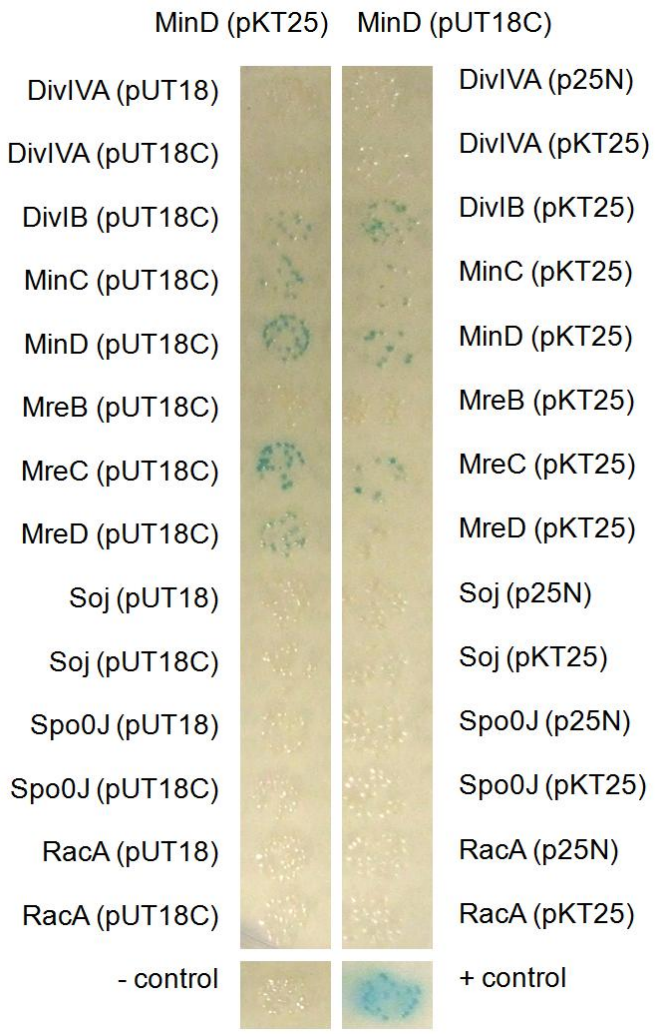

Figure 5.3: Bacterial-Two-Hybrid system screen for MinD.
The experiment was repeated 3 times independently. Positive interactions between MinD and the tested protein results in blue colour of the *E. coli* colony. MinD interacts with DivIB, MinC, MreC, MreD and itself. Different combinations were tested using different plasmids as described in 2.7.

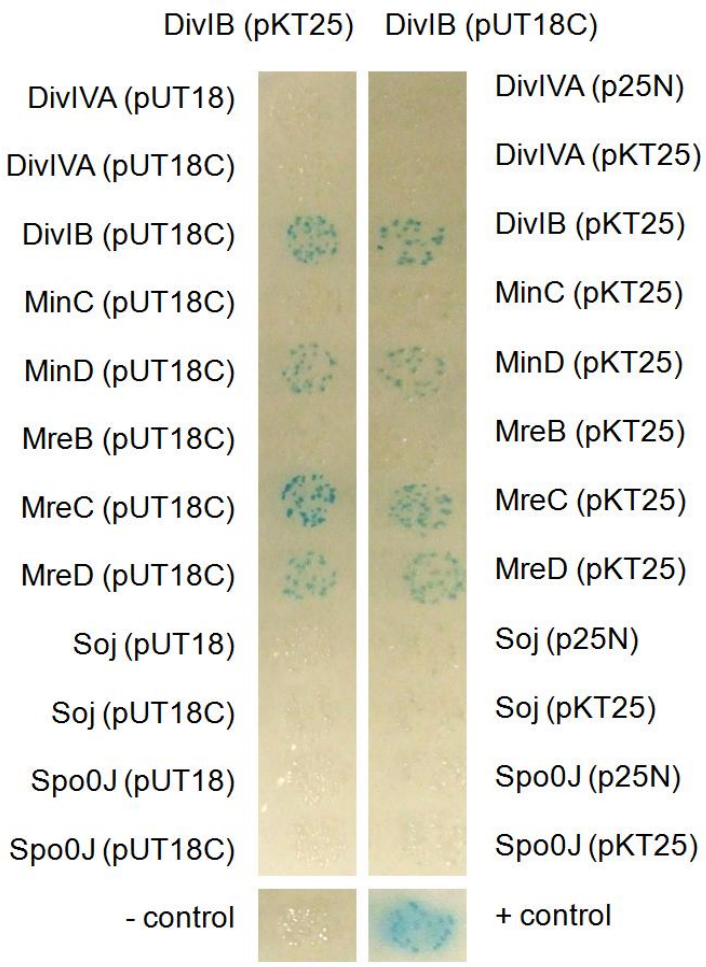

Figure 5.4: Bacterial-Two-Hybrid system screen for DivIB.
The experiment was repeated 3 times independently. Positive interactions between DivIB and the tested protein result in blue colour of the *E. coli* colony. DivIB interacts with DivIB, MinD, MreC, MreD and itself. Detailed description of plasmids used is in 2.7.

of *B. subtilis* but are not involved in sporulation (Divakaruni et al., 2007; Leaver and Errington, 2005; White et al., 2010). Positive interaction between MinD and MreC/MreD and previously described effect of Mg^{2+} on the trapping pattern might indicate also the involvement of MreB in this process.

5.2.4.2. Bacterial two-hybrid screen with DivIB

DivIB is conditionally required for cell division but has also been reported to affect Spo0J/Soj foci in sporulating cells (Real et al., 2005), suggesting a role for DivIB in prespore chromosome trapping. We therefore performed a Bacterial-Two-Hybrid screen for DivIB. Only 4 positive interactions were obtained for DivIB: with MinD, MreC and MreD (cell shape proteins) and DivIB itself (Figure 5.4).

5.2.5. Synthetic lethal screen

For the purpose of identifying proteins with functions homologous to MinCD complex, a Synthetic Lethal Screen was performed. The screen is based on an unstable plasmid, which carries the gene of interest that was deleted in the parental strain. After mutagenesis, only rare colonies maintain the unstable plasmid: the ones, in which the gene of interest became essential. The mapping of the mutation on the chromosome reveals which is the synthetic lethal gene: the redundant gene to the gene of interest.

For this purpose we first constructed a strain with a complete knockout of *minCD* (RL 33) then introduced into it pLOSS that carried the *minCD* genes under the IPTG

inducible P_{spac} promoter. The resulting strain (RL 59) strain was transformed with pMAR-B plasmid that carries TnYLB-1 mariner transposon and the resulting strain RL 60 was used for transposon mutagenesis.

When bacteria were grown for a few hours at 50°C, the unstable plasmid (pLOSS with *minCD*) could be lost, only the colonies with the transposon inserted in genes that had become essential in the absence of *minCD* would retain the unstable plasmid, as it is crucial for the colony to survive. pLOSS carries a *lacZ* reporter which allowed us to identify colonies that still contained the plasmid. One such mutant was isolated.

Further analysis showed that the transposon was inserted in the middle of the 531 base pairs long gene *yshB*, which is a gene of unknown function in *B.subtilis*. It encodes for a transmembrane protein, which might implicate it in a cell division process. However, the backcross of the *yshB* mutation into the wild type showed no obvious growth defect on agar plates, which is in agreement with previously published data (Gueiros-Filho and Losick, 2002). The *yshB* gene is located downstream from *yshA*, which encodes ZapA; a protein that is involved in promoting FtsZ polymerisation (Scheffers, 2008). ZapA has also been shown to suppress the division inhibition caused by *minD* overexpression. Since the screen was carried out in a *minCD* double mutant, it is not clear whether the synthetic effect with *yshB* is due to the absence of MinC or MinD alone or both. To understand the function of *yshB* better, a synthetic lethal screen with *minD* and *minC* separately should be done.

5.3. Discussion

To bring the chromosome to the cell pole during the early stages of sporulation is crucial for successful completion of the sporulation process. Therefore, the process is tightly regulated and employs many proteins. Functions of these proteins often overlap, which can explain why the absence of one protein that helps to anchor the chromosome to the cell pole does not cause a dramatic defect and most of the mutant cells can still manage to finish the sporulation process.

A lot has been known about the MinD protein and its main function during vegetative growth. It recruits MinC to the cell pole, where they inhibit septation. But this function is very distinct from its function in sporulation that is described in this thesis. In this work we have shown that MinD plays an important role during the early stage of sporulation, such that it ensures the polar position of the *oriC*. Not much is yet known which (if any) protein-protein interactions are important during this process. To characterise MinD further, we purified the protein and tested its binding activity for DNA and membranes. It would be expected that MinD somehow has a connection to the DNA molecule as it affects its structure and/or position during the early stage of sporulation. However, the results presented here show that MinD does not interact with DNA directly. It is possible that the purified MinD protein was not fully active, or that the reaction conditions were not suitable for MinD-DNA interaction. Due to the high instability of purified MinD we have only tested nonspecific binding to DNA, but additional tests of specific binding are needed to understand this process better. Most importantly, the *oriC* region of the chromosome should be tested for MinD binding activity to DNA molecules like we have previously tested non-specific

DNA binding activity of MinD. Alternatively, DNA binding activity could be tested by using chromatography method.

Interestingly, bacterial two-hybrid screen revealed a positive interaction between MinD and MreC/MreD proteins. Both, MreC and MreD are part of the machinery that helps to maintain celular shape. The interaction between these 3 proteins could partially explain the dependence of *minD* mutants on Mg^{2+}. However, more experiments should be done to investigate this further, because at this moment the effect of Mg^{2+} is still unknown.

Despite the absence of a transmembrane domain in the sequence of MinD, it has been shown to bind to membranes by its 8-12 residue motif at the C-terminal part. This motif is highly conserved across eubacteria, archea and chloroplasts. It forms a short amphipatic helix that probably mediates a direct interaction between MinD and membrane phospholipids (Szeto et al., 2003; Szeto et al., 2002; Zhou and Lutkenhaus, 2003). MinD can then effectively target other proteins to the cell membrane (Taghbalout et al., 2006). It is not clear whether the affinity of MinD for membranes plays a role during the chromosome attachment to the cell pole. Additional experiments are needed to address this question. The trapping pattern of a MinD mutant lacking the membrane binding domain should be tested by using *lacZ* reporter or fluorescence reporters.

DivIVA has been shown to be important for proper localisation of MinD (Marston et al., 1998), but the direct interaction between these 2 proteins has never been shown so far apart from the formation of a complex that DivIVA forms together with FtsZ and

MinD during vegative growth (Perry and Edwards, 2006). Moreover, none of our experiments could confirm a positive direct interaction between DivIVA and MinD. Recently Bramcamp *et al*. showed a link between DivIVA and MinD. They discovered a protein called MinJ which brings MinD to the cell pole and interacts with both, DivIVA and MinD (Bramkamp et al., 2008). Their result could explain why we were unable to show a positive, direct interaction between DivIVA and MinD.

We have also performed a Synthetic lethal screen, hoping to find proteins with similar function as MinCD. The gene that we found, *yshB*, is of unknown function. However, it is located downstream of *yshA*, which encodes ZapA that promotes FtsZ polymerisation. Additionally, ZapA has been shown to suppress the effect of MinD over-expression (Gueiros-Filho and Losick, 2002). An *yshB* mutant showed no obvious defect, however, more detailed analysis should be done, especially to understand its connection with MinCD; it would also be beneficial to test the trapping pattern of a *yshB* mutant and perform a Bacterial Two-Hybrid screen with *yshB*, to investigate its interactions with other proteins implicated in cell division and/or sporulation.

Chapter 6: DivIVA binds to the cell membrane and interacts with RacA directly in the process of anchoring chromosome to the cell poles

6.1. Introduction

DivIVA is a conserved protein in Gram positive bacteria. In all bacteria investigated so far it specifically localises to cell division sites and cell poles. DivIVA is involved in various processes; some related to cell division, some related to cell growth and others related to sporulation (Lenarcic et al., 2009). It is assumed that DivIVA functions as a scaffold for the localisation of other proteins.

In *B. subtilis*, DivIVA helps to localise the cell division inhibitor complex MinC/MinD/MinJ to the cell poles, where MinC inhibits FtsZ polymerisation during vegetative growth (Bramkamp et al., 2008; Edwards and Errington, 1997; Edwards et al., 2000). When DivIVA is inactive or absent, Min proteins are delocalised and cell division is largely inhibited causing elongated cells. Moreover, cells occasionally divide aberrantly close to the cell poles giving birth to small anucleate minicells (Cha and Stewart, 1997). Fluorescence microscopy has shown that DivIVA localises at mid-cell during the cell division and at matured cell poles.

DivIVA also plays an important role in sporulation (Thomaides et al., 2001). During the early stage of sporulation, it is important to anchor the chromosome to the cell pole, and later to incorporate one full copy of the chromosome in the prespore. RacA and DivIVA have been shown to be responsible to attach the chromosome to the cell pole (Ben-Yehuda et al., 2003; Wu and Errington, 2003).

In our study we were interested in how DivIVA localises to the cell poles and whether there are other proteins needed for its polar localisation. We also studied interactions of DivIVA with other proteins that require DivIVA for their localization.

6.2. Results

6.2.1. DivIVA binds to the membranes

DivIVA is a cell pole determinant protein, localized at the cell pole. We wanted to test why it binds to the cell membrane and why it localises to the cell poles. Experiments showed that DivIVA has an ability to bind directly to membranes which can be shown by pull down of DivIVA from suspension by the addition of lipid vesicles. Lipid vesicles were prepared as described in 2.8.2.1. Purified DivIVA was mixed with or without lipids in binding buffer and after 20 min incubation at room temperature, samples were centrifuged. Pellets were analysed on SDS-PAGE gel and Comassie stained. The signal intensity on SDS-PAGE gel was highly increased by the addition of lipid vesicles into the reaction mixture (Lenarcic et al., 2009).

6.2.2. Binding is not affected by the size of lipid vesicles

To test whether the size of lipid vesicles can affect DivIVA binding capacity, we made lipid vesicles of different diameter (0.1 μm, 0.4 μm or 5.0 μm) by extrusion through different size pore filters, and mixed them with purified DivIVA. Samples were centrifuged after 20 mins incubation at room temperature, and the pellets with lipid vesicles were analysed by SDS-PAGE and Comassie staining. The experiment was repeated 3x, with 3 different DivIVA concentrations. We could not observe any difference in binding capacity between lipid vesicles of different diameter (Figure 6.1).

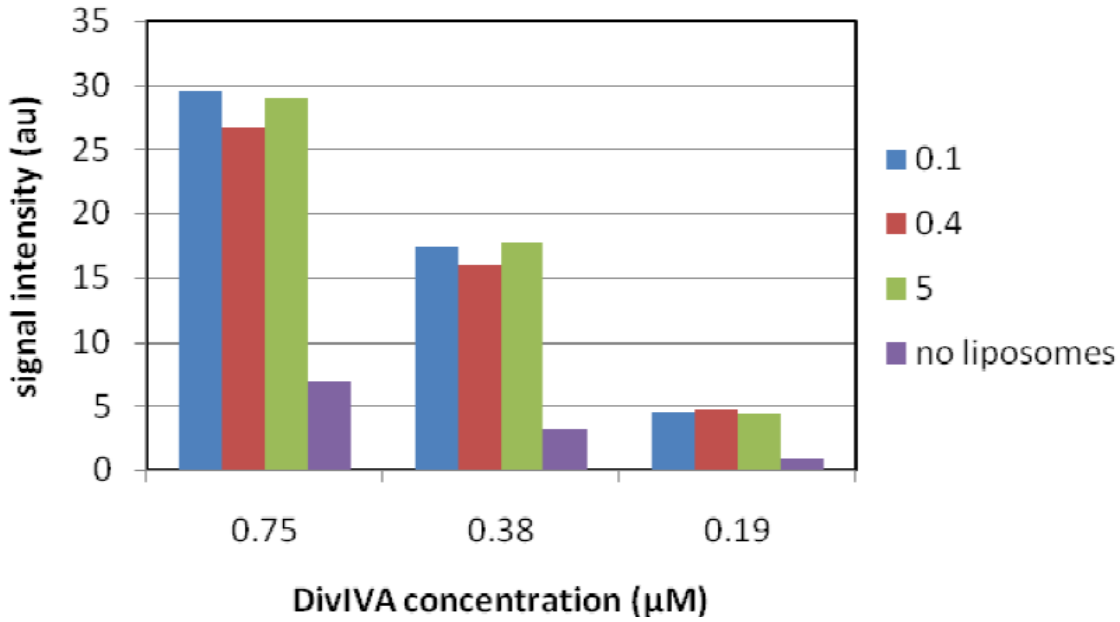

Figure 6.1: Binding of DivIVA to liposomes of different diameter (0.1 µm, 0.4 µm or 5.0 µm).
The DivIVA concentration was titrated (0.75 µm, 0.38 µm and 0.19 µm) and the amount of DivIVA in the pellet fractions was determined by gel scanning. As a control the pellet fractions of reactions without lipid vesicles were included. Signal intensity is presented in arbitrary units.

6.2.3. DivIVA localization in *E. coli*

To test if DivIVA binds preferably to curved membranes, we tested DivIVA-GFP localization *in vivo* in *E. coli* because the native *B. subtilis* DivIVA promoter is active also in *E. coli* and *E. coli* genome lacks a divIVA homologous sequence. It has been previously shown that DivIVA localises to division sites and cell poles in *E.coli* (Edwards et al., 2000). In our experiments, we tested DivIVA-GFP localization in wild type *E. coli* cells again, but in different Z-positions than previously reported. The Z-position in which we were interested is the transitional state between Y and X axis, where the membrane is most curved. We compared results obtained in wild type *E.coli* strain to the *E. coli* strain deficient in murein hydrolase. In this mutant, cells remain connected and are unable to split after cell division and therefore the cell poles are shaped differently. The comparison between the two different *E.coli* strains confirmed our prediction, that DivIVA is preferably localised to the most curved areas in the cell and is not spread homogeneously over the whole septal (or pole) area (Figure 6.3).

Wild type cells of *E. coli* form round poles and the curvature of the membrane is strongest at the poles. Our prediction that DivIVA binds to strongly curved membranes fits with the observation of DivIVA-GFP localization at the poles of wild type *E. coli* cells (Figure 6.2). However, fluorescence microscopy experiments showed that in wild type *E. coli* cells there is always one pole with more DivIVA accumulated than at the other pole. We investigated whether there is some oscillation of DivIVA between the two poles using time-lapse microscopy. The result showed that there is no oscillation but it appeared that DivIVA accumulates at the older cell

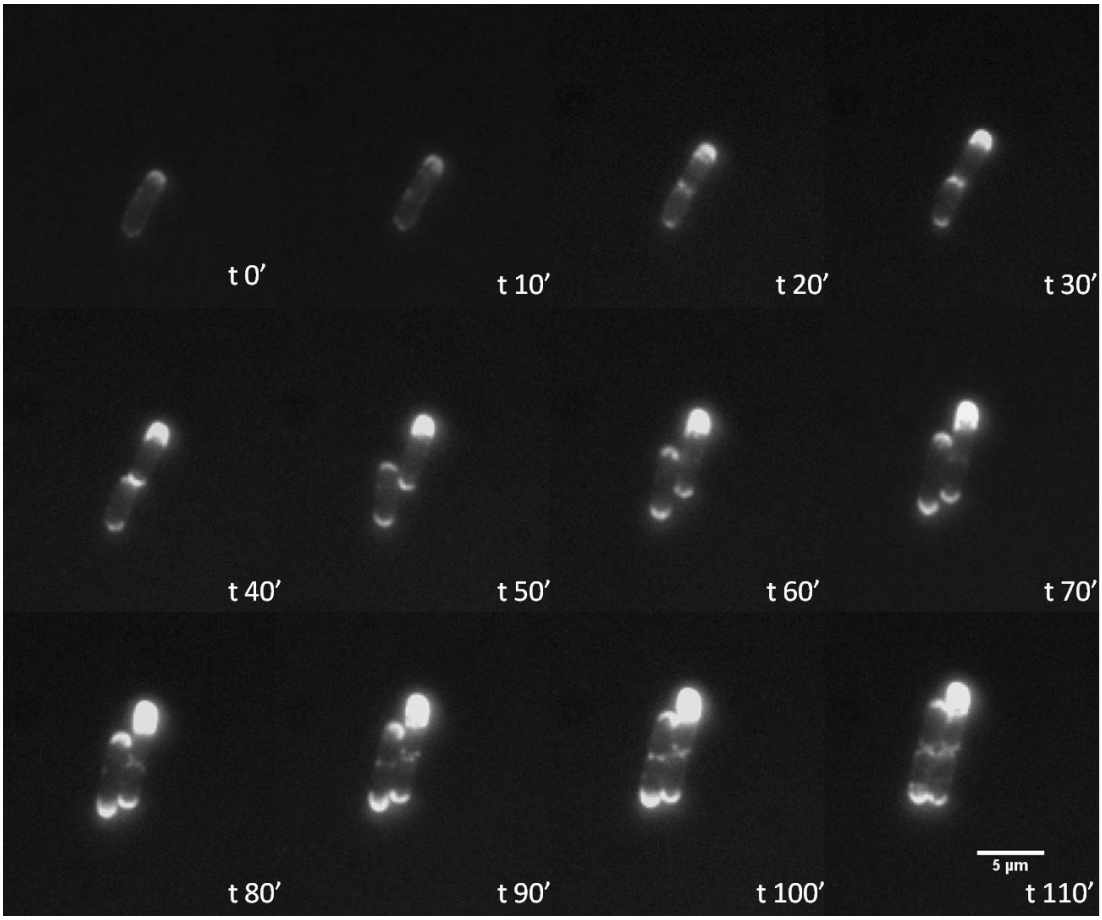

Figure 6.2: DivIVA localization in *E. coli*.
DivIVA localises in *E. coli* at the cell poles, where membrane is most curved. It seemed that one pole often has a stronger signal than the other one and the time-lapse microscopy showed that the pole with the stronger DivIVA-GFP signal remains the same; there is no DivIVA-GFP oscillation in the cell. The protein accumulates over the time more at one of the poles and less at the other one. It is not known what the reason is for significantly stronger DivIVA-GFP at usually the older cell pole. Additional figure with more cells is presented in Supplementary data in Figure A2. All the cell

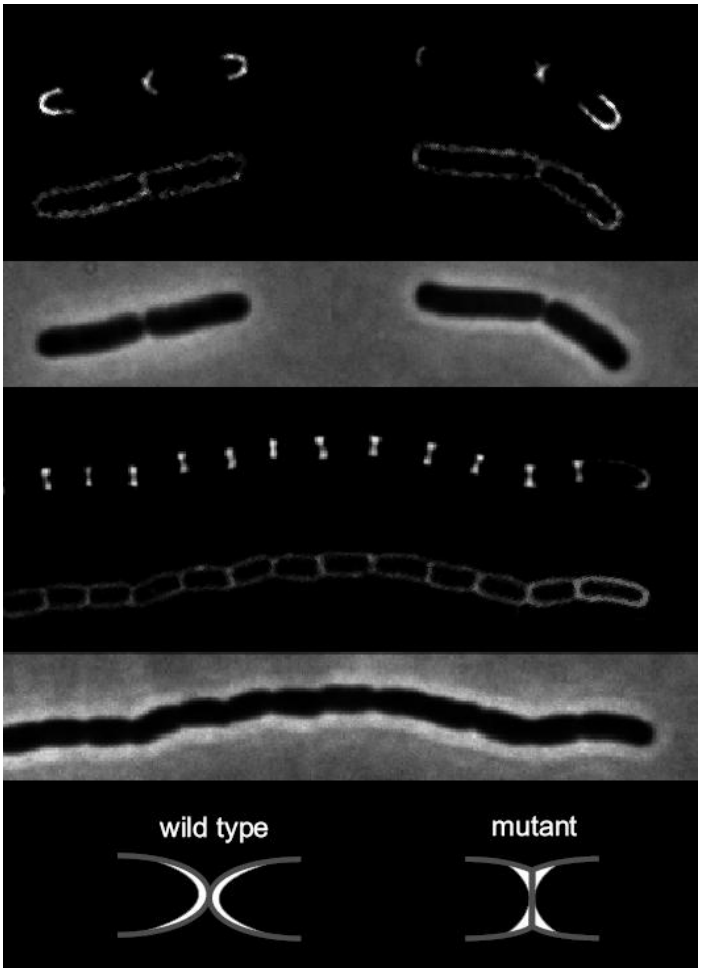

DivIVA-GFP (wild type)

membrain stain (wild type)

brightfield (wild type)

DivIVA-GFP (mutant)

membrain stain (mutant)

brightfield (mutant)

shematic comparison

Figure 6.3: Localisation of DivIVA in *E. coli* hydrolase mutant compared to wild type cell poles.
In wild type *E. coli* (the top of the figure), DivIVA localises at the cell poles, because membrane is most curved at this location. In contrast, *E. coli* hydrolase mutant have differently shaped cell poles: cells cannot separate after division and consequently, poles are flat. DivIVA localises in this mutant at the corners of the flat pole, where membrane is most curved (bottom figure).

poles over time (Figure 6.2). An additional figure that shows more cells with comparable DivIVA-GFP localization pattern is shown in supplementary data of appendix (Figure A2).

E. coli MHD63 strain is devoid of murein hydrolase, which is necessary to hydrolise peptidoglycan in the division septum. Cells of this mutant cannot separate after division and therefore they form long chains of cells (Heidrich et al. 2001). Consequently, poles of these cells are flat and not round as are poles of the wild type *E. coli* cells (see shematic presentation in figure 6.3). Flat poles have relatively sharp curved membrane at the transition from a pole to a lateral wall. It is therefore not surprising, that DivIVA-GFP gives a strong dumbbell-shaped fluorescence signal in such a mutant (Figure 6.3). The *in vivo* data are supported also by a Monte Carlo algorithm, which shows that DivIVA forms clusters that accumulate best at the curved membrane (Lenarcic et al., 2009). Another protein SpoVM, has also been reported to discriminate between the negative and positive membrane curvature and use this feature to localise to the membranes (Ramamurthi et al., 2009).

6.2.4. RacA interacts directly with DivIVA

RacA is expressed specifically during the early stage of sporulation. Ben-Yehuda *et al*. showed that the cell pole determinant protein DivIVA is required for the proper localisation of RacA, but it remained unclear whether this interaction is direct or indirect. Since MinD also requires DivIVA to be localized to the poles, it could be that these three proteins interact to anchor the *oriC* region of the chromosome to the

cell pole. Moreover, our previously described experiments showed that combining a *racA* null mutant with *soj* or *minD* null mutant causes a dramatic trapping defect (see 4.2.3.2.). Therefore we wanted to test if RacA localisation to the cell poles depends on MinD or Soj, or RacA interacts with DivIVA directly.

6.2.4.1. Effect of Soj and MinD on RacA localisation

To test if RacA localization at the cell poles during sporulation depends on MinD, strain RL 67, harbouring a GFP-RacA fusion and a deletion of *minD,* was investigated by fluorescence light microscopy and compared to an otherwise wild type strain RL 65 harbouring a GFP-RacA fusion. Cells were grown in CH and resuspended in SM to induce sporulation. After 1h at 37°C, localisation of GFP-RacA was investigated.

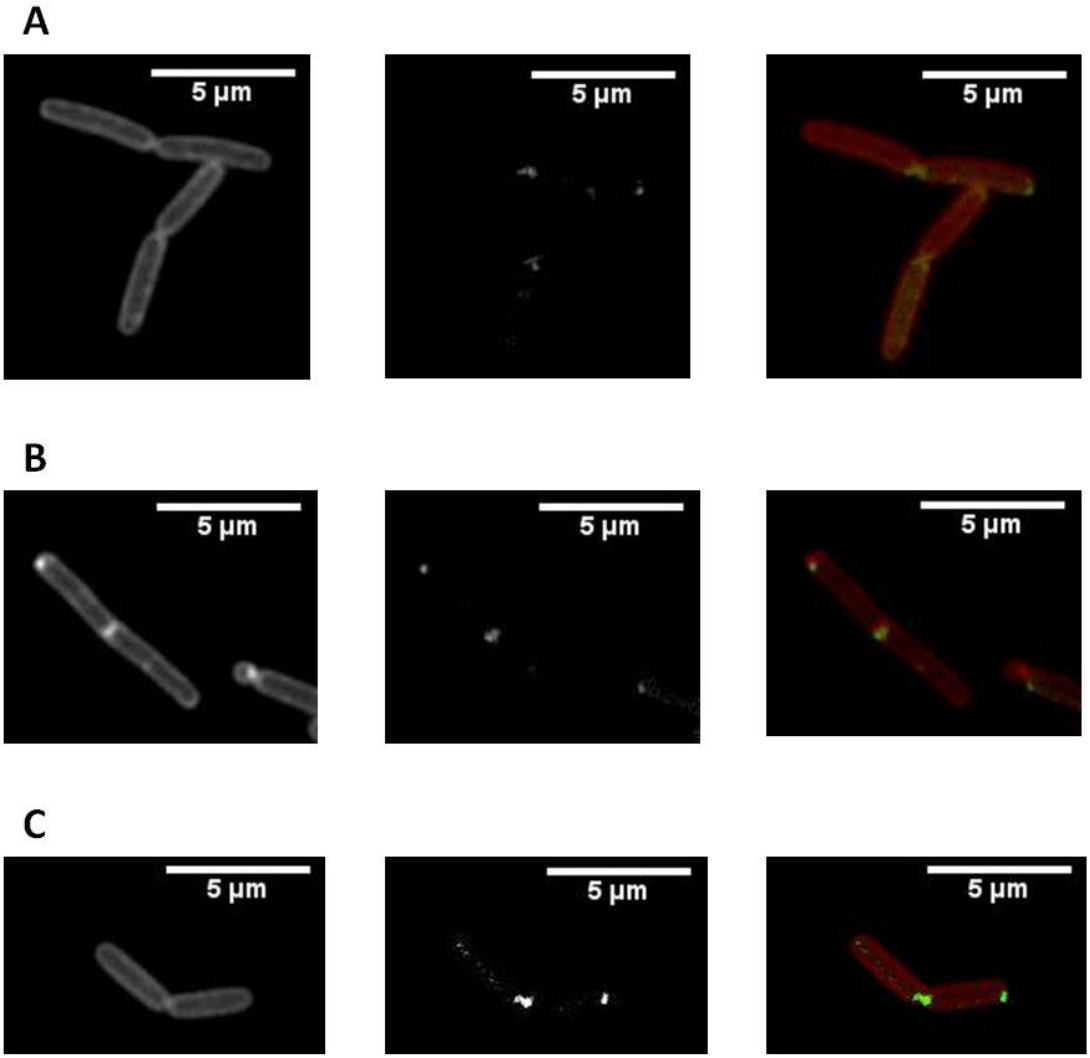

Figure 6.4: RacA-GFP localization.
Strain RL 65 shows localisation of RacA in wild type cells; RacA localises exclusively to the cell poles (A), from left to right: nile red membrane stain, RacA-GFP, merge. The absence of MinD has no effect on GFP-RacA localisation; RacA localises to the cell poles (B), from left to right: nile red membrane stain, RacA-GFP, merge. Also the absence of Soj has no effect on GFP-RacA localisation; RacA localises to the cell poles, comparably to wild type (C), from left to right: nile red membrane stain, RacA-GFP, merge.

In wild type cells RacA localised exclusively at the cell poles (Figure 6.4 A). Same localization pattern of RacA was observed in the strain lacking *minD* which suggests that MinD is not needed for proper RacA localisation (Figure 6.4 B).

Next, we examined whether RacA localization at the cell poles depends on Soj. Again, in strain lacking *soj*, a strong signal of GFP-RacA fusion at the cell poles was observed, suggesting that Soj has no effect on RacA localisation during the early stage of sporulation (Figure 6.4 C).

6.2.5. Bacterial two-hybrid screen

To further investigate potential interactions of RacA with other proteins, we performed a bacterial-two-hybrid screen. We found that RacA interacts with itself and with DivIVA (Figure 6.5), but not with MinD or Soj. This confirmed microscopy experiments that suggested that MinD or Soj have no effect on RacA localization.

To investigate RacA interaction with DivIVA in more detail, *divIVA* and *racA* were cloned in different expression vectors (high copy/low copy and N-termnial/C-terminal fusion) and different combinations screened for adenylate cyclase activity (blue colonies on X-gal plate). Among all the combinations, a positive interaction was observed only with a DivIVA-adenylate cyclase T25 fragment (low-copy plasmid p25N) and an adenylate cyclase T18 fragment-RacA fusion (high copy plasmid pUT18C) (Figure 6.6).

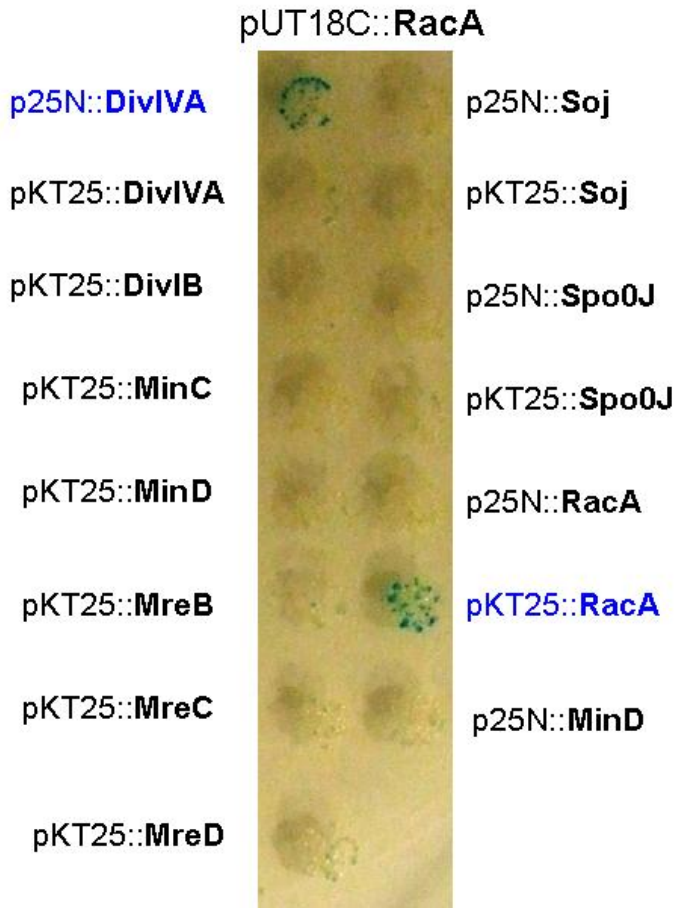

Figure 6.5: Bacterial-Two-Hybrid screen for RacA protein.
Positive interactions are shown in blue colour. RacA interacts with DivIVA and itself.

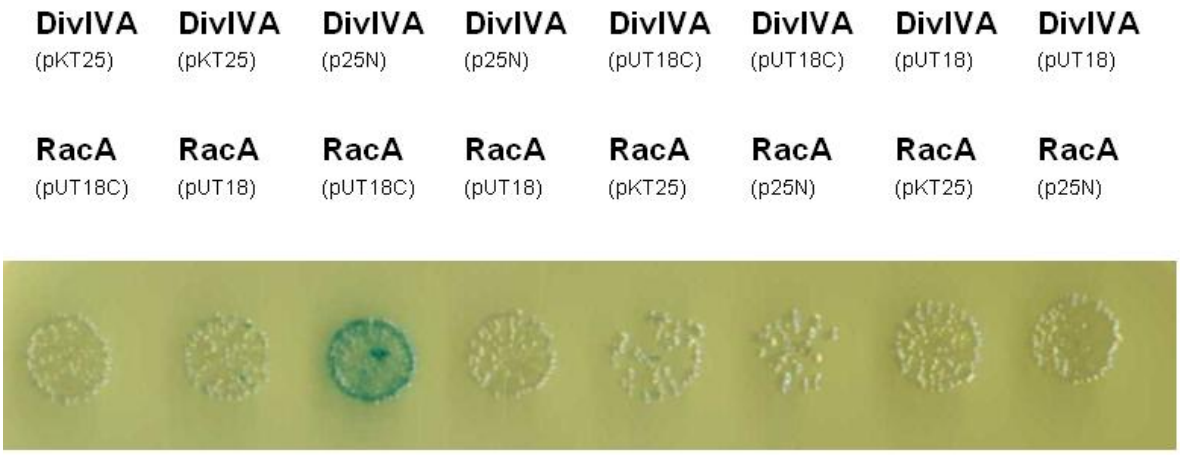

Figure 6.6: Bacterial-Two-Hybrid screen for RacA-DivIVA interaction.
All combinations of plasmid harbouring DivIVA or RacA were screened, the positive interaction was observed only between a DivIVA-adenylate cyclase T25 fragment (low-copy plasmid p25N) and an adenylate cyclase T18 fragment-RacA fusion (high copy plasmid pUT18C).

6.2.6. Flotation with lipid vesicles

DivIVA has been shown to bind lipid membranes, and we used this feature to confirm interaction between DivIVA and RacA revealed by Bacterial-two-hybrid screen. We expected to see RacA in the lipid fraction only when DivIVA was present in the reaction mixture. To test this, a gradient density flotation experiment was performed. Figure 6.7 shows that RacA remains at the bottom fractions when there are no liposomes present in the reaction mixture. The addition of lipid vesicles/liposomes resulted in some flotation of RacA together with the liposomes in the sucrose gradient. However, this fraction was significantly enhanced when DivIVA was also present in the reaction mixture (Figure 6.7). This confirmed a direct interaction between RacA and DivIVA. However, it should be noted that in our lipid vesicle flotation experiment we used a much higher molar ratio of DivIVA compared to RacA (1900:1) because we wanted to cover the lipid vesicles by DivIVA completely.

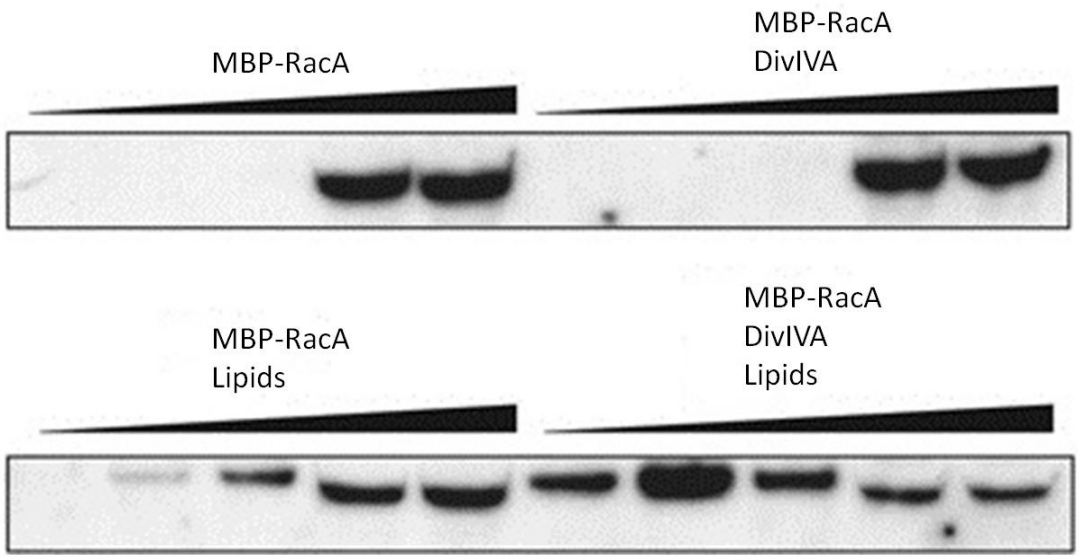

Figure 6.7: RacA interaction with DivIVA.
MBP-RacA (6.4 ng) and DivIVA (3.6 µg) were mixed with liposomes (90 µg) in a sucrose–containing buffer, and loaded at the bottom of a sucrose gradient. After centrifugation, gradients were sampled in five fractions (top fraction with low density sucrose to bottom fraction with high density sucrose run from left to right). Liposomes flotated to the two top fractions and were clearly visible. Gradient fractions were analysed by Western blotting using RacA-specific antibodies.

6.3. Discussion

It is crucial for sporulating cells to anchor the chromosome to the cell pole to ensure it enters the developing prespore. To do so, cells need to recognise the cell pole and prepare chromosome so that it can be anchored to the cell pole. Proteins that are involved in this process have to recognise DNA on one hand and the cell pole on the other hand.

DivIVA is a cell pole determinant which recruits other proteins to the cell pole. The absence of DivIVA causes mislocalisation of important cell division proteins MinD (and consequently MinC), and the sporulation specific protein RacA. Although DivIVA has been proved to play an important role as a cell pole determinant protein, it had been unclear until recent how DivIVA recognises the cell pole. Some proteins are localized to the membrane via the interaction with other membrane protein(s), but this is not the case for DivIVA. Together with colleagues we have shown that DivIVA binds to isolated cell membranes even after pre-treatment with proteases (Lenarcic et al., 2009): protease treated membranes do not contain proteins and therefore DivIVA cannot rely on binding to other membrane proteins. This result suggested that DivIVA has a direct affinity for the lipid membrane and should be considered a peripheral membrane protein.

We next addressed the question how DivIVA recognises membrane at the cell pole. Combining results obtained by fluorescent microscopy and mathematical modelling, we suggested that DivIVA recognises cell poles because membrane there is most curved. To show that DivIVA has an affinity for membranes we used positively curved lipid vesicles which is in contrast to negatively curved cell poles, but DivIVA

still bound to membranes. Taking together these results, although with general affinity for membranes, DivIVA preferentially binds to negatively curved membranes.

Being localised at the cell pole it is not surprising that DivIVA plays an important role in anchoring the chromosome to the cell pole. Previous studies have shown that it is important for proper localisation of RacA at the cell poles (Ben-Yehuda et al., 2003). It remained unclear whether this interaction is direct or indirect. First, we investigated this interaction by Bacterial Two-Hybrid screen, which revealed a positive interaction between DivIVA and RacA. Our *in vitro* biochemical experiment also supports a direct interaction between these two proteins as MBP-RacA can be pulled up in the flotation experiment only when DivIVA was present in the reaction mixture.

Fluorescence microscopy indicated that the absence of MinD or Soj had no effect on RacA localization. It is therefore most likely that the localization of RacA is directly dependent on DivIVA. It follows that the MinD trapping defect is most likely not due to delocalization of RacA during the early stage of sporulation.

Chapter 7: General discussion and conclusions

The ability of *B. subtilis* to differentiate into highly resistant endospore is often crucial in harsh living conditions and allows the organism to survive. The process involves well regulated cellular processes including chromosome replication, chromosome segregation, formation of an asymmetric septum, DNA transfer into the prespore and finally formation of a highly resistant spore coat (Driks, 2004; Errington, 1991, 2001; Wu and Errington, 2003). Many of the proteins implicated in these processes are also involved in cell division during vegetative growth. One example is the MinD protein, part of the 'Min' system that inhibits septum formation close to the cell poles and the formation of anucleate minicells (Marston et al., 1998). Here we show that MinD plays another role during the early stage of sporulation: it is involved in the process of attaching chromosome to the cell pole and allowing the prespore to trap 30 % of the chromosome around the *oriC*, when the asymmetric septum is formed.

The trapping defect of *minD* null mutants has been confirmed by various experimental methods. Reporter gene *lacZ* placed at different locations on the chromosome allowed us to identify parts of the DNA that are present in the prespore and the ones that are not. We then confirmed this result by using fluorescence microscopy to follow the locations of *oriC* in the mother-cell/prespore by using Spo0J-GFP. Finally, we used a dual reporter method, CFP close to the *oriC* and YFP more distant from the *oriC*, but still in the region of the chromosome that is trapped in the prespore in wild type cells. Although there were slight differences in the trapping results obtained by the different methods, all methods confirmed that about 30% of *minD* null mutant prespores do not trap *oriC* in the prespore when the asymmetric septum is formed.

The most obvious reason for this defect could be the cell length as a certain proportion of cells lacking the 'Min' function are longer, usually nearly double the size of the wild type cells. Longer cells could have difficulties moving chromosomes to the more distant cell poles. However, strains lacking different Min proteins have comparable phenotype; a *minC* null mutants form similarly long cells as a *minD* null mutants but *minC* null mutants trap the *oriC* region of the prespore chromosome very efficiently; trapping efficiency is only slightly reduced when compared to the one of the wild type, suggesting that the trapping defect of the *minD* mutants is not due to the loss of the Min function.

The number of Spo0J-GFP foci indicates the number of origins of replication in the cell. We observed higher numbers of Spo0J-GFP foci in a *minD* null mutants than in wild type cells, which suggests that *minD* null mutants over-initiate chromosome replication. Consistent with this suggestion, time-lapse microscopy showed that chromosome replication was still ongoing in *minD* mutants when sporulation had already been initiated, which was not the case in the wild type strain. These results indicated that chromosome replication during sporulation, probably due to over-initiation in *minD* null mutants could be the reason for its trapping defect.

A precise method to determine the number of origins in the cell is quantitative PCR. The *ori:ter* ratio (origin of replication compared to terminus of replication), to our surprise, clearly showed that *minD* null mutants did not over-replicate chromosomes (not during vegetative growth neither during sporulation): the *ori:ter* ratios were not different from wild type one. As several mutants (*spo0J, yabA, dnaA326L*) that over-initiate DNA replication did not show the same trapping defect, it can be concluded

that over-initiation of DNA replication during spore development cannot be the reason for the trapping defect observed. Also, quantitative PCR is a more reliable method than Spo0J-GFP foci counts, therefore we believe that for some unknown reason, Δ*minD* strains do not form a discrete Spo0J-GFP foci as wild type strain.

One possible partner of MinD during the establishment of the *oriC* of the chromosome attachment to the cell pole could be RacA; therefore we tested whether the absence of MinD affects localisation of RacA in the cell during the early stage of sporulation. The fluorescence microscopy results showed that the absence of MinD did not affect the recruitment of RacA to the cell pole, but we could not exclude the possibility that the activity of RacA had been affected.

Moreover, further analysis proved that RacA only needs DivIVA for its proper localization. The interaction between these two proteins is direct and plays an important role in sporulation. RacA is a DNA binding protein that can stick the chromosome to the cell pole by interacting with DivIVA. Localization of DivIVA relies on its ability to bind to membranes. It preferentially binds to negatively curved membranes, which is at the cell pole. There is no other protein needed for DivIVA to be positioned at the cell pole and so it serves as a cell pole determinant and the polar anchor for both, MinD and RacA, but also probably Spo0J (Lenarcic et al., 2009; Perry and Edwards, 2004).

DivIVA has also been shown to help to orientate chromosome correctly during sporulation in a coordinated action together with Spo0J/Soj and MinD. A modification of DivIVA is needed so that it forms a complex with Spo0J/Soj rather

than with FtsZ and MinD which takes place during the vegetative growth. These results suggested that there is a more direct link between DivIVA and Spo0J, which does not require MinD (Perry and Edwards, 2004, 2006).

Our speculation is that MinD, in the process of orienting the chromosome prior to asymmetric septum formation, somehow interacts with Soj. This is supported by our results which show that deletion of *soj* can suppress *minD* trapping defect: a *soj* point mutant that is unable to bind DNA molecule is also able to suppress the defect, whereas another mutant that can still bind DNA and stimulate DnaA does not. It is therefore possible that Soj somehow imposes some topological property on the *oriC* region of the chromosome, preventing its release from the usual quarter position during vegetative growth or its migration to the cell pole. This activity of Soj is inhibited by its association with MinD at the cell pole, probably by sequesting the majority of Soj to the division septum. A direct interaction between MinD and Soj has so far not yet been demonstrated. The Soj G12V no longer binds DNA and therefore this mutant does not interfere with the release of *oriC* to the cell poles. It is interesting that the *dnaS326L* mutants also have normal trapping pattern whether MinD is present or not. One possible explanation is that this mutant protein somehow is able to counteract the topological effect of Soj on the *oriC* region of the chromosome. It would be interesting to test whether Soj is still associated with the *oriC* region in this mutant.

The model (Figure 7.1) presents the possible situations in sporulating cell with and without MinD. When MinD is present, it can inhibit the negative effect of Soj on the release of the *oriC* and allows the *oriC* region to be attached to the cell pole, together

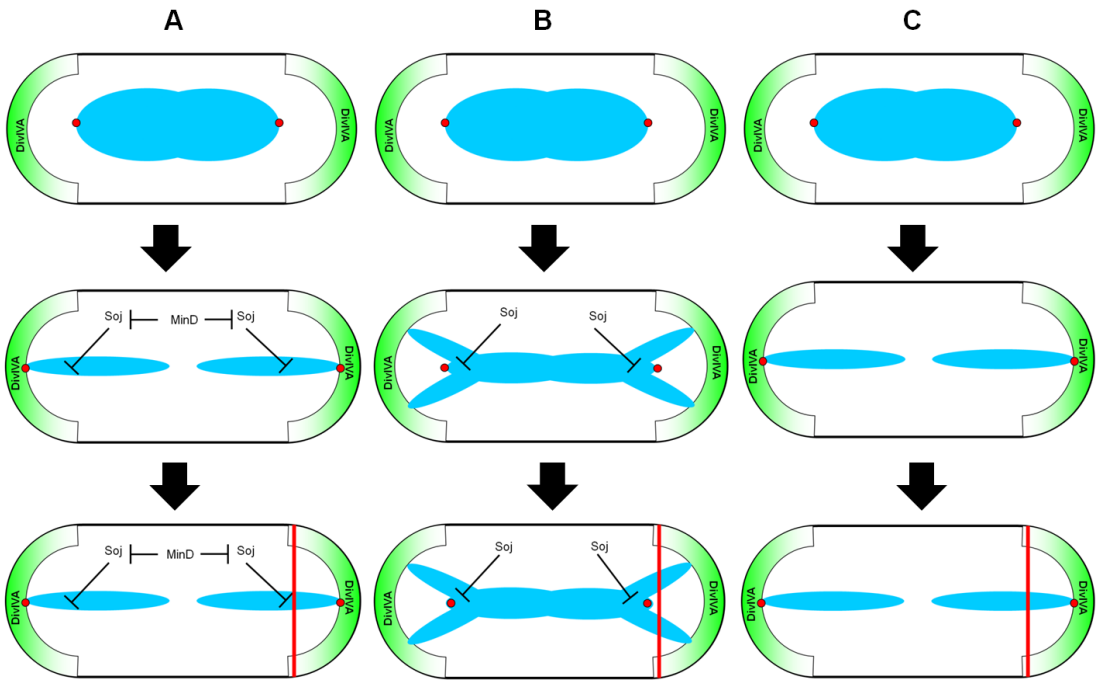

Figure 7.1: The model presenting involvement of Soj and MinD in chromosome segregation during the early stage of sporulation
In wild type sporulating cells, the negative effect of Soj on *oriC* movement to the cell pole is inhibited by MinD and therefore *oriC* of the chromosome can be attached to the cell pole (A). When MinD is absent, Soj inhibits *oriC* movement to the cell poles, and therefore *oriC* is not trapped in the prespore (B). However, when both Soj and MinD are absent, there is no inhibition of *oriC* movement and it can be released from the quarter position of the cell to be attached to the cell pole (C).

with other proteins involved: DivIVA, Spo0J, RacA. However, in the absence of MinD Soj can still inhibit the release of the *oriC* from the quarter position and its movement to the cell pole. Because the DivIVA/Spo0J complex described by Perry and Edwards (Perry and Edwards, 2006) can probably still be formed in these strains, and the RacA protein is active, the flanking regions left and right of *oriC* can be

properly attached to the cell pole. When in the cells that lack MinD we delete also Soj, there is no inhibition of the *oriC* movement to the cell pole and therefore *oriC* is properly attached to the pole prior to asymmetric septum formation. Wu and Errington reported difficulties to release the *oriC* form the quarter positions also in *divIVA* mutant and *soj racA* double mutant (the defect is comparable to *minD* single mutant) and the Spo0J foci are far from the cell poles in these strains (Wu and Errington, 2003). This might suggest the important role of Spo0J in chromosome relocation, which needs also DivIVA for the formation of the complex, and also Soj and MinD for its activity.

According to the model, it is possible that there are 3 important complexes involved in the *oriC* movement to the cell pole. One is the DivIVA/Spo0J complex, previously described by Perry and Edwards, which appears only during the early stage of sporulation (Perry and Edwards, 2006) and, similarly to the second complex RacA/DivIVA, helps to attach the chromosome to the cell pole. The third complex which involves MinD and Soj is important to allow the release of the *oriC* from the quarter positions of the cell prior to its attachment to the cell pole. The Soj/MinD complex is employed in the system prior to the other two complexes. This is also in

an agreement with the finding that Spo0J/DivIVA complex does not require MinD (Perry and Edwards, 2004).

This idea can also be supported by how the asymmetric septum can be formed in the presence of the MinD protein, which together with MinC inhibits FtsZ polymerisation during the vegetative growth. If the MinD is bound to a complex with Soj during the sporulation to help to release the *oriC* form the quarter positions of the cell, it is no longer available to inhibit the asymmetric septum formation and so the septum during sporulation can be formed at the cell pole.

To test our model in more detail, a time-lapse microscopy of *oriC* localisation is needed to test whether in the *minD* mutant *oriC* indeed cannot move from the midcell position to the cell pole as we proposed in the model, or that it moves to the cell pole, but is then moved back to the midcell position.

MinD is also known to affect the orientation of SpoIIIE assembly in the prespore: in the absence of MinD, SpoIIIE can assemble so that it exports DNA from the prespore into the mother cell (Becker and Pogliano, 2007). However, in our experiments we used SpoIIIE mutant that is unable to perform any DNA transfer. Therefore we believe that the observed *minD* defect is due to inability of *oriC* to move to the cell pole rather than being exported back into the mother cell after it has already been properly positioned to the cell pole.

To further understand the exact activity of MinD in this process, testing trapping efficiency of different MinD point mutants would be beneficial. This would reveal

which parts of MinD are required for the trapping function. Because MinD has an ability to bind membranes, it would be beneficial to test MinD mutants that are unable to bind membranes how they are able to trap the *oriC* region of the chromosome.

Bacterial Two-Hybrid screen with MinD and a library of different cell division related proteins did not reveal any new interaction that could be important for the trapping process. However, using a Synthetic Lethal Screen we identified the gene *yshB* gene of an unknown function. The product of *yshB* gene might play a similar role in the cell to that of the MinCD proteins, but during the vegetative growth and therefore is probably not involved in the trapping process directly. However, testing the trapping pattern of *yshB* strain should be done to exclude the possibility that it plays any role in sporulation. To answer the question which proteins interact with MinD during the early stage of sporulation, a pull down experiment using tagged MinD could be done. Preliminary data showed that MinD fused to a histidine tag is fully active and could be used to perform a pull down experiment during the early stage of sporulation.

In conclusion, we have shown and confirmed the trapping defect of strains lacking *minD* such that the *oriC* of the chromosome is not trapped in the prespore. This defect is not due to the initiation of over-replication of the chromosomes in the cells or the presence of more than two copies of the chromosome in the sporulating cell. The observed trapping defect can be suppressed by deletion of *soj*, leading us to speculate that MinD inhibits Soj when it prevents *oriC* to be trapped in the prespore.

References

Adams, D.W., and Errington, J. (2009). Bacterial cell division: assembly, maintenance and disassembly of the Z ring. Nat Rev Microbiol *7*, 642-653.

Adler, H.I., Fisher, W.D., Cohen, A., and Hardigree, A.A. (1967). MINIATURE escherichia coli CELLS DEFICIENT IN DNA. Proc Natl Acad Sci U S A *57*, 321-326.

Arigoni, F., Duncan, L., Alper, S., Losick, R., and Stragier, P. (1996). SpoIIE governs the phosphorylation state of a protein regulating transcription factor sigma F during sporulation in Bacillus subtilis. Proc Natl Acad Sci U S A *93*, 3238-3242.

Aronson, A.I., and Fitz-James, P. (1976). Structure and morphogenesis of the bacterial spore coat. Bacteriol Rev *40*, 360-402.

Autret, S., and Errington, J. (2003). A role for division-site-selection protein MinD in regulation of internucleoid jumping of Soj (ParA) protein in Bacillus subtilis. Mol Microbiol *47*, 159-169.

Autret, S., Nair, R., and Errington, J. (2001). Genetic analysis of the chromosome segregation protein Spo0J of Bacillus subtilis: evidence for separate domains involved in DNA binding and interactions with Soj protein. Mol Microbiol *41*, 743-755.

Baker, T.A., and Bell, S.P. (1998). Polymerases and the replisome: machines within machines. Cell *92*, 295-305.

Barak, I., Behari, J., Olmedo, G., Guzman, P., Brown, D.P., Castro, E., Walker, D., Westpheling, J., and Youngman, P. (1996). Structure and function of the Bacillus SpoIIE protein and its localization to sites of sporulation septum assembly. Mol Microbiol *19*, 1047-1060.

Barak, I., Muchova, K., Wilkinson, A.J., O'Toole, P.J., and Pavlendova, N. (2008). Lipid spirals in Bacillus subtilis and their role in cell division. Mol Microbiol *68*, 1315-1327.

Barak, I., Prepiak, P., and Schmeisser, F. (1998). MinCD proteins control the septation process during sporulation of Bacillus subtilis. J Bacteriol *180*, 5327-5333.

Barak, I., and Wilkinson, A.J. (2007). Division site recognition in Escherichia coli and Bacillus subtilis. FEMS Microbiol Rev *31*, 311-326.

Barre, F.X. (2007). FtsK and SpoIIIE: the tale of the conserved tails. Mol Microbiol *66*, 1051-1055.

Bates, D., and Kleckner, N. (2005). Chromosome and replisome dynamics in E. coli: loss of sister cohesion triggers global chromosome movement and mediates chromosome segregation. Cell *121*, 899-911.

Bath, J., Wu, L.J., Errington, J., and Wang, J.C. (2000). Role of Bacillus subtilis SpoIIIE in DNA transport across the mother cell-prespore division septum. Science *290*, 995-997.

Becker, E.C., and Pogliano, K. (2007). Cell-specific SpoIIIE assembly and DNA translocation polarity are dictated by chromosome orientation. Mol Microbiol *66*, 1066-1079.

Ben-Yehuda, S., Fujita, M., Liu, X.S., Gorbatyuk, B., Skoko, D., Yan, J., Marko, J.F., Liu, J.S., Eichenberger, P., Rudner, D.Z., *et al.* (2005). Defining a centromere-like element in Bacillus subtilis by Identifying the binding sites for the chromosome-anchoring protein RacA. Mol Cell *17*, 773-782.

Ben-Yehuda, S., and Losick, R. (2002). Asymmetric cell division in B. subtilis involves a spiral-like intermediate of the cytokinetic protein FtsZ. Cell *109*, 257-266.

Ben-Yehuda, S., Rudner, D.Z., and Losick, R. (2003). RacA, a bacterial protein that anchors chromosomes to the cell poles. Science *299*, 532-536.

Berkmen, M.B., and Grossman, A.D. (2006). Spatial and temporal organization of the Bacillus subtilis replication cycle. Mol Microbiol *62*, 57-71.

Bernhardt, T.G., and de Boer, P.A. (2005). SlmA, a nucleoid-associated, FtsZ binding protein required for blocking septal ring assembly over Chromosomes in E. coli. Mol Cell *18*, 555-564.

Blaesing, F., Weigel, C., Welzeck, M., and Messer, W. (2000). Analysis of the DNA-binding domain of Escherichia coli DnaA protein. Mol Microbiol *36*, 557-569.

Bogush, M., Xenopoulos, P., and Piggot, P.J. (2007). Separation of chromosome termini during sporulation of Bacillus subtilis depends on SpoIIIE. J Bacteriol *189*, 3564-3572.

Boye, E., and Nordstrom, K. (2003). Coupling the cell cycle to cell growth. EMBO Rep *4*, 757-760.

Bramkamp, M., Emmins, R., Weston, L., Donovan, C., Daniel, R.A., and Errington, J. (2008). A novel component of the division-site selection system of Bacillus subtilis and a new mode of action for the division inhibitor MinCD. Mol Microbiol *70*, 1556-1569.

Bramkamp, M., Weston, L., Daniel, R.A., and Errington, J. (2006). Regulated intramembrane proteolysis of FtsL protein and the control of cell division in Bacillus subtilis. Mol Microbiol *62*, 580-591.

Breier, A.M., and Grossman, A.D. (2007). Whole-genome analysis of the chromosome partitioning and sporulation protein Spo0J (ParB) reveals spreading and origin-distal sites on the Bacillus subtilis chromosome. Mol Microbiol *64*, 703-718.

Bruand, C., and Ehrlich, S.D. (1995). The Bacillus subtilis dnaI gene is part of the dnaB operon. Microbiology *141 (Pt 5)*, 1199-1200.

Bruand, C., Ehrlich, S.D., and Janniere, L. (1995). Primosome assembly site in Bacillus subtilis. EMBO J *14*, 2642-2650.

Budde, I., Steil, L., Scharf, C., Volker, U., and Bremer, E. (2006). Adaptation of Bacillus subtilis to growth at low temperature: a combined transcriptomic and proteomic appraisal. Microbiology *152*, 831-853.

Burbulys, D., Trach, K.A., and Hoch, J.A. (1991). Initiation of sporulation in B. subtilis is controlled by a multicomponent phosphorelay. Cell *64*, 545-552.

Burkholder, P.R., and Giles, N.H., Jr. (1947). Induced biochemical mutations in Bacillus subtilis. Am J Bot *34*, 345-348.

Burkholder, W.F., Kurtser, I., and Grossman, A.D. (2001). Replication initiation proteins regulate a developmental checkpoint in Bacillus subtilis. Cell *104*, 269-279.

Burton, B.M., Marquis, K.A., Sullivan, N.L., Rapoport, T.A., and Rudner, D.Z. (2007). The ATPase SpoIIIE transports DNA across fused septal membranes during sporulation in Bacillus subtilis. Cell *131*, 1301-1312.

Bussiere, D.E., and Bastia, D. (1999). Termination of DNA replication of bacterial and plasmid chromosomes. Mol Microbiol *31*, 1611-1618.

Cano, R.J., and Borucki, M.K. (1995). Revival and identification of bacterial spores in 25- to 40-million-year-old Dominican amber. Science *268*, 1060-1064.

Cha, J.H., and Stewart, G.C. (1997). The divIVA minicell locus of Bacillus subtilis. J Bacteriol *179*, 1671-1683.

Chary, V.K., Amaya, E.I., and Piggot, P.J. (1997). Neomycin- and spectinomycin-resistance replacement vectors for Bacillus subtilis. FEMS Microbiol Lett *153*, 135-139.

Chung, K.M., Hsu, H.H., Yeh, H.Y., and Chang, B.Y. (2007). Mechanism of regulation of prokaryotic tubulin-like GTPase FtsZ by membrane protein EzrA. J Biol Chem *282*, 14891-14897.

Churchward, G., Estiva, E., and Bremer, H. (1981). Growth rate-dependent control of chromosome replication initiation in Escherichia coli. J Bacteriol *145*, 1232-1238.

Claessen, D., Emmins, R., Hamoen, L.W., Daniel, R.A., Errington, J., and Edwards, D.H. (2008). Control of the cell elongation-division cycle by shuttling of PBP1 protein in Bacillus subtilis. Mol Microbiol *68*, 1029-1046.

Coppolecchia, R., DeGrazia, H., and Moran, C.P., Jr. (1991). Deletion of spoIIAB blocks endospore formation in Bacillus subtilis at an early stage. J Bacteriol *173*, 6678-6685.

Cutting, S., Driks, A., Schmidt, R., Kunkel, B., and Losick, R. (1991a). Forespore-specific transcription of a gene in the signal transduction pathway that governs Pro-sigma K processing in Bacillus subtilis. Genes Dev *5*, 456-466.

Cutting, S., Roels, S., and Losick, R. (1991b). Sporulation operon spoIVF and the characterization of mutations that uncouple mother-cell from forespore gene expression in Bacillus subtilis. J Mol Biol *221*, 1237-1256.

Dainty, S.J., Kennedy, C.A., Watt, S., Bahler, J., and Whitehall, S.K. (2008). Response of Schizosaccharomyces pombe to zinc deficiency. Eukaryot Cell *7*, 454-464.

Dajkovic, A., Lan, G., Sun, S.X., Wirtz, D., and Lutkenhaus, J. (2008). MinC spatially controls bacterial cytokinesis by antagonizing the scaffolding function of FtsZ. Curr Biol *18*, 235-244.

Daniel, R.A., Drake, S., Buchanan, C.E., Scholle, R., and Errington, J. (1994). The Bacillus subtilis spoVD gene encodes a mother-cell-specific penicillin-binding protein required for spore morphogenesis. J Mol Biol *235*, 209-220.

Daniel, R.A., and Errington, J. (2000). Intrinsic instability of the essential cell division protein FtsL of Bacillus subtilis and a role for DivIB protein in FtsL turnover. Mol Microbiol *36*, 278-289.

Daniel, R.A., Harry, E.J., and Errington, J. (2000). Role of penicillin-binding protein PBP 2B in assembly and functioning of the division machinery of Bacillus subtilis. Mol Microbiol *35*, 299-311.

Daniel, R.A., Harry, E.J., Katis, V.L., Wake, R.G., and Errington, J. (1998). Characterization of the essential cell division gene ftsL(yIID) of Bacillus subtilis and its role in the assembly of the division apparatus. Mol Microbiol *29*, 593-604.

Daniel, R.A., Noirot-Gros, M.F., Noirot, P., and Errington, J. (2006). Multiple interactions between the transmembrane division proteins of Bacillus subtilis and the role of FtsL instability in divisome assembly. J Bacteriol *188*, 7396-7404.

de Boer, P.A., Crossley, R.E., Hand, A.R., and Rothfield, L.I. (1991). The MinD protein is a membrane ATPase required for the correct placement of the Escherichia coli division site. EMBO J *10*, 4371-4380.

de Boer, P.A., Crossley, R.E., and Rothfield, L.I. (1989). A division inhibitor and a topological specificity factor coded for by the minicell locus determine proper placement of the division septum in E. coli. Cell *56*, 641-649.

de Boer, P.A., Crossley, R.E., and Rothfield, L.I. (1992). Roles of MinC and MinD in the site-specific septation block mediated by the MinCDE system of Escherichia coli. J Bacteriol *174*, 63-70.

Din, N., Quardokus, E.M., Sackett, M.J., and Brun, Y.V. (1998). Dominant C-terminal deletions of FtsZ that affect its ability to localize in Caulobacter and its interaction with FtsA. Mol Microbiol *27*, 1051-1063.

Divakaruni, A.V., Baida, C., White, C.L., and Gober, J.W. (2007). The cell shape proteins MreB and MreC control cell morphogenesis by positioning cell wall synthetic complexes. Mol Microbiol *66*, 174-188.

Doubrovinski, K., and Howard, M. (2005). Stochastic model for Soj relocation dynamics in Bacillus subtilis. Proc Natl Acad Sci U S A *102*, 9808-9813.

Driks, A. (2004). The bacillus spore coat. Phytopathology *94*, 1249-1251.

Driks, A., Roels, S., Beall, B., Moran, C.P., Jr., and Losick, R. (1994). Subcellular localization of proteins involved in the assembly of the spore coat of Bacillus subtilis. Genes Dev *8*, 234-244.

Duncan, L., Alper, S., Arigoni, F., Losick, R., and Stragier, P. (1995). Activation of cell-specific transcription by a serine phosphatase at the site of asymmetric division. Science *270*, 641-644.

Duncan, L., and Losick, R. (1993). SpoIIAB is an anti-sigma factor that binds to and inhibits transcription by regulatory protein sigma F from Bacillus subtilis. Proc Natl Acad Sci U S A *90*, 2325-2329.

Edwards, D.H., and Errington, J. (1997). The Bacillus subtilis DivIVA protein targets to the division septum and controls the site specificity of cell division. Mol Microbiol *24*, 905-915.

Edwards, D.H., Thomaides, H.B., and Errington, J. (2000). Promiscuous targeting of Bacillus subtilis cell division protein DivIVA to division sites in Escherichia coli and fission yeast. EMBO J *19*, 2719-2727.

Eichenberger, P., Fawcett, P., and Losick, R. (2001). A three-protein inhibitor of polar septation during sporulation in Bacillus subtilis. Mol Microbiol *42*, 1147-1162.

Errington, J. (1991). A model for asymmetric septum formation during sporulation in Bacillus subtilis. Mol Microbiol *5*, 785-789.

Errington, J. (1993). Bacillus subtilis sporulation: regulation of gene expression and control of morphogenesis. Microbiol Rev *57*, 1-33.

Errington, J. (2001). Septation and chromosome segregation during sporulation in Bacillus subtilis. Curr Opin Microbiol *4*, 660-666.

Errington, J. (2003). Regulation of endospore formation in Bacillus subtilis. Nat Rev Microbiol *1*, 117-126.

Errington, J., Appleby, L., Daniel, R.A., Goodfellow, H., Partridge, S.R., and Yudkin, M.D. (1992). Structure and function of the spoIIIJ gene of Bacillus subtilis: a

vegetatively expressed gene that is essential for sigma G activity at an intermediate stage of sporulation. J Gen Microbiol *138*, 2609-2618.

Errington, J., Daniel, R.A., and Scheffers, D.J. (2003). Cytokinesis in bacteria. Microbiol Mol Biol Rev *67*, 52-65, table of contents.

Errington, J., and Mandelstam, J. (1983). Variety of sporulation phenotypes resulting from mutations in a single regulatory locus, spoIIA, in Bacillus subtilis. J Gen Microbiol *129*, 2091-2101.

Fan, N., Cutting, S., and Losick, R. (1992). Characterization of the Bacillus subtilis sporulation gene spoVK. J Bacteriol *174*, 1053-1054.

Fawcett, P., Eichenberger, P., Losick, R., and Youngman, P. (2000). The transcriptional profile of early to middle sporulation in Bacillus subtilis. Proc Natl Acad Sci U S A *97*, 8063-8068.

Feucht, A., Abbotts, L., and Errington, J. (2002). The cell differentiation protein SpoIIE contains a regulatory site that controls its phosphatase activity in response to asymmetric septation. Mol Microbiol *45*, 1119-1130.

Feucht, A., Evans, L., and Errington, J. (2003). Identification of sporulation genes by genome-wide analysis of the sigmaE regulon of Bacillus subtilis. Microbiology *149*, 3023-3034.

Formstone, A., and Errington, J. (2005). A magnesium-dependent mreB null mutant: implications for the role of mreB in Bacillus subtilis. Mol Microbiol *55*, 1646-1657.

Frandsen, N., and Stragier, P. (1995). Identification and characterization of the Bacillus subtilis spoIIP locus. J Bacteriol *177*, 716-722.

Fukuoka, T., Moriya, S., Yoshikawa, H., and Ogasawara, N. (1990). Purification and characterization of an initiation protein for chromosomal replication, DnaA, in Bacillus subtilis. J Biochem *107*, 732-739.

Fuller, R.S., Funnell, B.E., and Kornberg, A. (1984). The dnaA protein complex with the E. coli chromosomal replication origin (oriC) and other DNA sites. Cell *38*, 889-900.

Gamba, P., Veening, J.W., Saunders, N.J., Hamoen, L.W., and Daniel, R.A. (2009). Two-step assembly dynamics of the Bacillus subtilis divisome. J Bacteriol *191*, 4186-4194.

Gerdes, K., Moller-Jensen, J., and Bugge Jensen, R. (2000). Plasmid and chromosome partitioning: surprises from phylogeny. Mol Microbiol *37*, 455-466.

Gholamhoseinian, A., and Piggot, P.J. (1989). Timing of spoII gene expression relative to septum formation during sporulation of Bacillus subtilis. J Bacteriol *171*, 5747-5749.

Glaser, P., Sharpe, M.E., Raether, B., Perego, M., Ohlsen, K., and Errington, J. (1997). Dynamic, mitotic-like behavior of a bacterial protein required for accurate chromosome partitioning. Genes Dev *11*, 1160-1168.

Glenn, A.R., and Mandelstam, J. (1971). Sporulation in Bacillus subtilis 168. Comparison of alkaline phosphatase from sporulating and vegetative cells. Biochem J *123*, 129-138.

Goranov, A.I., Breier, A.M., Merrikh, H., and Grossman, A.D. (2009). YabA of Bacillus subtilis controls DnaA-mediated replication initiation but not the transcriptional response to replication stress. Mol Microbiol *74*, 454-466.

Graumann, P.L., and Losick, R. (2001). Coupling of asymmetric division to polar placement of replication origin regions in Bacillus subtilis. J Bacteriol *183*, 4052-4060.

Gregory, J.A., Becker, E.C., and Pogliano, K. (2008). Bacillus subtilis MinC destabilizes FtsZ-rings at new cell poles and contributes to the timing of cell division. Genes Dev *22*, 3475-3488.

Grossman, A.D., and Losick, R. (1988). Extracellular control of spore formation in Bacillus subtilis. Proc Natl Acad Sci U S A *85*, 4369-4373.

Gueiros-Filho, F.J., and Losick, R. (2002). A widely conserved bacterial cell division protein that promotes assembly of the tubulin-like protein FtsZ. Genes Dev *16*, 2544-2556.

Haeusser, D.P., Schwartz, R.L., Smith, A.M., Oates, M.E., and Levin, P.A. (2004). EzrA prevents aberrant cell division by modulating assembly of the cytoskeletal protein FtsZ. Mol Microbiol *52*, 801-814.

Hamoen, L.W., Meile, J.C., de Jong, W., Noirot, P., and Errington, J. (2006). SepF, a novel FtsZ-interacting protein required for a late step in cell division. Mol Microbiol *59*, 989-999.

Harry, E.J. (2001). Bacterial cell division: regulating Z-ring formation. Mol Microbiol *40*, 795-803.

Harry, E.J., and Lewis, P.J. (2003). Early targeting of Min proteins to the cell poles in germinated spores of Bacillus subtilis: evidence for division apparatus-independent recruitment of Min proteins to the division site. Mol Microbiol *47*, 37-48.

Harry, E.J., Rodwell, J., and Wake, R.G. (1999). Co-ordinating DNA replication with cell division in bacteria: a link between the early stages of a round of replication and mid-cell Z ring assembly. Mol Microbiol *33*, 33-40.

Hayashi, I., Oyama, T., and Morikawa, K. (2001). Structural and functional studies of MinD ATPase: implications for the molecular recognition of the bacterial cell division apparatus. EMBO J *20*, 1819-1828.

Hayashi, M., Ogura, Y., Harry, E.J., Ogasawara, N., and Moriya, S. (2005). Bacillus subtilis YabA is involved in determining the timing and synchrony of replication initiation. FEMS Microbiol Lett *247*, 73-79.

Heidrich, C., Templin, M.F., Ursinus, A., Merdanovic, M., Berger, J., Schwarz, H., de Pedro, M.A., and Holtje, J.V. (2001). Involvement of N-acetylmuramyl-L-alanine amidases in cell separation and antibiotic-induced autolysis of Escherichia coli. Mol Microbiol *41*, 167-178.

Henriques, A.O., and Moran, C.P., Jr. (2000). Structure and assembly of the bacterial endospore coat. Methods *20*, 95-110.

Hilbert, D.W., and Piggot, P.J. (2004). Compartmentalization of gene expression during Bacillus subtilis spore formation. Microbiol Mol Biol Rev *68*, 234-262.

Hiraga, S. (2000). Dynamic localization of bacterial and plasmid chromosomes. Annu Rev Genet *34*, 21-59.

Hiragi, Y. (1972). Physical, chemical and morphological studies of spore coat of Bacillus subtilis. J Gen Microbiol *72*, 87-99.

Hu, Z., and Lutkenhaus, J. (1999). Topological regulation of cell division in Escherichia coli involves rapid pole to pole oscillation of the division inhibitor MinC under the control of MinD and MinE. Mol Microbiol *34*, 82-90.

Hu, Z., and Lutkenhaus, J. (2001). Topological regulation of cell division in E. coli. spatiotemporal oscillation of MinD requires stimulation of its ATPase by MinE and phospholipid. Mol Cell *7*, 1337-1343.

Hu, Z., Mukherjee, A., Pichoff, S., and Lutkenhaus, J. (1999). The MinC component of the division site selection system in Escherichia coli interacts with FtsZ to prevent polymerization. Proc Natl Acad Sci U S A *96*, 14819-14824.

Hu, Z., Saez, C., and Lutkenhaus, J. (2003). Recruitment of MinC, an inhibitor of Z-ring formation, to the membrane in Escherichia coli: role of MinD and MinE. J Bacteriol *185*, 196-203.

Huang, J., Cao, C., and Lutkenhaus, J. (1996). Interaction between FtsZ and inhibitors of cell division. J Bacteriol *178*, 5080-5085.

Illing, N., and Errington, J. (1991a). Genetic regulation of morphogenesis in Bacillus subtilis: roles of sigma E and sigma F in prespore engulfment. J Bacteriol *173*, 3159-3169.

Illing, N., and Errington, J. (1991b). The spoIIIA operon of Bacillus subtilis defines a new temporal class of mother-cell-specific sporulation genes under the control of the sigma E form of RNA polymerase. Mol Microbiol *5*, 1927-1940.

Ireton, K., and Grossman, A.D. (1994). A developmental checkpoint couples the initiation of sporulation to DNA replication in Bacillus subtilis. EMBO J *13*, 1566-1573.

Ireton, K., Gunther, N.W.t., and Grossman, A.D. (1994). spo0J is required for normal chromosome segregation as well as the initiation of sporulation in Bacillus subtilis. J Bacteriol *176*, 5320-5329.

Ishikawa, S., Kawai, Y., Hiramatsu, K., Kuwano, M., and Ogasawara, N. (2006). A new FtsZ-interacting protein, YlmF, complements the activity of FtsA during progression of cell division in Bacillus subtilis. Mol Microbiol *60*, 1364-1380.

Ishikawa, S., Ogura, Y., Yoshimura, M., Okumura, H., Cho, E., Kawai, Y., Kurokawa, K., Oshima, T., and Ogasawara, N. (2007). Distribution of stable DnaA-binding sites on the Bacillus subtilis genome detected using a modified ChIP-chip method. DNA Res *14*, 155-168.

Itaya, M. (1992). Construction of a novel tetracycline resistance gene cassette useful as a marker on the Bacillus subtilis chromosome. Biosci Biotechnol Biochem *56*, 685-686.

Jones, L.J., Carballido-Lopez, R., and Errington, J. (2001). Control of cell shape in bacteria: helical, actin-like filaments in Bacillus subtilis. Cell *104*, 913-922.

Kaimer, C., Gonzalez-Pastor, J.E., and Graumann, P.L. (2009). SpoIIIE and a novel type of DNA translocase, SftA, couple chromosome segregation with cell division in Bacillus subtilis. Mol Microbiol *74*, 810-825.

Karimova, G., Pidoux, J., Ullmann, A., and Ladant, D. (1998). A bacterial two-hybrid system based on a reconstituted signal transduction pathway. Proc Natl Acad Sci U S A *95*, 5752-5756.

Karow, M.L., Glaser, P., and Piggot, P.J. (1995). Identification of a gene, spoIIR, that links the activation of sigma E to the transcriptional activity of sigma F during sporulation in Bacillus subtilis. Proc Natl Acad Sci U S A *92*, 2012-2016.

Katis, V.L., Harry, E.J., and Wake, R.G. (1997). The Bacillus subtilis division protein DivIC is a highly abundant membrane-bound protein that localizes to the division site. Mol Microbiol *26*, 1047-1055.

Keijser, B.J., Ter Beek, A., Rauwerda, H., Schuren, F., Montijn, R., van der Spek, H., and Brul, S. (2007). Analysis of temporal gene expression during Bacillus subtilis spore germination and outgrowth. J Bacteriol *189*, 3624-3634.

Kelman, Z., and O'Donnell, M. (1995). DNA polymerase III holoenzyme: structure and function of a chromosomal replicating machine. Annu Rev Biochem *64*, 171-200.

King, N., Dreesen, O., Stragier, P., Pogliano, K., and Losick, R. (1999). Septation, dephosphorylation, and the activation of sigmaF during sporulation in Bacillus subtilis. Genes Dev *13*, 1156-1167.

Krause, M., Ruckert, B., Lurz, R., and Messer, W. (1997). Complexes at the replication origin of Bacillus subtilis with homologous and heterologous DnaA protein. J Mol Biol *274*, 365-380.

Kruse, K., Howard, M., and Margolin, W. (2007). An experimentalist's guide to computational modelling of the Min system. Mol Microbiol *63*, 1279-1284.

Lackner, L.L., Raskin, D.M., and de Boer, P.A. (2003). ATP-dependent interactions between Escherichia coli Min proteins and the phospholipid membrane in vitro. J Bacteriol *185*, 735-749.

Le Breton, Y., Mohapatra, N.P., and Haldenwang, W.G. (2006). In vivo random mutagenesis of Bacillus subtilis by use of TnYLB-1, a mariner-based transposon. Appl Environ Microbiol *72*, 327-333.

Leaver, M., Dominguez-Cuevas, P., Coxhead, J.M., Daniel, R.A., and Errington, J. (2009). Life without a wall or division machine in Bacillus subtilis. Nature *457*, 849-853.

Leaver, M., and Errington, J. (2005). Roles for MreC and MreD proteins in helical growth of the cylindrical cell wall in Bacillus subtilis. Mol Microbiol *57*, 1196-1209.

Lederberg, J. (1957). Mechanism of action of penicillin. J Bacteriol *73*, 144.

Lee, P.S., and Grossman, A.D. (2006). The chromosome partitioning proteins Soj (ParA) and Spo0J (ParB) contribute to accurate chromosome partitioning, separation of replicated sister origins, and regulation of replication initiation in Bacillus subtilis. Mol Microbiol *60*, 853-869.

Lee, P.S., Lin, D.C., Moriya, S., and Grossman, A.D. (2003). Effects of the chromosome partitioning protein Spo0J (ParB) on oriC positioning and replication initiation in Bacillus subtilis. J Bacteriol *185*, 1326-1337.

Lemon, K.P., and Grossman, A.D. (1998). Localization of bacterial DNA polymerase: evidence for a factory model of replication. Science *282*, 1516-1519.

Lemon, K.P., Kurtser, I., Wu, J., and Grossman, A.D. (2000). Control of initiation of sporulation by replication initiation genes in Bacillus subtilis. J Bacteriol *182*, 2989-2991.

Lenarcic, R., Halbedel, S., Visser, L., Shaw, M., Wu, L.J., Errington, J., Marenduzzo, D., and Hamoen, L.W. (2009). Localisation of DivIVA by targeting to negatively curved membranes. EMBO J *28*, 2272-2282.

Levin, P.A., and Grossman, A.D. (1998). Cell cycle and sporulation in Bacillus subtilis. Curr Opin Microbiol *1*, 630-635.

Levin, P.A., Kurtser, I.G., and Grossman, A.D. (1999). Identification and characterization of a negative regulator of FtsZ ring formation in Bacillus subtilis. Proc Natl Acad Sci U S A *96*, 9642-9647.

Levin, P.A., and Losick, R. (1994). Characterization of a cell division gene from Bacillus subtilis that is required for vegetative and sporulation septum formation. J Bacteriol *176*, 1451-1459.

Levin, P.A., and Losick, R. (1996). Transcription factor Spo0A switches the localization of the cell division protein FtsZ from a medial to a bipolar pattern in Bacillus subtilis. Genes Dev *10*, 478-488.

Levin, P.A., Shim, J.J., and Grossman, A.D. (1998). Effect of minCD on FtsZ ring position and polar septation in Bacillus subtilis. J Bacteriol *180*, 6048-6051.

Lewis, P.J., and Errington, J. (1997). Direct evidence for active segregation of oriC regions of the Bacillus subtilis chromosome and co-localization with the SpoOJ partitioning protein. Mol Microbiol *25*, 945-954.

Lewis, P.J., and Marston, A.L. (1999). GFP vectors for controlled expression and dual labelling of protein fusions in Bacillus subtilis. Gene *227*, 101-110.

Lewis, P.J., Smith, M.T., and Wake, R.G. (1989). A protein involved in termination of chromosome replication in Bacillus subtilis binds specifically to the terC site. J Bacteriol *171*, 3564-3567.

Lewis, P.J., and Wake, R.G. (1991). Termination of chromosome replication in Bacillus subtilis. Res Microbiol *142*, 893-900.

Lin, D.C., and Grossman, A.D. (1998). Identification and characterization of a bacterial chromosome partitioning site. Cell *92*, 675-685.

Londono-Vallejo, J.A., Frehel, C., and Stragier, P. (1997). SpoIIQ, a forespore-expressed gene required for engulfment in Bacillus subtilis. Mol Microbiol *24*, 29-39.

Lowe, J., and Amos, L.A. (1998). Crystal structure of the bacterial cell-division protein FtsZ. Nature *391*, 203-206.

Margolin, W. (2001). Spatial regulation of cytokinesis in bacteria. Curr Opin Microbiol *4*, 647-652.

Marquis, K.A., Burton, B.M., Nollmann, M., Ptacin, J.L., Bustamante, C., Ben-Yehuda, S., and Rudner, D.Z. (2008). SpoIIIE strips proteins off the DNA during chromosome translocation. Genes Dev *22*, 1786-1795.

Marston, A.L., and Errington, J. (1999a). Dynamic movement of the ParA-like Soj protein of B. subtilis and its dual role in nucleoid organization and developmental regulation. Mol Cell *4*, 673-682.

Marston, A.L., and Errington, J. (1999b). Selection of the midcell division site in Bacillus subtilis through MinD-dependent polar localization and activation of MinC. Mol Microbiol *33*, 84-96.

Marston, A.L., Thomaides, H.B., Edwards, D.H., Sharpe, M.E., and Errington, J. (1998). Polar localization of the MinD protein of Bacillus subtilis and its role in selection of the mid-cell division site. Genes Dev *12*, 3419-3430.

Matsui, M., Oka, A., Takanami, M., Yasuda, S., and Hirota, Y. (1985). Sites of dnaA protein-binding in the replication origin of the Escherichia coli K-12 chromosome. J Mol Biol *184*, 529-533.

Mazor, S., Regev, T., Mileykovskaya, E., Margolin, W., Dowhan, W., and Fishov, I. (2008a). Mutual effects of MinD-membrane interaction: I. Changes in the membrane properties induced by MinD binding. Biochim Biophys Acta *1778*, 2496-2504.

Mazor, S., Regev, T., Mileykovskaya, E., Margolin, W., Dowhan, W., and Fishov, I. (2008b). Mutual effects of MinD-membrane interaction: II. Domain structure of the membrane enhances MinD binding. Biochim Biophys Acta *1778*, 2505-2511.

Messer, W. (2002). The bacterial replication initiator DnaA. DnaA and oriC, the bacterial mode to initiate DNA replication. FEMS Microbiol Rev *26*, 355-374.

Messer, W., Blaesing, F., Jakimowicz, D., Krause, M., Majka, J., Nardmann, J., Schaper, S., Seitz, H., Speck, C., Weigel, C., *et al.* (2001). Bacterial replication initiator DnaA. Rules for DnaA binding and roles of DnaA in origin unwinding and helicase loading. Biochimie *83*, 5-12.

Messer, W., Blaesing, F., Majka, J., Nardmann, J., Schaper, S., Schmidt, A., Seitz, H., Speck, C., Tungler, D., Wegrzyn, G., *et al.* (1999). Functional domains of DnaA proteins. Biochimie *81*, 819-825.

Min, K.T., Hilditch, C.M., Diederich, B., Errington, J., and Yudkin, M.D. (1993). Sigma F, the first compartment-specific transcription factor of B. subtilis, is regulated by an anti-sigma factor that is also a protein kinase. Cell *74*, 735-742.

Moir, A. (1981). Germination properties of a spore coat-defective mutant of Bacillus subtilis. J Bacteriol *146*, 1106-1116.

Moir, A., Kemp, E.H., Robinson, C., and Corfe, B.M. (1994). The genetic analysis of bacterial spore germination. J Appl Bacteriol *77*, 9S-16S.

Moriya, S., Kato, K., Yoshikawa, H., and Ogasawara, N. (1990). Isolation of a dnaA mutant of Bacillus subtilis defective in initiation of replication: amount of DnaA protein determines cells' initiation potential. EMBO J *9*, 2905-2910.

Mott, M.L., and Berger, J.M. (2007). DNA replication initiation: mechanisms and regulation in bacteria. Nat Rev Microbiol *5*, 343-354.

Murray, H., and Errington, J. (2008). Dynamic control of the DNA replication initiation protein DnaA by Soj/ParA. Cell *135*, 74-84.

Nguyen, T.H., Kumagai, T., Matoba, Y., Suzaki, T., and Sugiyama, M. (2008). Molecular cloning and functional analysis of minD gene from streptomyces lavendulae ATCC25233. J Biosci Bioeng *106*, 303-305.

Nicholson, W.L., Munakata, N., Horneck, G., Melosh, H.J., and Setlow, P. (2000). Resistance of Bacillus endospores to extreme terrestrial and extraterrestrial environments. Microbiol Mol Biol Rev *64*, 548-572.

Nogales, E., Downing, K.H., Amos, L.A., and Lowe, J. (1998). Tubulin and FtsZ form a distinct family of GTPases. Nat Struct Biol *5*, 451-458.

Noirot-Gros, M.F., Dervyn, E., Wu, L.J., Mervelet, P., Errington, J., Ehrlich, S.D., and Noirot, P. (2002). An expanded view of bacterial DNA replication. Proc Natl Acad Sci U S A *99*, 8342-8347.

Ogasawara, N., Moriya, S., Mazza, P.G., and Yoshikawa, H. (1986). Nucleotide sequence and organization of dnaB gene and neighbouring genes on the Bacillus subtilis chromosome. Nucleic Acids Res *14*, 9989-9999.

Osawa, M., and Erickson, H.P. (2006). FtsZ from divergent foreign bacteria can function for cell division in Escherichia coli. J Bacteriol *188*, 7132-7140.

Partridge, S.R., and Errington, J. (1993). The importance of morphological events and intercellular interactions in the regulation of prespore-specific gene expression during sporulation in Bacillus subtilis. Mol Microbiol *8*, 945-955.

Partridge, S.R., Foulger, D., and Errington, J. (1991). The role of sigma F in prespore-specific transcription in Bacillus subtilis. Mol Microbiol *5*, 757-767.

Patrick, J.E., and Kearns, D.B. (2008). MinJ (YvjD) is a topological determinant of cell division in Bacillus subtilis. Mol Microbiol *70*, 1166-1179.

Pavlendova, N., Muchova, K., and Barak, I. (2007). Chromosome segregation in Bacillus subtilis. Folia Microbiol (Praha) *52*, 563-572.

Perry, S.E., and Edwards, D.H. (2004). Identification of a polar targeting determinant for Bacillus subtilis DivIVA. Mol Microbiol *54*, 1237-1249.

Perry, S.E., and Edwards, D.H. (2006). The Bacillus subtilis DivIVA protein has a sporulation-specific proximity to Spo0J. J Bacteriol *188*, 6039-6043.

Peters, P.C., Migocki, M.D., Thoni, C., and Harry, E.J. (2007). A new assembly pathway for the cytokinetic Z ring from a dynamic helical structure in vegetatively growing cells of Bacillus subtilis. Mol Microbiol *64*, 487-499.

Piggot, P.J. (1973). Mapping of asporogenous mutations of Bacillus subtilis: a minimum estimate of the number of sporeulation operons. J Bacteriol *114*, 1241-1253.

Popham, D.L., Helin, J., Costello, C.E., and Setlow, P. (1996). Muramic lactam in peptidoglycan of Bacillus subtilis spores is required for spore outgrowth but not for spore dehydration or heat resistance. Proc Natl Acad Sci U S A *93*, 15405-15410.

Ptacin, J.L., Nollmann, M., Becker, E.C., Cozzarelli, N.R., Pogliano, K., and Bustamante, C. (2008). Sequence-directed DNA export guides chromosome translocation during sporulation in Bacillus subtilis. Nat Struct Mol Biol *15*, 485-493.

Ramamurthi, K.S., Lecuyer, S., Stone, H.A., and Losick, R. (2009). Geometric cue for protein localization in a bacterium. Science *323*, 1354-1357.

Ramirez-Arcos, S., Szeto, J., Beveridge, T., Victor, C., Francis, F., and Dillon, J. (2001). Deletion of the cell-division inhibitor MinC results in lysis of Neisseria gonorrhoeae. Microbiology *147*, 225-237.

Ramirez-Arcos, S., Szeto, J., Dillon, J.A., and Margolin, W. (2002). Conservation of dynamic localization among MinD and MinE orthologues: oscillation of Neisseria gonorrhoeae proteins in Escherichia coli. Mol Microbiol *46*, 493-504.

Raskin, D.M., and de Boer, P.A. (1999a). MinDE-dependent pole-to-pole oscillation of division inhibitor MinC in Escherichia coli. J Bacteriol *181*, 6419-6424.

Raskin, D.M., and de Boer, P.A. (1999b). Rapid pole-to-pole oscillation of a protein required for directing division to the middle of Escherichia coli. Proc Natl Acad Sci U S A *96*, 4971-4976.

Real, G., Autret, S., Harry, E.J., Errington, J., and Henriques, A.O. (2005). Cell division protein DivIB influences the Spo0J/Soj system of chromosome segregation in Bacillus subtilis. Mol Microbiol *55*, 349-367.

Regamey, A., Harry, E.J., and Wake, R.G. (2000). Mid-cell Z ring assembly in the absence of entry into the elongation phase of the round of replication in bacteria: co-ordinating chromosome replication with cell division. Mol Microbiol *38*, 423-434.

Ricca, E., Cutting, S., and Losick, R. (1992). Characterization of bofA, a gene involved in intercompartmental regulation of pro-sigma K processing during sporulation in Bacillus subtilis. J Bacteriol *174*, 3177-3184.

Rong, S., Rosenkrantz, M.S., and Sonenshein, A.L. (1986). Transcriptional control of the Bacillus subtilis spoIID gene. J Bacteriol *165*, 771-779.

Rothfield, L., Taghbalout, A., and Shih, Y.L. (2005). Spatial control of bacterial division-site placement. Nat Rev Microbiol *3*, 959-968.

Rowland, S.L., Fu, X., Sayed, M.A., Zhang, Y., Cook, W.R., and Rothfield, L.I. (2000). Membrane redistribution of the Escherichia coli MinD protein induced by MinE. J Bacteriol *182*, 613-619.

Rudner, D.Z., and Losick, R. (2001). Morphological coupling in development: lessons from prokaryotes. Dev Cell *1*, 733-742.

Rudner, D.Z., and Losick, R. (2002). A sporulation membrane protein tethers the pro-sigmaK processing enzyme to its inhibitor and dictates its subcellular localization. Genes Dev *16*, 1007-1018.

Ryter, A., Schaeffer, P., and Ionesco, H. (1966). [Cytologic classification, by their blockage stage, of sporulation mutants of Bacillus subtilis Marburg]. Ann Inst Pasteur (Paris) *110*, 305-315.

Sakamoto, Y., Nakai, S., Moriya, S., Yoshikawa, H., and Ogasawara, N. (1995). The Bacillus subtilis dnaC gene encodes a protein homologous to the DnaB helicase of Escherichia coli. Microbiology *141 (Pt 3)*, 641-644.

Schaper, S., and Messer, W. (1995). Interaction of the initiator protein DnaA of Escherichia coli with its DNA target. J Biol Chem *270*, 17622-17626.

Scheffers, D.J. (2008). The effect of MinC on FtsZ polymerization is pH dependent and can be counteracted by ZapA. FEBS Lett *582*, 2601-2608.

Scheffers, D.J., den Blaauwen, T., and Driessen, A.J. (2000). Non-hydrolysable GTP-gamma-S stabilizes the FtsZ polymer in a GDP-bound state. Mol Microbiol *35*, 1211-1219.

Schmidt, R., Margolis, P., Duncan, L., Coppolecchia, R., Moran, C.P., Jr., and Losick, R. (1990). Control of developmental transcription factor sigma F by sporulation regulatory proteins SpoIIAA and SpoIIAB in Bacillus subtilis. Proc Natl Acad Sci U S A *87*, 9221-9225.

Schwarz, U., Asmus, A., and Frank, H. (1969). Autolytic enzymes and cell division of Escherichia coli. J Mol Biol *41*, 419-429.

Setlow, P. (1995). Mechanisms for the prevention of damage to DNA in spores of Bacillus species. Annu Rev Microbiol *49*, 29-54.

Sharp, M.D., and Pogliano, K. (1999). An in vivo membrane fusion assay implicates SpoIIIE in the final stages of engulfment during Bacillus subtilis sporulation. Proc Natl Acad Sci U S A *96*, 14553-14558.

Sharp, M.D., and Pogliano, K. (2002). MinCD-dependent regulation of the polarity of SpoIIIE assembly and DNA transfer. EMBO J *21*, 6267-6274.

Sharpe, M.E., and Errington, J. (1996). The Bacillus subtilis soj-spo0J locus is required for a centromere-like function involved in prespore chromosome partitioning. Mol Microbiol *21*, 501-509.

Sharpe, M.E., and Errington, J. (1999). Upheaval in the bacterial nucleoid. An active chromosome segregation mechanism. Trends Genet *15*, 70-74.

Sharpe, M.E., Hauser, P.M., Sharpe, R.G., and Errington, J. (1998). Bacillus subtilis cell cycle as studied by fluorescence microscopy: constancy of cell length at initiation of DNA replication and evidence for active nucleoid partitioning. J Bacteriol *180*, 547-555.

Sherratt, D.J. (2003). Bacterial chromosome dynamics. Science *301*, 780-785.

Shih, Y.L., Fu, X., King, G.F., Le, T., and Rothfield, L. (2002). Division site placement in E.coli: mutations that prevent formation of the MinE ring lead to loss of the normal midcell arrest of growth of polar MinD membrane domains. Embo J *21*, 3347-3357.

Shiomi, D., and Margolin, W. (2007). The C-terminal domain of MinC inhibits assembly of the Z ring in Escherichia coli. J Bacteriol *189*, 236-243.

Sievers, J., and Errington, J. (2000a). Analysis of the essential cell division gene ftsL of Bacillus subtilis by mutagenesis and heterologous complementation. J Bacteriol *182*, 5572-5579.

Sievers, J., and Errington, J. (2000b). The Bacillus subtilis cell division protein FtsL localizes to sites of septation and interacts with DivIC. Mol Microbiol *36*, 846-855.

Sievers, J., Raether, B., Perego, M., and Errington, J. (2002). Characterization of the parB-like yyaA gene of Bacillus subtilis. J Bacteriol *184*, 1102-1111.

Singh, J.K., Makde, R.D., Kumar, V., and Panda, D. (2008). SepF increases the assembly and bundling of FtsZ polymers and stabilizes FtsZ protofilaments by binding along its length. J Biol Chem *283*, 31116-31124.

Smith, K., and Youngman, P. (1993). Evidence that the spoIIM gene of Bacillus subtilis is transcribed by RNA polymerase associated with sigma E. J Bacteriol *175*, 3618-3627.

Sonenshein, A.L. (2000). Control of sporulation initiation in Bacillus subtilis. Curr Opin Microbiol *3*, 561-566.

Steinmetz, M., and Richter, R. (1994). Plasmids designed to alter the antibiotic resistance expressed by insertion mutations in Bacillus subtilis, through in vivo recombination. Gene *142*, 79-83.

Stephenson, K., and Hoch, J.A. (2002). Evolution of signalling in the sporulation phosphorelay. Mol Microbiol *46*, 297-304.

Sterlini, J.M., and Mandelstam, J. (1969). Commitment to sporulation in Bacillus subtilis and its relationship to development of actinomycin resistance. Biochem J *113*, 29-37.

Stragier, P., and Losick, R. (1996). Molecular genetics of sporulation in Bacillus subtilis. Annu Rev Genet *30*, 297-241.

Suefuji, K., Valluzzi, R., and RayChaudhuri, D. (2002). Dynamic assembly of MinD into filament bundles modulated by ATP, phospholipids, and MinE. Proc Natl Acad Sci U S A *99*, 16776-16781.

Sullivan, N.L., Marquis, K.A., and Rudner, D.Z. (2009). Recruitment of SMC by ParB-parS organizes the origin region and promotes efficient chromosome segregation. Cell *137*, 697-707.

Sun, D.X., Cabrera-Martinez, R.M., and Setlow, P. (1991). Control of transcription of the Bacillus subtilis spoIIIG gene, which codes for the forespore-specific transcription factor sigma G. J Bacteriol *173*, 2977-2984.

Sun, D.X., Stragier, P., and Setlow, P. (1989). Identification of a new sigma-factor involved in compartmentalized gene expression during sporulation of Bacillus subtilis. Genes Dev *3*, 141-149.

Sun, Q., and Margolin, W. (1998). FtsZ dynamics during the division cycle of live Escherichia coli cells. J Bacteriol *180*, 2050-2056.

Sun, Y.L., Sharp, M.D., and Pogliano, K. (2000). A dispensable role for forespore-specific gene expression in engulfment of the forespore during sporulation of Bacillus subtilis. J Bacteriol *182*, 2919-2927.

Szeto, J., Acharya, S., Eng, N.F., and Dillon, J.A. (2004). The N terminus of MinD contains determinants which affect its dynamic localization and enzymatic activity. J Bacteriol *186*, 7175-7185.

Szeto, J., Ramirez-Arcos, S., Raymond, C., Hicks, L.D., Kay, C.M., and Dillon, J.A. (2001). Gonococcal MinD affects cell division in Neisseria gonorrhoeae and Escherichia coli and exhibits a novel self-interaction. J Bacteriol *183*, 6253-6264.

Szeto, T.H., Rowland, S.L., Habrukowich, C.L., and King, G.F. (2003). The MinD membrane targeting sequence is a transplantable lipid-binding helix. J Biol Chem *278*, 40050-40056.

Szeto, T.H., Rowland, S.L., Rothfield, L.I., and King, G.F. (2002). Membrane localization of MinD is mediated by a C-terminal motif that is conserved across eubacteria, archaea, and chloroplasts. Proc Natl Acad Sci U S A *99*, 15693-15698.

Taghbalout, A., Ma, L., and Rothfield, L. (2006). Role of MinD-membrane association in Min protein interactions. J Bacteriol *188*, 2993-3001.

Thomaides, H.B., Freeman, M., El Karoui, M., and Errington, J. (2001). Division site selection protein DivIVA of Bacillus subtilis has a second distinct function in chromosome segregation during sporulation. Genes Dev *15*, 1662-1673.

van den Ent, F., Amos, L., and Lowe, J. (2001). Bacterial ancestry of actin and tubulin. Curr Opin Microbiol *4*, 634-638.

van den Ent, F., and Lowe, J. (2006). RF cloning: a restriction-free method for inserting target genes into plasmids. J Biochem Biophys Methods *67*, 67-74.

Vats, P., and Rothfield, L. (2007). Duplication and segregation of the actin (MreB) cytoskeleton during the prokaryotic cell cycle. Proc Natl Acad Sci U S A *104*, 17795-17800.

Veening, J.W., Murray, H., and Errington, J. (2009). A mechanism for cell cycle regulation of sporulation initiation in Bacillus subtilis. Genes Dev *23*, 1959-1970.

Vreeland, R.H., Rosenzweig, W.D., and Powers, D.W. (2000). Isolation of a 250 million-year-old halotolerant bacterium from a primary salt crystal. Nature *407*, 897-900.

Waites, W.M., Kay, D., Dawes, I.W., Wood, D.A., Warren, S.C., and Mandelstam, J. (1970). Sporulation in Bacillus subtilis. Correlation of biochemical events with morphological changes in asporogenous mutants. Biochem J *118*, 667-676.

Wake, R.G. (1997). Replication fork arrest and termination of chromosome replication in Bacillus subtilis. FEMS Microbiol Lett *153*, 247-254.

Wakeley, P.R., Dorazi, R., Hoa, N.T., Bowyer, J.R., and Cutting, S.M. (2000). Proteolysis of SpolVB is a critical determinant in signalling of Pro-sigmaK processing in Bacillus subtilis. Mol Microbiol *36*, 1336-1348.

Wang, J.D., and Levin, P.A. (2009). Metabolism, cell growth and the bacterial cell cycle. Nat Rev Microbiol *7*, 822-827.

Ward, J.B., Jr., and Zahler, S.A. (1973). Genetic studies of leucine biosynthesis in Bacillus subtilis. J Bacteriol *116*, 719-726.

Warth, A.D., Ohye, D.F., and Murrell, W.G. (1963). Location and composition of spore mucopeptide in Bacillus species. J Cell Biol *16*, 593-609.

Weart, R.B., Lee, A.H., Chien, A.C., Haeusser, D.P., Hill, N.S., and Levin, P.A. (2007). A metabolic sensor governing cell size in bacteria. Cell *130*, 335-347.

Weart, R.B., and Levin, P.A. (2003). Growth rate-dependent regulation of medial FtsZ ring formation. J Bacteriol *185*, 2826-2834.

Wei, Y., Havasy, T., McPherson, D.C., and Popham, D.L. (2003). Rod shape determination by the Bacillus subtilis class B penicillin-binding proteins encoded by pbpA and pbpH. J Bacteriol *185*, 4717-4726.

White, C.L., Kitich, A., and Gober, J.W. (2010). Positioning cell wall synthetic complexes by the bacterial morphogenetic proteins MreB and MreD. Mol Microbiol *76*, 616-633.

Williams, D.R., and Thomas, C.M. (1992). Active partitioning of bacterial plasmids. J Gen Microbiol *138*, 1-16.

Wold, S., Skarstad, K., Steen, H.B., Stokke, T., and Boye, E. (1994). The initiation mass for DNA replication in Escherichia coli K-12 is dependent on growth rate. EMBO J *13*, 2097-2102.

Woldringh, C.L., Mulder, E., Valkenburg, J.A., Wientjes, F.B., Zaritsky, A., and Nanninga, N. (1990). Role of the nucleoid in the toporegulation of division. Res Microbiol *141*, 39-49.

Wu, L.J. (2004). Structure and segregation of the bacterial nucleoid. Curr Opin Genet Dev *14*, 126-132.

Wu, L.J., and Errington, J. (1994). Bacillus subtilis SpoIIIE protein required for DNA segregation during asymmetric cell division. Science *264*, 572-575.

Wu, L.J., and Errington, J. (1997). Septal localization of the SpoIIIE chromosome partitioning protein in Bacillus subtilis. EMBO J *16*, 2161-2169.

Wu, L.J., and Errington, J. (2003). RacA and the Soj-Spo0J system combine to effect polar chromosome segregation in sporulating Bacillus subtilis. Mol Microbiol *49*, 1463-1475.

Wu, L.J., and Errington, J. (2004). Coordination of cell division and chromosome segregation by a nucleoid occlusion protein in Bacillus subtilis. Cell *117*, 915-925.

Wu, L.J., Feucht, A., and Errington, J. (1998). Prespore-specific gene expression in Bacillus subtilis is driven by sequestration of SpoIIE phosphatase to the prespore side of the asymmetric septum. Genes Dev *12*, 1371-1380.

Wu, L.J., Franks, A.H., and Wake, R.G. (1995). Replication through the terminus region of the Bacillus subtilis chromosome is not essential for the formation of a division septum that partitions the DNA. J Bacteriol *177*, 5711-5715.

Wu, L.J., Ishikawa, S., Kawai, Y., Oshima, T., Ogasawara, N., and Errington, J. (2009). Noc protein binds to specific DNA sequences to coordinate cell division with chromosome segregation. EMBO J *28*, 1940-1952.

Yan, K., Pearce, K.H., and Payne, D.J. (2000). A conserved residue at the extreme C-terminus of FtsZ is critical for the FtsA-FtsZ interaction in Staphylococcus aureus. Biochem Biophys Res Commun *270*, 387-392.

Yanouri, A., Daniel, R.A., Errington, J., and Buchanan, C.E. (1993). Cloning and sequencing of the cell division gene pbpB, which encodes penicillin-binding protein 2B in Bacillus subtilis. J Bacteriol *175*, 7604-7616.

Zhou, H., and Lutkenhaus, J. (2003). Membrane binding by MinD involves insertion of hydrophobic residues within the C-terminal amphipathic helix into the bilayer. J Bacteriol *185*, 4326-4335.

Zhou, H., Schulze, R., Cox, S., Saez, C., Hu, Z., and Lutkenhaus, J. (2005). Analysis of MinD mutations reveals residues required for MinE stimulation of the MinD ATPase and residues required for MinC interaction. J Bacteriol *187*, 629-638.

Appendices

Solutions used in this work

Name	Concentration /volume/mass	Substance
Binding buffer BD	20 mM	Tris-HCl pH 8
	200 mM	KCl
	2 mM	$MgCl_2$
	0.2 mM	DTT
	0.5 mg/ml	BSA
Binding buffer BM	20 mM	Tris-HCl
	200 mM	KCl
	5 mM	$MgCl_2$
	1 mM	EDTA
	0.5 mM	DTT
Binding buffer BR	20 mM	Tris-HCl
	200 mM	KCl
	2 mM	$MgCl_2$
	0.2 mM	DTT
Binding buffer DM	100 mM	Tris-HCl
	25 mM	$MgCl_2$
	500 mM	KCl
	2.5 mM	DTT
	5 mM	EDTA
	50 %	glycerol
Buffer M1	20 mM	Tris-HCl pH 8
	200 mM	NaCl
	1 mM	EDTA
	0.5 mM	DTT
Buffer M2	20 mM	Tris-HCl pH 8
	1 M	NaCl
	1 mM	EDTA
	0.5 mM	DTT
Buffer M3	20 mM	Tris-HCl pH 8
	100 mM	NaCl
	0.5 mM	DTT
Buffer R1	20 mM	Tris-HCl pH 8
	200 mM	NaCl
	1 mM	EDTA
	0.5 mM	DTT

	0.25 %	Tween20
Buffer R2	20 mM	Tris-HCl pH 8
	1 M	NaCl
	1 mM	EDTA
	0.5 mM	DTT
	0.25 %	Tween20
Buffer R3	20 mM	Tris-HCl pH 8
	100 mM	NaCl
	0.5 mM	DTT
Column Buffer M	20 mM	Tris-HCl pH 8
	200 mM	NaCl
	1 mM	EDTA
CAA (casamino acids)	20 %	casamino acids
DNA loading dye	0.04 %	bromphenol blue in 50 % glycerol
10000x mineral stock	5 g/l	boric acid
	4 g/l	$MnSO_4$
	4 g/l	$ZnSO_4*7H_2O$
	2 g/l	$FeCl_2*6H_2O$
	0.4 g/l	molybdic acid
	1 g/l	KI
	0.4 g/l	$CuSO_4*5H_2O$
	10 g/l	citric acid
ONPG solution	40mg	ONPG (*ortho*-Nitrophenyl-β-galactoside)
	fill up to 10 ml with Z-buffer	
50x salt stock (for EMM)	52.5 g/l	$MgCl_2*6H_2O$
	0.735 g/l	$CaCl_2*2H_2O$
	50 g/l	KCl
	2 g/l	Na_2SO_4
10 x SDS	0.25 M	Tris
	1.92 M	Glycine
	1 %	SDS
SMM medium	0.2 %	$(NH_4)_2SO_4$
	1.4 %	K_2HPO_4
	0.6 %	KH_2PO_4
	0.1 %	sodium citrate
	0.02 %	$MgSO_4$
	fill up to 1 l with dH_2O	
Solution A	1.979 g	$MnCl_2*6H_2O$
	0.098 g	$FeCl_3*6H_2O$

	0.083 g	$MgCl_2*6H_2O$
	fill up to 100 ml with dH_2O	
Solution B	53.3 g	NH_4Cl
	10.6 g	Na_2SO_4
	6.8 g	KH_2PO_4
	9.7 g	NH_4NO_3
	fill up to 1 l with dH_2O and adjust to pH 7.0	
Solution C	50 g	L-glutamic acid
	fill up to 1 l with dH_2O and adjust to pH 7.0	
Solution D	0.1 M	$CaCl_2$
Solution E	40 %	D-glucose
Solution F	1 M	$MgSO_4$
Solution G	25 g	Oxoid Casein hydrolysate
	11.7 g	sodium glutamate
	3.125 g	L-alanine
	3.48 g	L-aspargine
	3.4 g	KH_2PO_4
	1.34 g	NH_4Cl_2
	0.27 g	Na_2SO_4
	0.24 g	NH_4NO_3
	2.45 g	$FeCl_3*6H_2O$
Solution H	50 mM	$MnSO_4$
	fill up to 1 l with dH_2O	
SSC	0.15 M	NaCl
	0.01 M	sodium tricitrate
	adjust to pH 7.0	
Staining solution A	50 %	methanol
	10 %	acetic acid
Staining solution B	60 g	$(NH_4)SO_4$
	15 ml	phosphoric acid 85 %
	fill up to 750 ml with dH_2O	
Staining solution C	0.8 g CBB-G	CBB-G
	50 ml	dH_2O
50 x TAE buffer	2 M	Tris pH8
	50 mM	acetic acid
	100 mM	EDTA
TE buffer	10 mM	Tris, pH 8

	1 mM	EDTA
Transfer buffer	25 ml	10x SDS
	200 ml	methanol
	775 ml	dH_2O
Tryptophane solution	2 mg/ml	trypthophan
1000x vitamin stock (for EMM)	1 g/l	pantothenic acid
	10 g/l	nicotinic acid
	10 g/l	inositol
	10 mg/l	biotin
Z-buffer	3.04 g	$NaH_2PO_4*2H_2O$
	4.33 g	Na_2HPO_4
	0.75 g	KCl
	0.25 g	$MgSO_4*7H_2O$
	fill up to 1 l with dH_2O	

Growth media

Name	Volume/mass	Substance/solution
CH medium	100 ml	solution G
	1 ml	tryptophan solution
	0.2 ml	solution H
	0.1 ml	solution D
	0.04 ml	solution F
Competence medium (MM)	10 ml	SMM
	0.125 ml	solution E
	0.1 ml	trypthophan solution
	0.06 ml	solution F
	0.01 ml	CAA
	0.005 ml	Ferric ammonium citrate
EMM	3 g/l	potassium hydrogen phthalate
	2.2 g/l	Na_2HPO_4
	5 g/l	NH_4Cl
	20 g/l	glucose
	20 ml/l	salts
	1 ml/l	vitamins
	0.1 ml/l	minerals
LB	10 g	Tryptone
	5 g	Yeast extract
	10 g	NaCl
	fill up to 1l with dH_2O and autoclave	
Nutrient agar	28 g	Oxoid Nutrient Agar
	fill up to 1l with dH_2O and autoclave	
PAB medium	17.5 g	Oxoid Antibiotic medium no.3
	fill up to 1l with dH_2O and autoclave	
Starvation medium	10 ml	SMM
	0.125 ml	solution E
	0.06 ml	solution F
2TY medium	5g	Yeast extract
	16g	Tryptone
	5g	NaCl
	fill up to 1l with dH_2O and autoclave	
Sporulation	90 ml	A+B (sporulation salts)

medium (SM)	4 ml	solution C
	1 ml	solution D
	0.5 ml	solution F
	1 ml	trypthophan
YE5S	30 g	glucose
	5 g	yeast extract
	0.225 g	ade/his/lys/ura
	0.25	leucine
	20 g	agar
	fill up to 1l with dH_2O and autoclave	

Media supplements

Supplement	**Final concentration**	
	B. subtilis	***E. coli***
Amino acids		
tryptophan	20 µg/ml	
Antibiotics		
ampicilin		100 µg/ml
chloramphenicol	5 µg/ml	
erythromycin	1 µg/ml	
kanamycin	5 µg/ml	25 µg/ml
lincomycin	25 µg/ml	
phleomycin	1 µg/ml	
spectinomycin	50 µg/ml	
tetracycline	10 µg/ml	
Other supplements		
IPTG	1 mM	1 mM
Starch	0.2 %	
X-gal	200 µg/ml	40 µg/ml
xylose	0.1-1 %	

Supplementary data

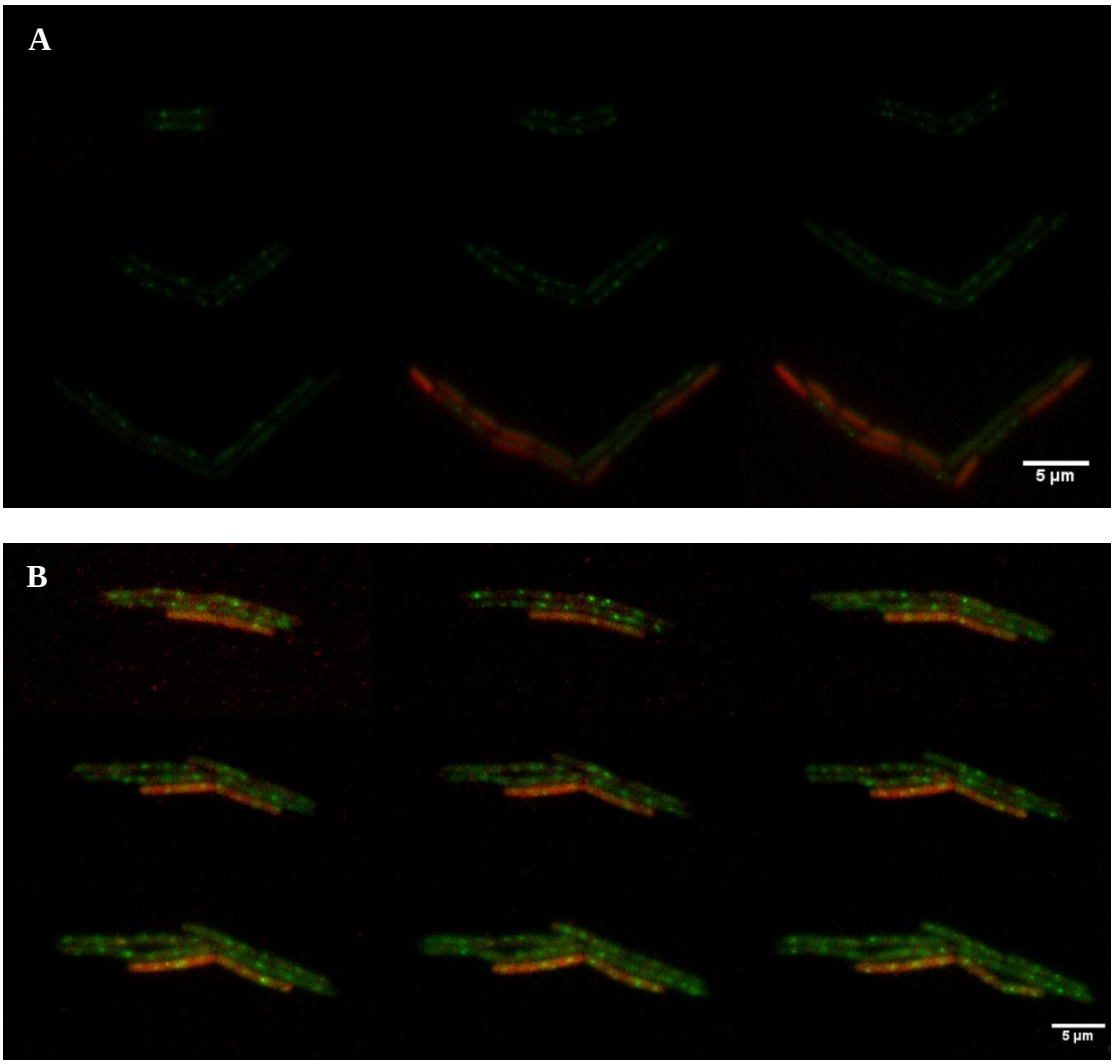

Figure A1: Chromosome replication and sporulation initiation.
DnaX-YFP forms foci when cells are replicating the chromosome (green signal), and SpoIIAA-mCherry signal (red signal spread through the cell) indicates initiation of sporulation. Wild type cells (A) finish chromosome replication prior to sporulation initiation: cells expressing SpoIIAA-mCherry (red signal through the cell) do not contain green DnaX-YFP foci (A). In contrast to wild type cells, not all cells of strain lacking *minD* stop chromosome replication at the time when sporulation has been initiated: some cells contain both, red SpoIIAA-mCherry signal and green DnaX-YFP foci (B).

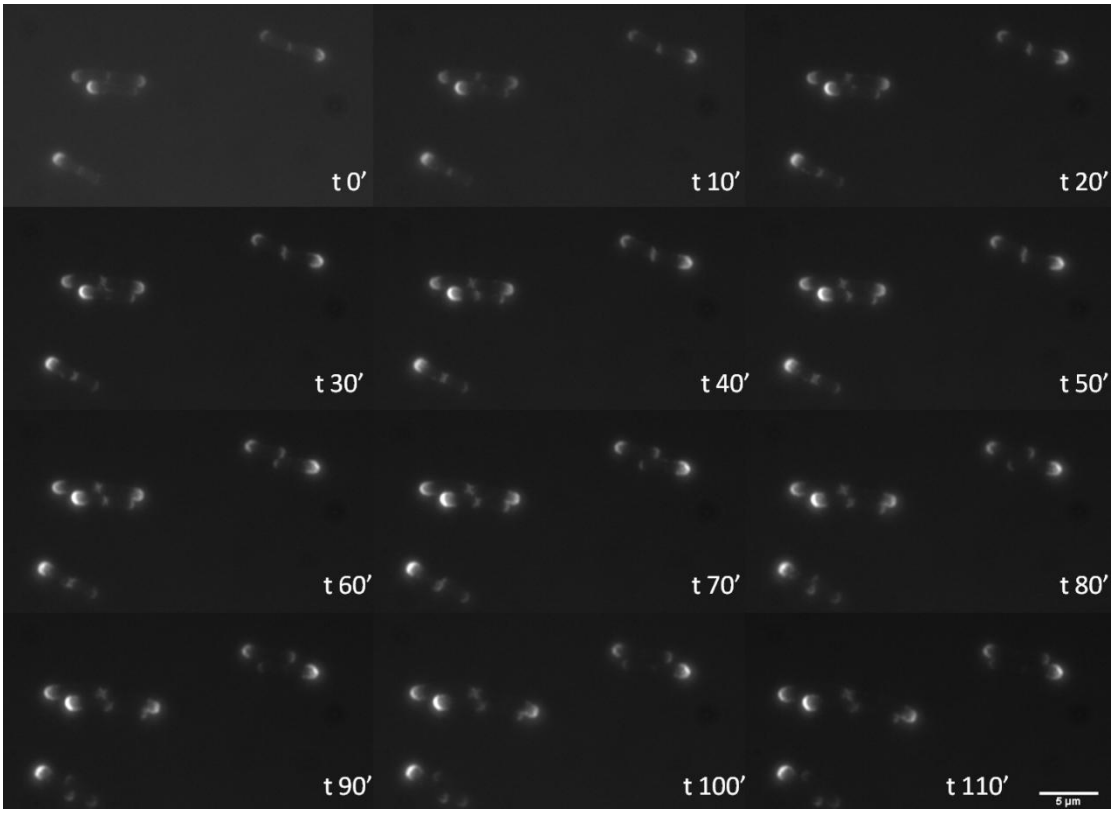

Figure A2: DivIVA localisation in wild type *E.coli* cells.
DivIVA preferentialy localizes to the cell poles in *E.coli*, because the curvature there is strongest. It accumulates at the older cell pole through the time and no oscillation of the protein can be observed.